From the:
Comprehensive Pneumology Center (CPC), Helmholtz Center Munich
and the
Institute of Experimental Pneumology, Ludwig-Maximilians-Universität München

Director: Dr. Ali Önder Yildirim

Dissertation

zum Erwerb des Doctor of Philosophy (Ph.D.) an der

Medizinischen Fakultät der

Ludwig-Maximilians-Universität zu München

Differential effects of prolyl-3-hydroxylases 1 and 4 on collagen biosynthesis highlight prolyl-3-hydroxylase 4 as a potential novel drug target in pulmonary fibrosis

vorgelegt von:

Ceylan Onursal

aus:

Yüksekova, Turkey

Jahr:

2023

Mit Genehmigung der Medizinischen Fakultät der

Ludwig-Maximilians-Universität zu München

First evaluator (1. TAC member): *PD Dr. Claudia Staab-Weijnitz*

Second evaluator (2. TAC member): *Prof. Dr. med. Susanne Mayer*

Dean: **Prof. Dr. med. Thomas Gudermann**

Datum der Verteidigung:

18.07.2023

Affidavit

LMU LUDWIG-MAXIMILIANS-UNIVERSITÄT MÜNCHEN | Promotionsbüro Medizinische Fakultät | MMRS

Affidavit

ONURSAL, CEYLAN

Surname, first name

München, GERMANY

town, country

I hereby declare, that the submitted thesis entitled:

Differential effects of prolyl-3-hydroxylases 1 and 4 on collagen biosynthesis highlight prolyl-3-hydroxylase 4 as a potential novel drug target in pulmonary fibrosis

is my own work. I have only used the sources indicated and have not made unauthorised use of services of a third party. Where the work of others has been quoted or reproduced, the source is always given.

I further declare that the dissertation presented here has not been submitted in the same or similar form to any other institution for the purpose of obtaining an academic degree.

München,12.08.2023 — **CEYLAN ONURSAL**

place, date — Signature doctoral candidate

Confirmation of congruency

LMU LUDWIG-MAXIMILIANS-UNIVERSITÄT MÜNCHEN | Promotionsbüro Medizinische Fakultät | MMRS

Confirmation of congruency between printed and electronic version of the doctoral thesis

ONURSAL CEYLAN

Surname, first name

München, GERMANY

town, country

I hereby declare, that the submitted thesis entitled:

Differential effects of prolyl-3-hydroxylases 1 and 4 on collagen biosynthesis highlight prolyl-3-hydroxylase 4 as a potential novel drug target in pulmonary fibrosis

is congruent with the printed version both in content and format.

CEYLAN ONURSAL

München,12.08.2023

place, date

Signature doctoral candidate

“It appears to me that doing what little one can to increase the general stock of knowledge is as respectable an object of life, as one can in any likelihood pursue.”

Charles Darwin

Table of Contents

Summary

Idiopathic pulmonary fibrosis (IPF) is a chronic, progressive, and incurable interstitial lung disease (ILD) with an average life expectancy of generally 2-5 years following diagnosis and an increasing worldwide incidence. Many questions about the etiology of IPF remain unanswered. IPF is characterized by an abnormal deposition of extracellular matrix (ECM) proteins, primarily collagen, leading to irreversible loss of lung function due to fibrosis, which occurs as symptoms of dyspnea and worsening cough, as well as poor life quality. Currently, only two therapeutics, Pirfenidone and Nintedanib, have been approved by US Food and Drug Administration (FDA) for the treatment of IPF. Treatment with these drugs slows disease progression but does nothing to prevent or reverse lung scarring. Therefore, there is a critical need for more effective treatment options for IPF.

FK506-binding protein 10 (FKBP10), a peptidyl-prolyl isomerase and endoplasmic reticulum (ER) resident collagen chaperone, has been defined as a therapeutic target for IPF treatment. Here, transcriptomic and proteomic analysis of global knockout FKBP10 mouse embryonic lungs identified prolyl-3-hydroxylase 4 (P3H4) as the most downregulated protein upon FKBP10 deficiency. P3H4 is an essential component of an ER resident collagen folding complex comprised of P3H3, peptidyl-prolyl cis-trans isomerase B (PPIB), and lysyl-hydroxylase 1 (LH1). It has been shown in osteoblasts and skin fibroblasts that P3H4 deficiency reduces the stability of this ER resident complex, as well as altered lysine (Lys) hydroxylation and cross-linking in collagen, and disrupted collagen fibrillogenesis, resulting in significant connective tissue defects in skin and bone (Heard et al., 2016b). However, its regulation and function in lung fibrosis are unknown.

Expression of *LEPRE1* (encoding another member of the collagen prolyl-3-hydroxylase family, P3H1) is increased in human lung fibrosis. Together with cartilage-associated protein (CRTAP) and PPIB, P3H1 forms another collagen folding ER resident complex and provides the enzymatic activity for prolyl 3-hydroxylation, a rare but conserved type of collagen post-translational modification (PTM). Similar to P3H4, P3H1 deficiency leads to instability of this complex and results

in changes in overall collagen PTM levels, fibril assembly and growth, and collagen fibril growth. The effect of P3H1 deficiency on the collagen gene expression and biosynthetic enzymes of collagen, however, has not been determined.

Therefore, the aims of this thesis were to (1) validate the effects of FKBP10 deficiency on P3H4 in a human *in vitro* model of lung fibrosis, (2) assess *P3H4* expression in *in vivo* and *in vitro* lung fibrosis models as well as IPF lung tissue sections, (3) monitor changes of profibrotic gene expression and collagen secretion following RNA-interference-mediated downregulation of P3H4, and (4) assess changes in expression of collagen biosynthesis genes in P3H1 knockout mouse-derived samples.

Similar to the results in embryonic mouse lungs of FKBP10-knockout mice, knockdown of FKBP10, by using small interfering RNA(siRNA), in primary human lung fibroblasts (phLFs) resulted in P3H4 downregulation at both protein and RNA level. *P3H4* expression was increased by transforming growth factor β (TGF-β), a profibrotic cytokine, in phLFs. Next, we showed increased levels of *P3H4* in the mouse model of bleomycin-induced lung fibrosis, with less P3H4 staining in phosphate-buffered saline(PBS)–instilled control mice. P3H4 was mainly detected in interstitial fibroblasts, as shown by colocalization with α-smooth muscle actin (α-SMA) which is a myofibroblast marker. P3H4 furthermore colocalized and interacted with FKBP10 in fibrotic lung sections from mouse. Upregulation of P3H4 and its colocalization with FKBP10 was equally observed in fibrotic lung sections from IPF patients. Publicly available scRNA-seq analysis data suggested the expression of *P3H4* and *FKBP10* in Hyaluronan Synthase 1 (HAS1)^{high} fibroblasts, which was confirmed by immunofluorescence colocalization analysis of P3H4 and FKBP10 with HAS1 in phLFs. Subcellular localization analysis of the interaction of P3H4 and FKBP10 in phLFs revealed not only direct interaction within the ER, but also that P3H4, in sharp contrast to the strictly ER resident FKBP10, is able to translocate to the nucleus. Furthermore, we performed siRNA-mediated knockdown of P3H4 in phLFs to investigate the effects of P3H4 knockdown on expression of *FKBP10* and other profibrotic marker genes. Knockdown of P3H4 in phLFs reduced *FKBP10* and fibrotic marker expression including type I collagen, α-SMA, Collagen Triple Helix Repeat Containing 1 (CTHRC1), as well as attenuated secretion of collagen into the cell supernatant.

These findings identify P3H4 as a potential novel therapeutic target for treatment of IPF. Furthermore, reciprocal regulation of P3H4 and FKBP10 in lung fibroblasts was observed. Thus, P3H4 may mediate some of the previously identified FKBP10-regulating effects on the ECM, and downregulating P3H4 may strengthen the antifibrotic effects of FKBP10 inhibition in lung fibroblasts.

Finally, the results from P3H1 null and WT mouse tail tendon experiments revealed significantly increased expression of *Col1a1, P4ha2*, and *Lh2,* together with a trend for increased transcript levels for all other genes assessed except for *P3h2* and *P4ha3*, and upregulation of type I collagen, P3H2, P3H3, and FKBP10 on the protein level. Amino acid analysis revealed that type I collagen isolated from P3H1 knockout mice was characterized by an increase in overall collagen PTM levels including prolyl-3-, prolyl-4-, and lysyl hydroxylation. These gene expression and modification changes upon P3H1 deficiency emphasize the importance of target specificity when aiming to block the collagen biosynthesis pathway for antifibrotic treatment and highlight our findings of P3H4 and FKBP10 as drug targets in pulmonary fibrosis.

In summary, the findings obtained in the thesis identified P3H4 as a novel modulator of collagen biosynthesis and secretion in lung fibroblasts, and thus a potential therapeutic target for IPF. This thesis highlights P3H4 as an important regulator of the ECM in the lung and inhibition of collagen biosynthesis *via* P3H4 and FKBP10, but not *via* P3H1, as promising approaches for IPF treatment. Besides the possibility that the interaction of P3H4 and FKBP10 can be a therapeutic target for IPF treatment, comparison of the effects of P3H4 deficiency with FKBP10 deficiency confirms that P3H4 loss alone reveals beneficial antifibrotic effects, which strengthens P3H4 as a novel drug target to prevent IPF disease progression.

1. Introduction

1.1 Idiopathic Pulmonary Fibrosis (IPF)

IPF, the most prevalent ILD, is a chronic and progressive lung disease with an average survival of up to 5 years after diagnosis (Aburto et al., 2018; Hoyer et al., 2019; L. Liu et al., 2021; Wollin et al., 2015). Even though the etiology of IPF is not completely understood, evidence from molecular characterization of clinical samples, genome-wide association studies (GWAS), as well as single-cell RNA-Sequencing (scRNA-Seq) indicates that besides repetitive micro-injuries to the alveolar epithelium, IPF also tends to involve an abnormal response of the bronchiolar and bronchial epithelium, overall resulting in abnormal wound repair initiating disease development (Chakraborty et al., 2022). Presumably as a result of environmental triggers and micro-injuries, lung epithelial cells release profibrotic mediators, growth factors, and chemokines, which activate fibroblasts to proliferate and differentiate into myofibroblasts. These myofibroblasts secrete increased amounts of ECM proteins, particularly collagen, which results in a subsequent decline in lung function and, eventually, death (Chakraborty et al., 2022; Coward et al., 2010; Glass et al., 2022; L. Liu et al., 2021; Michalski & Schwartz, 2020; Park et al., 2021).

1.1.1 Epidemiology of IPF

IPF is a disease that primarily affects males and is associated with aging, with an average diagnosis age of 66 years. IPF is a lung disease defined by usual interstitial pneumonia (UIP) pattern and by excessive deposition of ECM. During the disease progression, patients suffer from dry cough, fatigue, and progressive exertional dyspnea and the median survival rate is generally no longer than 5 to 10 years after diagnosis (Confalonieri et al., 2022; Glass et al., 2022). The predicted worldwide incidence of IPF, which is 3 to 9 cases per 100,000 individuals each year in North America and Europe, appears to be rising. Also, IPF seems to have contributed significantly to the increase in ILD mortality rates that were revealed globally between 1990 and 2013 (Confalonieri et al., 2022; Glass et al.,

2022; Kreuter et al., 2015). Even though the etiology of IPF is not fully understood, many potential risk factors and pathological pathways have been described that could be responsible for the disease process including aging, environmental factors, smoking, viral infections, gastroesophageal reflux disease (GERD), and genetic factors including mutations in the genes that encode the Mucin 5B or toll-interacting protein (TOLLIP) (Ley & Collard, 2013; López-Ramírez et al., 2018; Michalski & Schwartz, 2020; Puglisi et al., 2016; Reyfman et al., 2019; Schäfer et al., 2020; Wollin et al., 2015). Furthermore, abnormal telomere shortening and epigenetic mechanisms including histone tail modification, and DNA methylation occur in aging lungs, resulting in epithelial integrity loss and senescence (Wollin et al., 2015). However, it is unknown exactly how much each of these mechanisms contributes to the etiology of excessive fibrogenesis that characterizes IPF (Ley & Collard, 2013; López-Ramírez et al., 2018).

1.1.2 Histopathological features of IPF

IPF is associated with the characteristic imaging and histological pattern of UIP (Aburto et al., 2018). Histological hallmarks are represented by dense fibrosis, microscopic honeycombing, and fibrotic areas termed fibroblastic foci, usually located within the paraseptal and sub-pleural regions damaged by scarring, adjacent to regions of normal lung tissue and associated with a basal predominance (Glass et al., 2022; Torrisi et al., 2020). Honeycombs are enlarged airspaces that are often irregular in size and lined with fibrous tissue that contains macrophages and neutrophils, along with other inflammatory and mucous cells (Tanabe et al., 2020). Fibrotic foci, one of the key characteristics of UIP, are characterized by myofibroblast proliferation within a pathological ECM and defined by α-SMA expression, and their presence is associated with increased disease progression (Herrera et al., 2022; Hewlett et al., 2018). The architecture of the lungs is disrupted, resulting in impaired gas exchange (**Figure 1**) (Aburto et al., 2018; Glass et al., 2022).

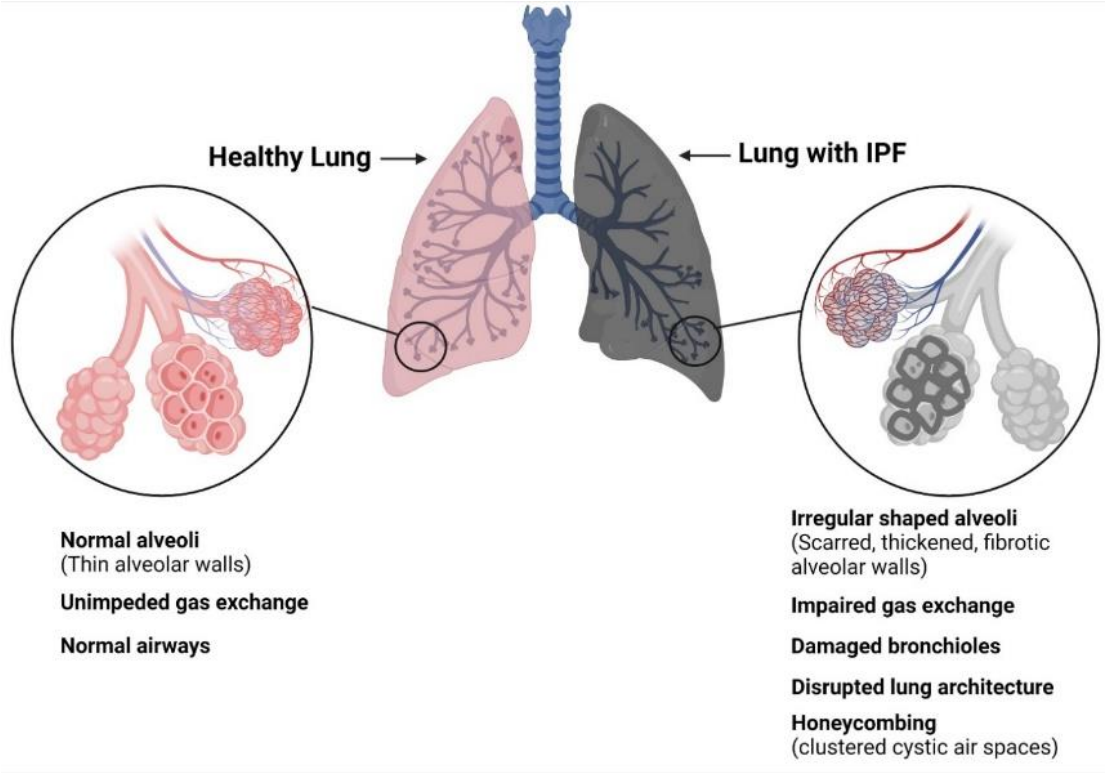

Figure 1: Illustration of healthy lung and lung with IPF. Normal airways with thin alveolar walls and unhindered gas exchange characterize the healthy lung. The lung with IPF represents pathological features of IPF including damaged bronchi, disrupted lung architecture, honeycombing, and scarred alveolar walls resulting in impaired gas exchange within the alveoli. Figure created using BioRender (https://biorender.com/) and modified from (Ghumman et al., 2021; Glass et al., 2022).

1.1.3 Pathogenesis of IPF

IPF is characterized by an increase in activated fibroblasts, collagen deposition, and ECM remodeling. These activated fibroblasts are identified by *ACTA2* expression, thus called myofibroblasts, and are believed to be the main effector cell type in lung fibrosis. In IPF lung tissues, myofibroblasts proliferate abnormally, prevent apoptosis, and impair fibrosis resolution (Ghumman et al., 2021; Noguchi et al., 2017; Zhu et al., 2017). The imbalance between the production and lysis of myofibroblasts leads to increased collagen deposition and eventually ventilation problems, and impaired oxygen levels in the body (Ghumman et al., 2021).

Most of the recent studies support resident fibroblasts, that differentiate into myofibroblasts, as the primary progenitor of myofibroblasts (Habermann et al., 2020; Ortiz-Zapater et al., 2022; Tsukui et al., 2015; Ushakumary et al., 2021). Additional potential myofibroblast progenitors have been proposed, *e.g.* bone marrow-derived circulating fibrocytes which are attracted to injured tissue sites by profibrotic factors and inflammatory cytokines. It has moreover been proposed that fibroblasts and myofibroblasts can also be produced, by a process known as "epithelial-mesenchymal transition"(EMT), in lung alveolar epithelial cells. However, research has shown that epithelial cells undergoing EMT only produce limited amounts of ECM, and lineage-tracing research has not provided evidence that they directly contribute to the mesenchymal population. Furthermore, it was revealed that α-SMA did not colocalize with EMT-derived cells. Thus, in the context of IPF, the significance of EMT and the ability of these cells to contribute to the mesenchymal population remains highly questionable (Degryse et al., 2011; Hill et al., 2019; Tanjore et al., 2009).

It has been shown that myofibroblast differentiation is induced by TGF-β (Blokland et al., 2021; B. C. Willis, 2006; Yang et al., 2022; Zanoni et al., 2019; Zhu et al., 2017). A number of cell types involved in the development of lung fibrosis produce TGF-β. Following an injury, functional TGF-β is released by alveolar macrophages and epithelial cells, and platelet granules (Hewlett et al., 2018; Zhu et al., 2017). TGF-β promotes the development of fibroblast foci and the excessive deposition of ECM in conjunction with other growth factors such as fibroblast growth factor (FGF2). These growth factors work together *via* multiple signaling pathways including TGF-β1-SMAD (Ghumman et al., 2021; Roach et al., 2018). Secretion of TGF-β leads to myofibroblast accumulation in alveolar areas and the accumulation of pathological ECM with aberrant composition, stiffness, and architecture in the lung tissue (Grigorieva et al., 2021). Myofibroblasts produce increased levels of ECM proteins, included collagen type I, III, and V, and also fibronectin (FN), a glycoprotein found in the ECM (**Figure 2**) (Ghumman et al., 2021; Knüppel et al., 2017; Lehtonen et al., 2016; Wei et al., 2019).

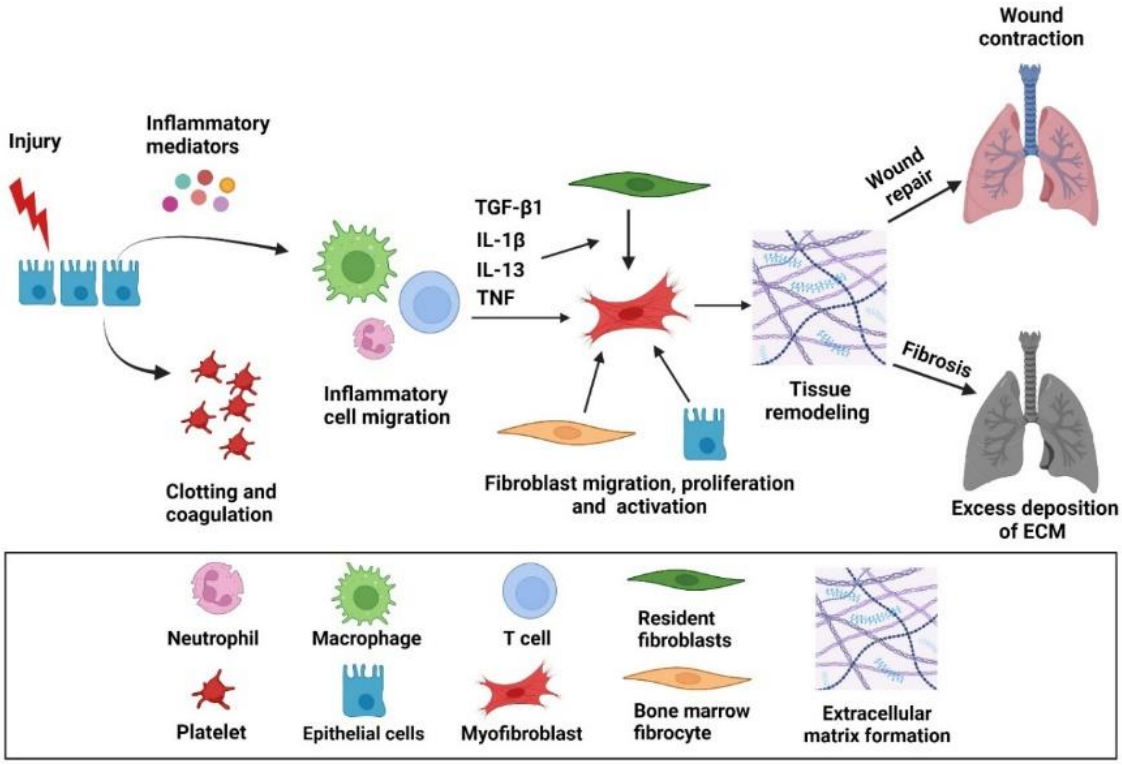

Figure 2: Illustration of the pathogenesis of IPF. Microinjuries of lung epithelial cells trigger release of inflammatory mediators, followed by inflammatory cell migration, clotting, and coagulation, as well as fibroblast activation, proliferation, and differentiation into myofibroblasts. During the phase of remodeling and resolution, activated myofibroblasts can enhance wound repair, resulting in wound contraction and blood vessel restoration. However, abnormal pulmonary wound repair and increased irreversible scar tissue formation promote the progression and development of IPF. Figure created using BioRender (https://biorender.com/) and modified from (Dudala et al., 2021; Zanoni et al., 2019).

1.1.4 ECM Accumulation in IPF

The pulmonary ECM is a highly dynamic 3D structural network that functions as a structure for migrating and adherent cells. Collagen, elastin, glycoproteins, laminins, and proteoglycans comprise the majority of the ECM (Hewlett et al., 2018; Onursal et al., 2021). By binding to integrins capable of signal transduction and by regulating tissue dynamics, ECM proteins regulate numerous mechanisms, such as cell migration and adhesion, differentiation, and the synthesis of growth factors. ECM proteins perform this function by controlling complicated developmental processes and maintaining tissue homeostasis. The development of pulmonary fibrosis, however, has been linked to the abnormal ECM protein deposi-

tion that enhance inflammation, fibroblast proliferation, and abnormal cell differentiation (Upagupta et al., 2018; Watson et al., 2016; Wight & Potter-Perigo, 2011). Aside from structural elements, the ECM also contains numerous signaling molecules including connective tissue growth factor, TGF-β, fibulin, osteopontin, and FN which affect cell adhesion, morphogenesis, and differentiation (Clause & Barker, 2013; Hewlett et al., 2018; Sorushanova et al., 2019a; Upagupta et al., 2018). These signaling molecules contribute to the regulation of pulmonary fibrosis by altering epithelial repair, enabling fibroblast recruitment, and activating myofibroblasts (Hewlett et al., 2018; Todd et al., 2012). The interaction between lung cells and ECM, as well as the alteration in lung ECM composition and structure, are well known to be critical factors in the pathogenesis of IPF (**Figure 3**) (Confalonieri et al., 2022; Deng et al., 2020; Onursal et al., 2021). Increased and disordered deposition of ECM is a characteristic of IPF. The role of growth factors including TGF-β1 in regulating this process has also been extensively studied**.** There is also strong evidence that enhanced ECM stiffness, in addition to alterations in the content and architecture of the fibrotic matrix, induces myofibroblast differentiation and increased the release of different types of ECM proteins (Blaauboer et al., 2014; Confalonieri et al., 2022; Deng et al., 2020; Suki & Bates, 2008; Tomasek et al., 2002).

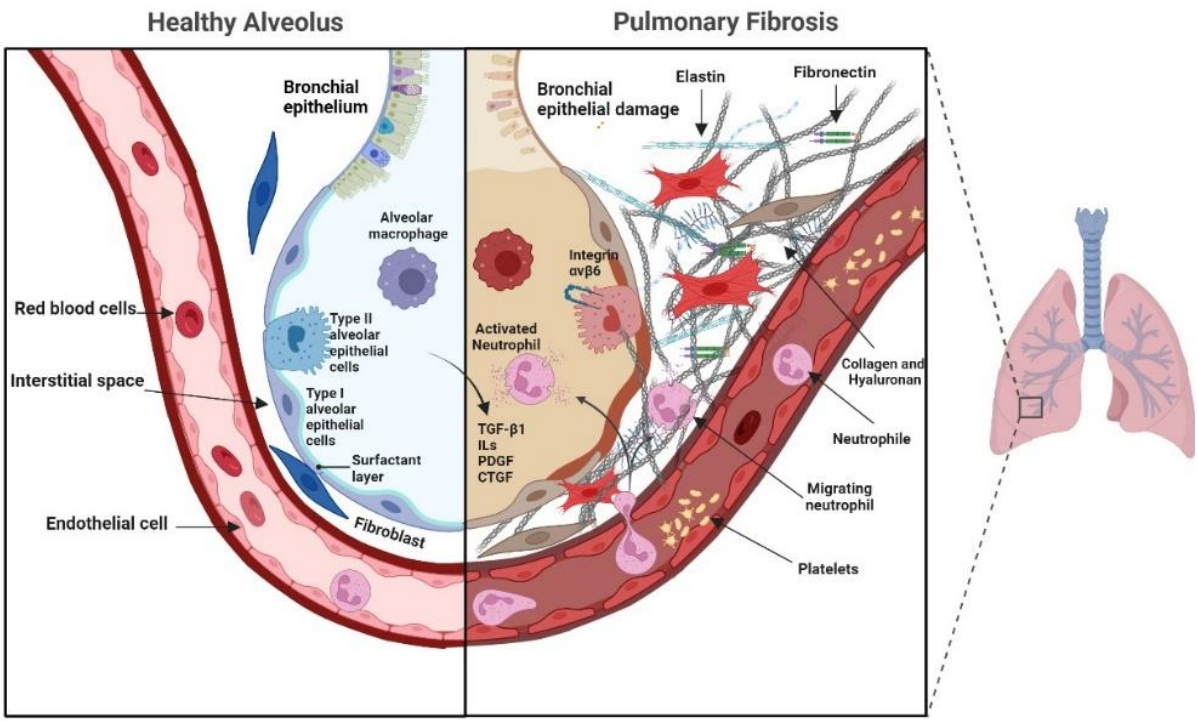

Figure 3: Illustration represents the pathological alterations in the interstitial ECM of the fibrotic lung. Interstitial ECM, comprised of a soft network of elastin, FN, and collagen connected to the basal membrane of the epithelial cell surface, is regulated by resident fibroblast activity in healthy lungs. In IPF, resident fibroblasts differentiate into myofibroblasts, resulting in an abundance of ECM proteins in the interstitium and a significant increase in ECM stiffness due to enzymatically cross-linked collagen and elastin. Figure created using BioRender (https://biorender.com/) and modified from (Burgstaller et al., 2017; Martinez et al., 2017).

1.2 Collagens

Collagens, which account for ~30% of all proteins in mammals, are the most abundant connective tissue proteins and are found in almost all organs and tissues (Karsdal, 2016; Sylvie Ricard-Blum, 2011). There are 28 different types of collagens that contain a minimum of one triple-helical collagenous domain (Gelse et al., 2003; Karsdal, 2016; Onursal et al., 2021; Sylvie Ricard-Blum, 2011). Based on their macromolecular assembly and domain formation, collagens are classified into different types including fibril-associated collagens with interrupted triple helices (FACITs, collagen types IX, XII, XIV, XVI, XIX, XX, XXI, XXII), fibrillar collagens (types I, II, III, V, XI, XXIV, XXVII), network forming collagens (types IV, VIII, X), endostatin-producing collagens/multiplexing (XV, XVIII), transmembrane collagens (types XIII, XVII, XXIII, XXV), beaded-filament-forming collagen

(type VI), and anchoring fibrils (type VII). Types XXVI and XXVIII don`t match into any of the subgroups (**Figure 4**) (Onursal et al., 2021).

All collagens have at minimum one triple-helical collagenous region formed by three polypeptide α-chains that repeat the $(Gly\text{-}X\text{-}Y)_n$ sequence, in which X is typically proline (Pro), or 3-hydroxyproline (3-Hyp) and Y proline, or 4-hydroxy-proline (4-Hyp). This triplet motif produces a left-handed helix that can conjoin with two other helices to build a right-handed triple-helical structure, that, depending on the type of collagens, can be homotrimeric or heterotrimeric (Canty & Kadler, 2005b; Heard et al., 2016a; Hudson et al., 2015; Röder, 2022; Weis et al., 2010).

Collagens typically contain non-triple-helical (NC) domains in addition to triple-helical domains, which are later removed by specific proteases before the collagens are assembled into dense fibrils (Bourgot et al., 2020). The majority of collagens interact with other ECM proteins and bind a variety of proteins to form supramolecular structures (Karsdal, 2016). Collagens, in addition to their structural functions, also act as ligands for particular cell receptors including glycoprotein VI and integrins to regulate cellular activities such as cell adhesion and migration and ECM remodeling (Muiznieks & Keeley, 2013; Yamauchi & Sricholpech, 2012).

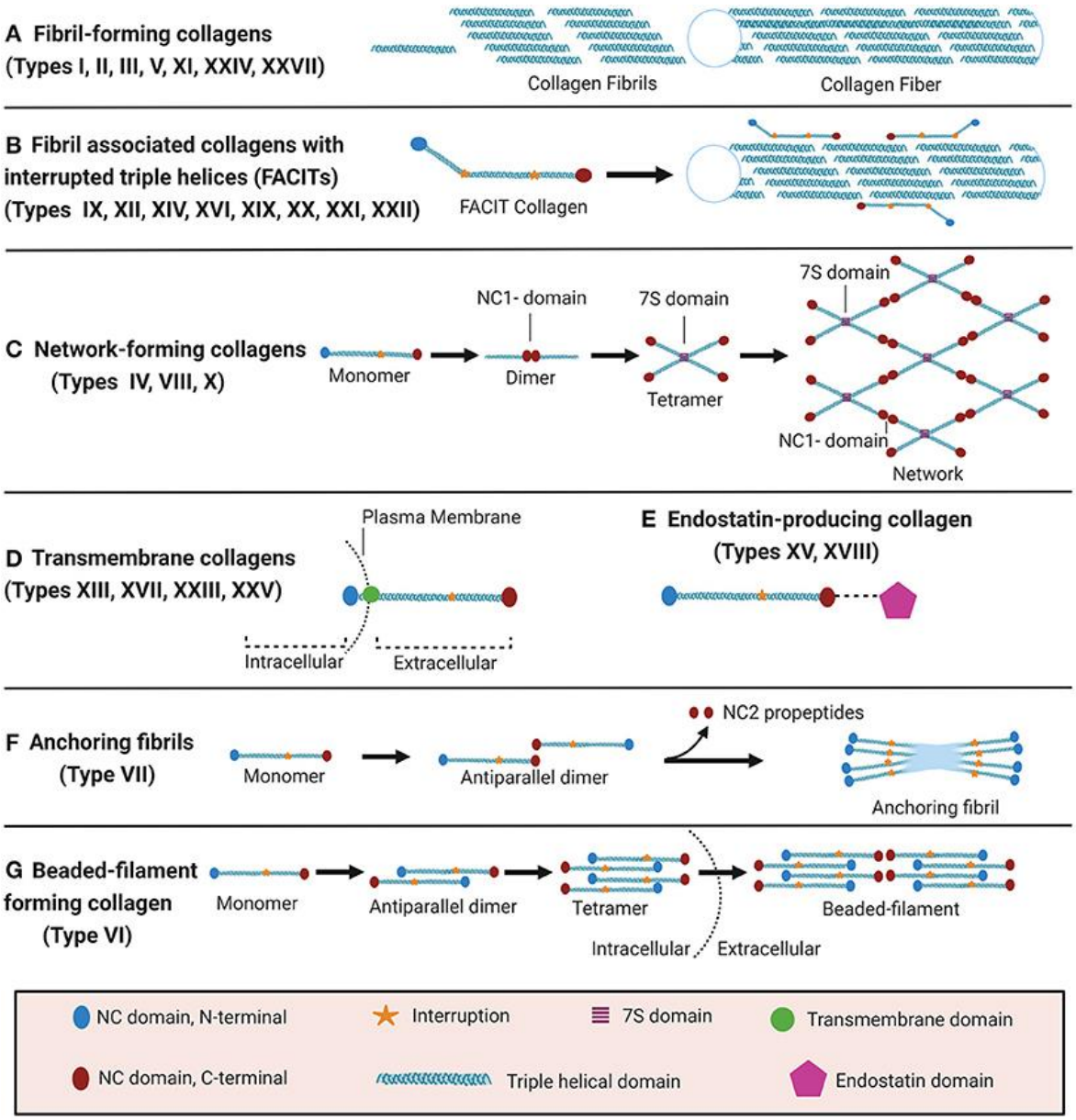

Figure 4*:* Categorization of collagens according to their supramolecular assembly. The main collagen supramolecular assembly forms are shown in the illustration. Since some of them are given specific names in publications, the figure specifies non-collagenous (NC) domains: The 7S and NC1 domains of type IV collagen network are critical nodes (C). NC2 refers to the C-terminal domain of anchoring fibrils that is cleaved off during fibril formation (F). Biorender.com was used to create the figure. This figure and the figure legend has been published in (Onursal et al., 2021) Front. Med., May 2021 under a Creative Commons Attribution License (CC BY).

1.2.1 Collagens in IPF

Collagen is the most prevalent ECM component in the airway and the key determinant of mechanical pulmonary features (L. Liu et al., 2021; Park et al., 2021). In the airway, several collagen subtypes have been identified: The basement membrane primarily consists of collagen type IV, while type II collagen predominates in cartilage of airway. The alveolar wall and septa are comprised primarily collagen type I and type III, which contribute significantly to mechanical properties of lung since they are abundant in alveoli (L. Liu et al., 2021). The pathogenesis and development of airway disease are associated with abnormal collagen deposition in the airways. There is a balance between the degradation and synthesis of collagen and other ECM proteins in healthy lungs, which is disrupted in fibrotic lungs (L. Liu et al., 2021; Organ et al., 2019; Park et al., 2021). Collagen deposition in the interalveolar space, a hallmark of IPF, distorts normal alveolar architecture during disease progression (L. Liu et al., 2021). It is assumed that collagen types I, III, and V are play a critical role in IPF pathogenesis (Jessen et al., 2021; Lei et al., 2016; L. Liu et al., 2021). Ultimately, targeting pathological collagen biosynthesis and deposition is a promising strategy for treatment of IPF (Claudia A. Staab-Weijnitz, 2022; Yang et al., 2022).

1.2.2 Biosynthesis and maturation of collagen

Collagen biosynthesis and maturation are highly complicated processes that differ depending on the type of collagen and supramolecular structure, however they are better defined for type I collagen (**Figure 6**) (Onursal et al., 2021). The process begins with collagen gene transcription, the procollagen is then translated and translocated to the rough endoplasmic reticulum (rER), where several molecular chaperones and enzymes assist in its folding and trimerization *via* its C-propeptides from its C-terminus to its N-terminus in a zipper-like style (Hulmes, 2002; Onursal et al., 2021). There are several steps required before collagen forms its triple helix.

Firstly, three different enzyme families hydroxylate unfolded procollagen: including lysyl hydroxylases (LHs), prolyl 3-hydroxylases (P3Hs),and prolyl 4-hydroxylases (P4Hs) (Ishikawa & Bächinger, 2013a). These hydroxylases have a dioxygenase domain and are 2-oxoglutarate- and Fe(II)-dependent dioxygenases.

Ascorbic acid is required as a cofactor by all hydroxylases because it is essential for returning iron to its oxidized form (Shao *et al.,* 2018). Three lysyl hydroxylase isoenzymes have been identified which are termed LH3, LH2, and LH1 and encoded by the genes procollagen-lysine 2-oxoglutarate 5-dioxygenase 3 (*PLOD3*), *PLOD2*, and *PLOD1* respectively. LH1 predominantly hydroxylates lysine in collagen triple helical regions. In telopeptides, however, LH2 is primarily responsible for lysine hydroxylation (Salo & Myllyharju, 2021). Lysyl hydroxylases require to form as dimers in order to function. FKBP10 facilitates LH2 dimerization in the telopeptides region. However, for LH1, an ER resident complex composed of four distinct proteins, known as the LH1/P3H4/P3H3/PPBI complex, potentially drives dimerization and facilitates LH1 activity in the helical region of the α-chains **(Figure 7)** (Gjaltema & Bank, 2017). It has been shown that LH3 also exhibits collagen glycosyltransferase activity in addition to LH activity (Salo & Myllyharju, 2021). PTMs such as prolyl or lysyl residue hydroxylation and hydroxylysine glycosylation are required for adequate stability, triple helix formation, procollagen secretion, and collagen maturation, and thus define the composition of collagen cross-links (Hudson & Eyre, 2013a; Ishikawa & Bächinger, 2013a; Shao et al., 2018a; Yamauchi & Sricholpech, 2012)**.** For instance, P4H is required to convert Pro to 4Hyp, which is the most abundant PTM that contributes significantly to the thermal stability of collagen triple helix structure (Canty & Kadler, 2005a; Ishikawa & Bächinger, 2013a; Shao et al., 2018a). Excessive collagen accumulation in various tissues, including the lung, has been associated with increased hydroxylysine cross-links (Onursal et al., 2021; Shao et al., 2018b; C. Wang et al., 2000)**.** Despite many decades of collagen research, the role of some collagen PTMs remains poorly understood. For instance, as mentioned previously, while prolyl-4-hydroxylations are well established to contribute to triple helical thermodynamic stability (Burjanadze, 1992; Sakakibara et al., 1973), the function of prolyl-3-hydroxylation in collagen type I is not well known (Eyre et al., 2011; Weis et al., 2010). Prolyl 3-hydroxylation is a uncommon PTM in collagenous sequences that, when defective, is linked to a broad range of human diseases (Hudson & Eyre, 2013a; Ishikawa & Bächinger, 2013b).

Prolyl-3-hydroxylase 1 (P3H1), P3H2, and P3H3, that are encoded by *LEPRE1, LEPREL1,* and *LEPREL2*, correspondingly, are the three collagen prolyl-3-hydroxylases that initiate prolyl-3-hydroxylation. All prolyl-3-hydroxylases have a common N-terminal domain and a 2-oxoglutarate-dependent dioxygenase domain at the C-terminus that also has hydroxylase activity, and their enzymatic activity is dependent on Fe2+, 2-oxoglutarate, O2, and ascorbic acid (Gjaltema & Bank, 2017; Marini et al., 2007)**.** P3H1 has been ascribed a function in prolyl-3-hydroxylation of type I collagen (Gjaltema & Bank, 2017; Pokidysheva, Zientek, et al., 2013; Vranka et al., 2010). Using tissues from P3H1 knockout mice and low- to medium-resolution mass spectrometry of protein digests, type I collagen has been shown to contain three P3H1-dependent prolyl-3-hydroxylation sites. The so-called A1 site P986 (referring to the pepsin-cleaved α1 chain of type I collagen, P1153 in Uniprot Entry P11087-1), has been reported to be fully hydroxylated by P3H1 in all murine tissues assessed, whereas the A3 site P707 (P874 in Uniprot Entry P11087-1), found in α1 and the α2 chain of collagen type I, was only dependent on P3H1 in bone (Gjaltema & Bank, 2017; Pokidysheva, Zientek, et al., 2013; Vranka et al., 2010)**.**

In type IV collagen, P3H2 has been linked to prolyl-3-hydroxylation (Pokidysheva et al., 2014; Tiainen et al., 2008), whereas, P3H3-dependent prolyl-3-hydroxylations have not yet been identified, to the best of our knowledge. However, collagens from *P3h3* null mice have deficiency of cross-linking and under-hydroxylated lysines (Hudson et al., 2017b).

In terms of collagen biosynthesis, P3H1 is a part of a trimeric complex that also includes the peptidyl-prolyl isomerase PPIB and CRTAP (Chang et al., 2010; Gjaltema & Bank, 2017; Ishikawa et al., 2009) which 3-hydroxylates the fibrillar collagen a1(I) Pro986 residue (Gjaltema & Bank, 2017; Pokidysheva, Zientek, et al., 2013) **(Figure 5).** In this trimeric complex, P3H1 provides the enzymatic activity for collagen modification, whereas CRTAP acts like a helper protein. Only the α1(I)Pro986 residue of type I collagen is 3-hydroxylated by this complex. Both P3H1 and CRTAP play independent roles. Aside from that, the two proteins share a high level of homology (Marini et al., 2007). This complex combines three functions that act on the collagen chain: prolyl-3-hydroxylation, chaperone function,

and peptidyl-prolyl isomerization (Chang et al., 2010; Ishikawa et al., 2009). Deficiency of CRTAP or P3H1 leads to destabilization of this complex (Chang et al., 2010; Morello et al., 2006), and results in changes in overall collagen PTM levels, fibril assembly and growth. Deficiency or mutations in P3H1 or CRTAP have been shown to alter lateral collagen fibril growth (Morello et al., 2006; Pokidysheva, Zientek, et al., 2013; Valli et al., 2012). P3H1 and CRTAP deficiency both result in general over-hydroxylation and over-glycosylation of lysine residues; for P3H1, a slight increase in prolyl-4-hydroxylation has also been found (Morello et al., 2006; Vranka et al., 2010). CRTAP, P3H1, and PPIB mutations cause recessive *osteogenesis imperfecta*, emphasizing the clinical significance of these changes (Barnes et al., 2006; van Dijk et al., 2009). Because P3H1 is essential for the formation and stability of this multiprotein complex, a deficiency in P3H1 might cause changes to collagen characteristics by preventing prolyl-3-hydroxylase activity or the formation of the trimeric complex (Pokidysheva, Zientek, et al., 2013).

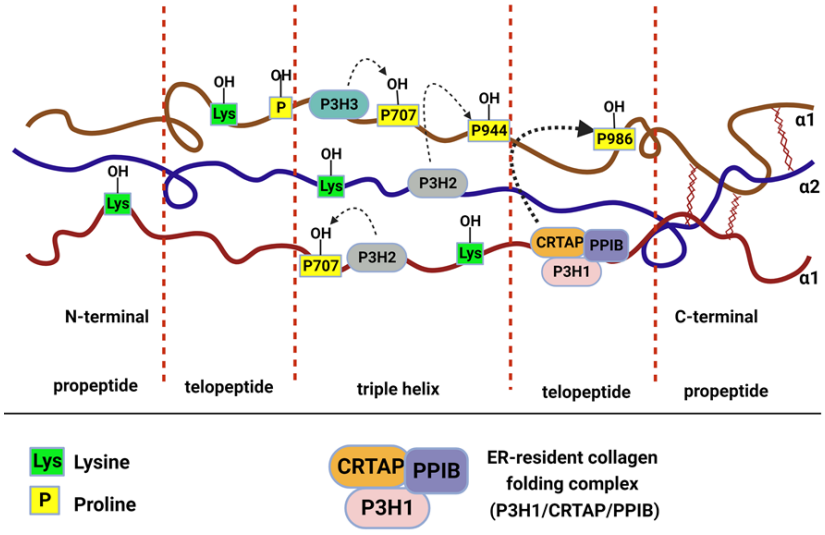

Figure 5: Collagen prolyl (P) 3-hydroxylation. P3H1, P3H2, and P3H3 are the P3H isoforms that initiate prolyl-3-hydroxylation. The CRTAP/PPBI/P3H1 complex is responsible for hydroxylation of P986 of the collagen a1(I) and a1(II) chains, while P3H2 hydroxylates the a-chains at P944 and P707. Hydroxylation P707 of the a-chains performed by P3H3. Figure created using BioRender (https://biorender.com/) and modified from (Gjaltema & Bank, 2017; Weis et al., 2010)

Next, collagen glycosyl transferases known as GLT25D1 and GLT25D2 facilitate, in addition to LH3, the 5-hydroxyl group-mediated O-glycosylation of hydroxylysines resulting in galactosyl-hydroxylysine (Gal-Hyl) or glucosyl-galactosyl-hydroxylysine (Glc-Gal-Hyl), correspondingly (De Giorgi et al., 2021; Onursal et al., 2021). Prior to the formation of triple helix, folding of both N- and C-propeptides occurs. Grp78 (BiP), PDI, calnexin, and cyclophilin are general rER resident molecular chaperones that play an active role during the folding process and chain selection via C-propeptides, which includes peptidyl-prolyl cis-trans isomerization, N-linked glycosylation, and disulfide bond formation (Ishikawa & Bächinger, 2013a; Onursal et al., 2021; Pyott et al., 2011; Ulrike Schwarze et al., 2013).

The proline residues *cis-trans* isomerization which performed by peptidyl-prolyl isomerases located in the rER, is one of the rate-limiting processes that forms the triple helix (Ishikawa & Bächinger, 2013a; Schiene-Fischer, 2015)**.** Peptidyl prolyl cis-trans isomerase activity is essential for converting proline residues into the *trans* form, allowing for the triple helix to be linearly prolonged (Canty & Kadler, 2005a; Myllyharju, 2003). The collagen chaperones FKBP10 and heat-shock protein 47 (HSP47), have demonstrated to be essential in this multistep process (Y. Chen et al., 2017; Ishikawa et al., 2017). HSP47 interacts with helical procollagen during its folding and assists in the transport of effectively folded procollagen from the ER to the Golgi apparatus *by* COPII vesicles (Gelse et al., 2003; Tasab et al., 2000). After that, procollagen is released into the extracellular space. In the extracellular space, after procollagen is secreted, specific proteinases cleave the C- and N-terminal of procollagen. Following propeptide cleavage, tropocollagen molecules with telopeptides on their cleaved ends spontaneously assemble into collagen fibrils (Gelse et al., 2003; Ishikawa & Bächinger, 2013a; Onursal et al., 2021). Finally, hydroxylysine and telopeptide lysines are undergo intra- and intermolecular cross-linking of collagen fibrils, which strengthens the fibrils. Collagen cross-linking is catalyzed by enzymes transglutaminase 2 (TG2) and lysyl oxidases (LOX) in the extracellular space. Collagen fibrils formed by the cross-linking of many triple helices are then further built to form collagen fibers (**Figure 8**) (Gelse et al., 2003; Onursal et al., 2021; Sylvie Ricard-Blum, 2011).

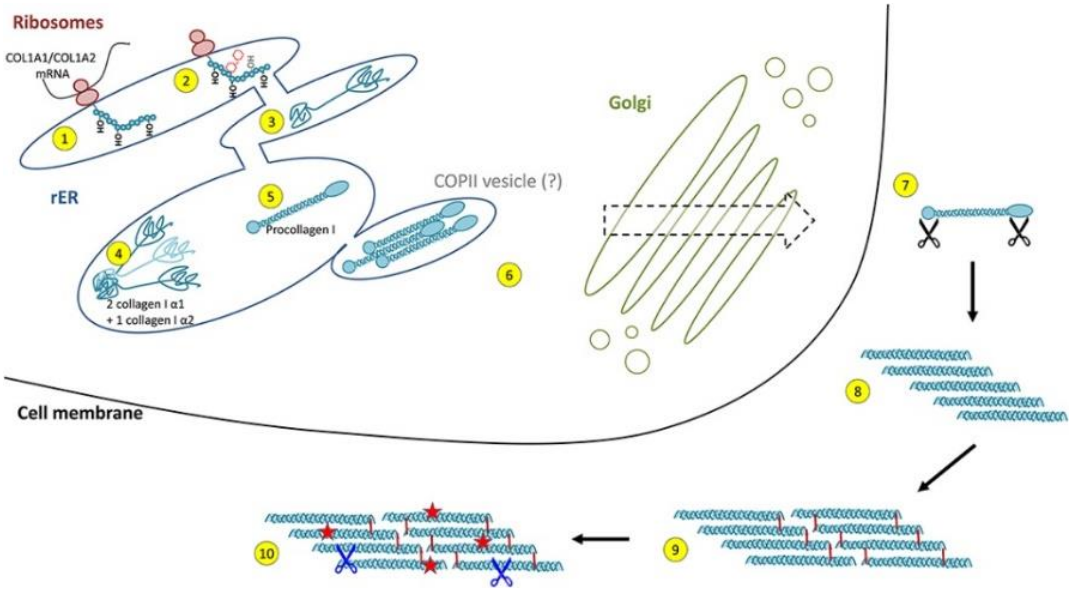

Figure 6: Intracellular biosynthesis and extracellular maturation of collagen I. The initial collagen polypeptide chain is first cotranslationally prolyl-4- and lysyl-hydroxylated in the rER (1), following by prolyl-3-hydroxylation and glycosylation (2) and folding of the N- and C-terminus propeptides (3). The triple helix nucleus of collagen I is produced by the assembly of two correctly folded α1 and a2 chain C-propeptides (4). Peptidyl-prolyl isomerases and collagen chaperones are needed for the zipper-like assembly of the collagen triple-helix (5). Upon forming the triple helix, procollagens are transported from ER to the Golgi apparatus, and then exported to the extracellular space. The concept that this happens *via* COPII vesicles has lately been questioned (6). Propeptide cleavage by at least three proteases in the extracellular space triggers (7) collagen fibril auto-assembly (8). Lastly, collagen fibrils are stabilized by cross-linking (9). *Via* extracellular proteases, the mature collagen fibers are damaged and degraded (10). This figure and the figure legend has been published in (Onursal et al., 2021) Front. Med., May 2021 under a Creative Commons Attribution License (CC BY).

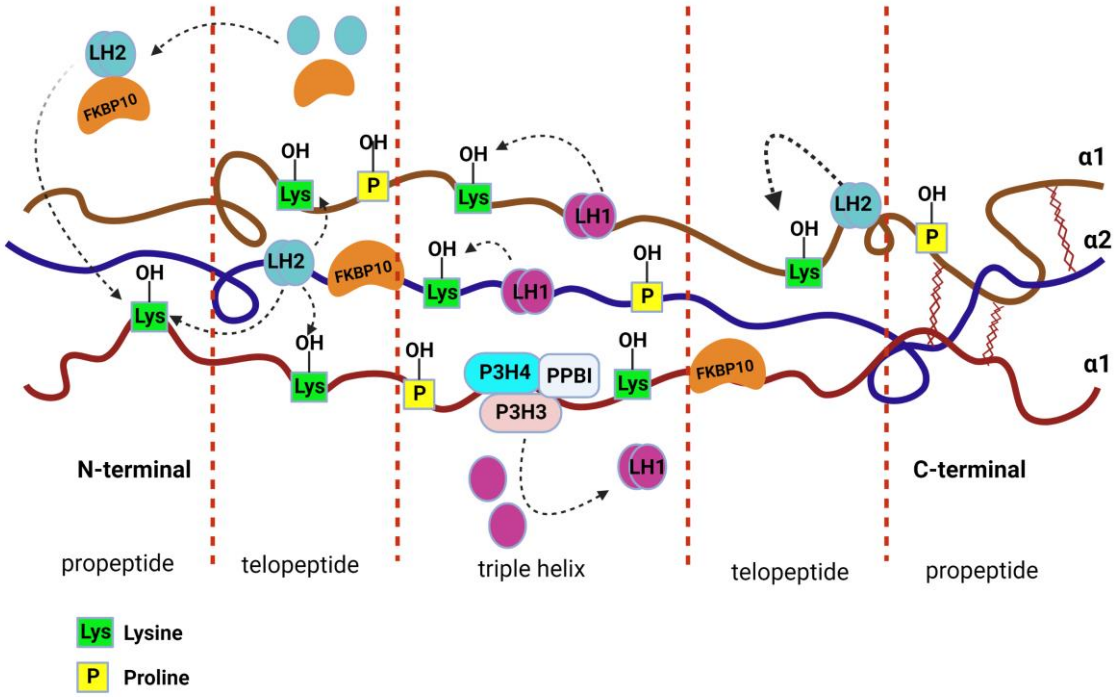

Figure 7: A graphical illustration of collagen lysyl hydroxylation of a fibrillar collagen molecule. Lysyl hydroxylases require to form as dimers in order to function. FKBP10 facilitates LH2 dimerization in the telopeptides region. However, for LH1, an ER resident complex (LH1/P3H4/P3H3/PPBI), potentially drives dimerization and facilitates LH1 activity in the helical region of the α-chains. LH2 particularly 5-hydroxylates telopeptide regions. In the triple helical domain of the α-chains of collagen type I, LH1 is likely the main isoform that catalyzes the 5-hydroxylation of lysine residues. Figure created using BioRender (https://biorender.com/) and modified from (Gjaltema & Bank, 2017; Heard et al., 2016a)

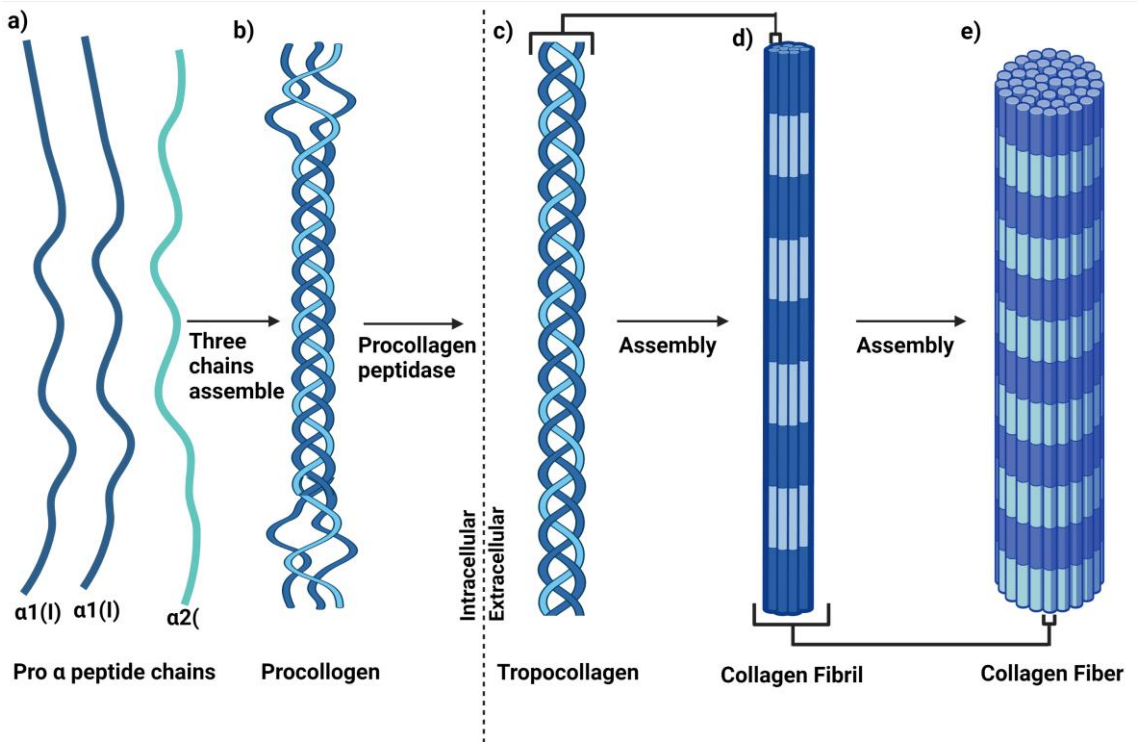

Figure 8: The hierarchical structure of collagen type I fiber Two α1(I) chains and one α2(I) chain self-assembled into procollagen(a,b). Each terminus was then cleaved by procollagen peptidase, generating a type I tropocollagen molecule(c). Collagen fibrils are generated by the self-assembly of tropocollagen molecules(d). Finally, collagen fibrils self-assemble to form type I collagen fiber (e). Figure created using BioRender (https://biorender.com/) and modified from (Kruger et al., 2013; B. Sun, 2021).

1.2.3 Assembly of extracellular matrix collagen fibrils

Procollagen is processed into collagen, secreted into the extracellular space, and assembled into protofibrils, which are closely linked to the cell membrane. Interaction between at least two collagens that can form fibrils is required for protofibril assembly. At the cell surface, assembly of protofibril is initiated by collagen types V and XI. Besides collagens, also small leucine-rich proteoglycans (SLRPs), such as fibromodulin and decorin bind to the protofibril surface to regulate collagen fibril formation (Birk et al., 1990; Canty & Kadler, 2005b; S. Chen & Birk, 2013; Wenstrup et al., 2004). The formation of fibrillar collagen I *in vivo* is dependent on the presence of the ECM components including FN- and collagen-binding integrins, FN, and other collagen types (Nashchekina et al., 2022). FN is a large extracellular protein that is released like a disulfide-bonded dimer with three types

of repeated modules that facilitate integrin receptors bind to the cell surface and interact with ECM components, such as collagen α1(I) chain (Canty & Kadler, 2005a; Kadler et al., 2008; Nashchekina et al., 2022). Integrins are essential for maintaining the ECM-cell and cell-cell adhesion, as well as the transduction of signals from extracellular matrix to the intracellular compartment (Hewlett et al., 2018; Musiime et al., 2021). FN, collagen V and α2β1 integrins appear to be essential for collagen fibril assembly (Kadler et al., 2008).

Collagens, as fibrillogenic proteins, regulate cell-extracellular matrix interactions. Collagen fibrils and other ECM proteins function as binding sites for cells (Nashchekina et al., 2022). During ECM synthesis, collagen and other ECM proteins interact and self-associate to create fibrillar networks (Ishikawa et al., 2017; Singh et al., 2010). ECM glycoproteins typically bind to cell surface receptors to trigger matrix formation. Receptor binding stimulates activation and self-association of FN; FN then promotes fibril assembly *via* interaction with other cell-associated FN dimers. FN structural changes reveal more binding sites involved in fibril assembly and fibril conversions to an insoluble and stable form. FN matrix, once formed, affects tissue structure by assisting in the formation of other ECM proteins (Singh et al., 2010; Wierzbicka-Patynowski & Schwarzbauer, 2003). The cytoplasmic domains of integrin receptors coordinate intracellular proteins to form into intracellular functional structures, as FN fibrils form extracellularly (Hastings et al., 2019). Thus, the formation of a functional ECM is dependent on the regulation of extracellular and intracellular processes (Wierzbicka-Patynowski & Schwarzbauer, 2003).

1.2.4 Regulation of extracellular matrix homeostasis

The ECM in healthy lungs is a complex mixture of polysaccharides, glycoproteins, and collagens that are neatly formed to sustain tissue integrity and divide mesenchymal and epidermal cell surfaces. It is also a highly dynamic structure that is continuously modified by both enzymatic and non-enzymatic processes (Upagupta et al., 2018; Watson et al., 2016). Together with controlling homeostasis, tissue development, and repair, these dynamics also control cell migration, differentiation, apoptosis, and proliferation (Bonnans et al., 2014; Decaris et al., 2014). Following an acute injury, tissue repair is often defined by the recruitment

of immune cells, the enzymatic ECM degradation close to the site of injury, and the later infiltration of fibroblasts depositing new ECM (Decaris et al., 2014; Hynes, 2009).

However, aberrant signaling pathways can be triggered in the case of chronic lung damage, and this remodeling is disrupted with abnormalities in protein secretion, organization, and degradation. This leads to a pathological accumulation of proteoglycans, collagen, elastin, and FN which ultimately results in fibrosis and distortion of the natural lung architecture (Decaris et al., 2014; Upagupta et al., 2018; Watson et al., 2016). The elastic recoil of the lung is assisted by the attachment of elastin fibers to collagen (Upagupta et al., 2018; Watson et al., 2016). Proteoglycans, along with glycoproteins, builds the essential hydrated gel that links collagen and elastin fibers to provide the alveolar structure mechanical stability (Upagupta et al., 2018).

Matrix turnover is normally regulated by a variety of mechanical and chemical signals like TGF-β1, serine proteases, growth factors, ECM-modifying enzymes, and mechanical stresses. The preservation of normal tissue activity is depends on the maintenance of this homeostasis (Bardou et al., 2016; Hastings et al., 2019). To prevent fibrosis, collagen production and degradation *via* intracellular or extracellular collagen degradation are coordinated during homeostasis (Clarke et al., 2013; Kay et al., 2021).

Matrix metalloproteinases (MMPs) have typically been considered as a major group of proteases involved in the degradation of ECM proteins, together with their tissue inhibitors (TIMPs). Under normal conditions, the activity of MMPs and other extracellular proteases, such as certain serine and cysteine proteases, is low. However, during repair or remodeling processes, as well as in pathological conditions, this activity increases and promotes fibrosis development by activating a broad range of growth factors, cytokines, and chemokines (Caley et al., 2015; Chuliá-Peris et al., 2022; Clarke et al., 2013; Pardo et al., 2016; Robert et al., 2016; Vidak et al., 2019). Moreover, MMPs are also able to activate TGF-β1 which is released in an inactive form, by attaching to a latent TGF-β1 binding protein and a latent-associated peptide (Clarke et al., 2013; Fernandez & Eickelberg, 2012). It is believed that MMP12 is crucial for the TGF-β1 signaling

pathway activation (Pardo *et al*., 2016). Macrophages are also important ECM regulators in fibrosis since, in addition to secreting MMPs, they ingest and digest ECM components *via* the lysosomal pathway (X. Zhao et al., 2022). Plasminogen activator inhibitor-1 (PAI-1) has been found to contribute to the pathological process of pulmonary fibrosis by inhibiting the activity of specific MMPs and collagen degradation (Flevaris & Vaughan, 2016; Iwaki *et al*., 2012; Oh *et al*., 2002; Shioya *et al*., 2018). MMPs and cathepsin K are primarily responsible for extracellular collagen degradation (Onursal et al., 2021). Intracellular collagen degradation occurs in the lysosomal network of the cell. A variety of cathepsins present in lysosomes cleave collagen into low-molecular-weight peptides (Onursal et al., 2021; Wagenaar-Miller et al., 2007). To sum up, all of these delicately balanced mechanisms are susceptible to being dysregulated, during pulmonary fibrosis, resulting in excessive ECM deposition and lung architecture distortion (Clarke et al., 2013; Upagupta et al., 2018)**.**

1.3 Treatment and Management of IPF

IPF, a progressive and fatal interstitial lung disease, is defined by the UIP pattern in radiology or histology. IPF patients who are not getting antifibrotic therapies have an extremely poor prognosis, with a typical life expectancy of 3 to 5 years. Lung function declines as the disease progresses, followed by worsening dyspnea and functional capacity, as well as a decline in quality of life (Heukels et al., 2019; Maher & Strek, 2019). IPF is difficult to diagnose because the symptoms are comparable to those of other respiratory disorders (G. Raghu, 2011). Despite significant research attempts over the last few years, no effective pharmaceutical therapy has been found (G. Raghu, 2011; Reyfman et al., 2019). Since IPF is currently incurable, the therapeutic objective remained to slow the progression of fibrosis, feel comfortable, and, in later stages, provide palliative care (Glass et al., 2022).

IPF treatment is classified as either pharmacological or non-pharmacological (G. Raghu, 2011). Non-pharmacological treatment includes the use of non-invasive ventilation (NIV) in combination with oxygen therapy to improve dyspnea and life quality in IPF patients. Additionally, interdisciplinary palliative care programs may

be beneficial for symptom management and psychological support throughout the disease progression (Glass et al., 2022; Millan-Billi et al., 2018).

In some patients, lung transplantation can greatly increase life expectancy and may be a viable option for treating IPF. Lung transplantation has a significant advantage over treatment options given the fact that it is the only effective treatment for IPF that improves both symptoms and survival time (Glass et al., 2022; Kistler et al., 2014; Laporta Hernandez et al., 2018; Weill et al., 2015). However, the number of lung transplants performed is limited primarily by the availability of donor organs, and only few patients are eligible for lung transplantation. It is challenging to determine the need for a transplant, but the mortality rate and chances of survival following transplantation are important factors to consider when selecting IPF patients for transplant. Strict post-transplant follow-up is important to prevent graft rejection, the primary cause of long-term mortality, and to identify problems such as infections (Kistler et al., 2014; Laporta Hernandez et al., 2018).

1.3.1 Past treatment strategies targeting inflammation

Until 2014, IPF was treated with immunosuppressants and corticosteroids since it was thought that permanent fibrosis was caused by chronic inflammation in the initial stage of the disease. Thus, immunosuppressant therapy in form of a combination of azathioprine, prednisone, and N-acetyl cysteine was widely used to treat IPF, until evidence accumulated that this therapy not only was ineffective, but also increased risks for hospitalization and death (Decaris et al., 2014; Glass et al., 2022; Kreuter et al., 2015; Pleasants & Tighe, 2019; Raghu et al., 2012). These findings combined with experimental evidence indicated that inflammation is not necessary for fibrosis progression. As a result, the current concept has gradually shifted toward the primary focus of IPF management being an incorrect repair of epithelial damage which results in chronic fibrosis (Datta et al., 2011; Decaris et al., 2014; Pleasants & Tighe, 2019).

Importantly, overexpression of TGF-β1 in mice results in progressive fibrosis without any significant inflammatory component. On the other hand, it has been argued that a pathogenic role for inflammation in the early (subclinical) stages of the disease cannot be excluded. Therefore, rather than a broad-based anti-inflammatory strategy, selective modulation of key inflammatory pathways and

newer strategies that target pro-fibrogenic and inflammatory mediators, fibroblast activation and proliferation may be worth considering for therapeutic development in IPF (Datta et al., 2011; Sime et al., 1997).

1.3.2 Current pharmacologic treatments

There are currently only two antifibrotic therapies approved by the FDA (2014) for IPF therapy: Pirfenidone and Nintedanib which are currently effective options as the primary treatment for IPF (Glass et al., 2022; Lehtonen et al., 2016; Yang et al., 2022). These two oral drugs can slow down disease progression, development of scar tissue, and forced vital capacity (FVC) deterioration while also providing the patient more comfort for a significantly longer time period (Confalonieri et al., 2022; Glass et al., 2022; Yang et al., 2022). However, they cannot stop the disease and reverse the lung damage. Furthermore, the use of these medications may result in a financial burden (a treatment cost of 25,000USD/person-year, that is higher than the costs of treating breast cancer and several other lethal chronic diseases) without changing the high mortality rate and overall disease progression. Particularly due to their considerable side effect profile, some patients may not respond to these medications (Confalonieri et al., 2022; Glass et al., 2022; Claudia A. Staab-Weijnitz et al., 2015a; Yang et al., 2022).

Gastroesophageal reflux disease is a well-known comorbid condition in IPF patients. It has been proposed that GERD-induced micro aspiration contributes to the IPF pathogenesis by injuring the lung epithelium and initiating inflammatory cascades. However, a link between GERD and IPF has yet to be established (Costabel et al., 2018). Using anti-acid medications in patients with asymptomatic GERD and IPF was recommended, with conditions, in the latest recent international treatment guideline. Treatment with antacids used to treat GERD has been linked to a slower decrease rate in FVC and improved survival in patients with IPF. Randomized controlled studies, however, have not given any evidence that anti-acid medication improves outcomes in IPF patients, and the benefits and risks of anti-acid therapy in patients with IPF are still being questioned (Costabel et al., 2018; Fujimoto et al., 2015; Maher & Strek, 2019). Therefore, there is an

urgent need for more effective treatments (Roach et al., 2018; Claudia A. Staab-Weijnitz et al., 2015a).

Table 1 summarizes some of the most important pharmaceutical options for IPF treatment, including Nintedanib and Pirfenidone, which are further explained in the following sections.

Table 1: Pharmacological treatments for IPF

	Treatment	Mechanism of action
Current therapies	Pirfenidone	Antifibrotic and anti-inflammatory
	Nintedanib	Antifibrotic and anti-inflammatory
	Oral corticosteroids, opioids	Antitussive
	Anti-acids, proton pump inhibitors	Reduces GERD (gastroesophageal reflux disease)
	Lung transplantation	Surgical replacement of one lung or both lungs
Therapies in development	PRM-151	Recombinant human pentraxin-2; actsas an antifibrotic agent
	Pamrevlumab	Fully human recombinant monoclonal antibody against CTGF(connective tissue growth factor)
	TD139	Small molecule inhibitor of galectin-3
	PLN-74809	Blocks activation of the TGFβ pathway
	TRK-250	Suppresses expression of TGFβ
	MRG-229 (a 2nd generation miR-29 mimic)	Decrease collagen production
	ND-L02-s0201	Inhibits expression of heat shock protein 47;anti-fibrotic effects

Modified from (Chioccioli et al., 2022; Glass et al., 2022; Y. Liu et al., 2021)

1.3.2.1 Nintedanib

Nintedanib (BIBF1120), originally developed as an anticancer drug, is an orally available intracellular inhibitor of tyrosine kinase that interacts with binding sites of adenosine triphosphate. Therefore, the signaling pathways associated with VEGFR receptor, FGF receptor, and PDGF receptor are suppressed (Glass et al., 2022; Myllärniemi & Kaarteenaho, 2015). PDGF, FGF, and VEGF mediate a variety of processes such as fibrogenesis, and have been linked to the IPF pathogenesis. Nintedanib inhibits fibroblast activity by inhibiting receptor tyrosine ki-

nases (Kreuter et al., 2015; Roach et al., 2018). Nintedanib inhibits TGF-β1 signaling indirectly by reducing the activity of PDGF and FGF-2, which mediate TGF-β1 profibrotic actions (Azuma et al., 2015). Nintedanib treatment inhibited bleomycin-induced activation of focal adhesion kinase (FAK), a key endothelial mesenchymal transition regulator, and thus inhibited bleomycin-induced endothelial mesenchymal transition both *in vitro* and *in vivo* (W.-K. Yu et al., 2022). Most importantly, Nintedanib decreased the expression of *FN* and type I collagen and V in IPF cells. Additionally, Nintedanib reduced the profibrotic gene expression, and secretion of collagen, inhibited the formation of collagen I fibrils, and reduced and changed the appearance of collagen fibril bundles (Knüppel et al., 2017).

The INPULSIS phase 3 trials I and II demonstrated that, despite the death rate remained unchanged, treatment with Nintedanib at 300 mg/day resulted in a significant reduction in the FVC deterioration rate in patients with IPF. The side effects, particulary nausea and diarrhea, are tolerable with medications; however, liver dysfunction and hepatotoxicity are uncommon risks, and the treatment is not suggested for people with severe liver disease (Glass et al., 2022; Kato et al., 2019; Richeldi et al., 2014).

1.3.2.2 Pirfenidone

Pirfenidone (5-methyl-1-phenylpyridin-2(1H)-one), is an oral small pyridine molecule with combined anti-inflammatory, antioxidant, and antifibrotic effects (Azuma et al., 2015; Glass et al., 2022; Kreuter et al., 2015). Although the exact mechanism of action is unknown, experimental evidence suggests that Pirfenidone exerts these effects by downregulating key profibrotic growth factors such as TGF-β1, inhibiting inflammatory cells and cytokines, and scavenging oxygen radicals (Kreuter et al., 2015).

Pirfenidone reduces collagen production, slows the development of fibrosis by suppressing TGF-β1, and decreases the rate of decline in FVC (Glass et al., 2022; King et al., 2014). Pirfenidone inhibited collagen V and delayed the formation of collagen I fibrils (Knüppel et al., 2017). In a clinical study, Pirfenidone was shown to be effective in decreasing the decline of FVC and carbon monoxide

diffusing capacity (DLCO) in IPF patients when administered throughout a 24-month research (Ghumman et al., 2021).

Pirfenidone significantly reduced lung fibrotic fibroblast-mediated fibrotic processes by inhibiting CTHRC1-induced lung fibroblast activity and restoring migration, TGF-β1-triggered collagen gel stiffness, and CTHRC1 secretion in fibrotic fibroblasts (J. Jin et al., 2019).

Over a year of treatment, Pirfenidone decreases the likelihood of respiratory-related hospitalization. Even though Pirfenidone is normally well tolerated and has only slight adverse effects including weight loss, fatigue, and nausea, cases of abnormal liver function were observed, specifically increases in bilirubin and the activity of serum alanine aminotransferase and aspartate aminotransferase (Glass et al., 2022).

Given that the pleiotropic effects of Nintedanib and Pirfenidone are believed to target different fibrotic cascade pathways, recent studies suggested that combination therapy will be the ideal therapeutic option for IPF in the future and combination therapy may have additive or even synergistic effects that lead to better results than either monotherapy. The majority of IPF patients tolerated combination therapy for 24 weeks (Flaherty et al., 2018; Huh et al., 2021; Vancheri et al., 2018).

Although Pirfenidone and Nintedanib both slow the progression of IPF, the disease still develops and is eventually fatal (Vancheri et al., 2018). Therefore, it is clear that there is an urgent requirement for additional consideration and comprehensive research into the development of targeted therapies that increase patient lifespan and quality of life (Glass et al., 2022).

1.3.3 Targeting ECM and collagen biosynthesis in IPF treatment

Excessive accumulation of collagen-rich ECM contributes to the development of IPF, resulting in increased stiffness, impaired gas exchange, and, subsequently, lung function decline (Chakraborty et al., 2022; Glass et al., 2022; Kreuter et al., 2015). The biochemical formation of the matrix and its constituents, as well as

PTMs including transglutamination, glycosylation, and cross-linking, all, have an impact on the ECM's biomechanical properties (Upagupta et al., 2018).

1.3.3.1 Targeting the myofibroblasts

ECM components, including collagen, provide promising novel therapeutic targets for the treatment of IPF, in which folding or stiffness of ECM proteins alters the functioning of important cell types, such as fibroblasts.

In IPF, activated fibroblasts restructure the ECM abnormally, as a response to a positive feedback cycle between fibroblasts and the defective ECM. Therefore, preventing this cycle may be a treatment strategy for IPF (Blaauboer et al., 2014; Parker et al., 2014).

One important pathway in remodeling processes is fibroblast activation and myofibroblast differentiation, which is induced by TGF-β and leads to increased ECM production and loss of organ function and structure (Bernard, 2018; Gang Liu et al., 2021). Thus, targeting activated myofibroblasts has been proposed as a strategy to slow and possibly reverse the progression of fibrosis (Bernard, 2018).

1.3.3.2 Targeting extracellular events of collagen biosynthesis

Previous research has investigated the link between IPF progression and ECM cross-linking. The ECM cross-linking enzymes LOX and LOX-like proteins, and transglutaminases, are known to play roles the in pathogenesis of fibrosis. The concept of targeting extracellular collagen cross-linking as an anti-fibrotic strategy has received much interest recently, due mainly to the identification of LOX-like 2 (LOXL2), the collagen cross-linking enzyme, as a potential therapeutic target for IPF (Barry-Hamilton et al., 2010b; Chien et al., 2014; Sgalla et al., 2019). Nevertheless, a recently completed phase 2 clinical trial using the LOXL2 inhibitor simtuzumab, a monoclonal anti-LOXL2 antibody, to target LOXL2 did not show a therapeutic benefit, indicating that more research of these enzymes is required (Ganesh Raghu et al., 2017; Sgalla et al., 2019; Tjin, White, Faiz, Sicard, Tschumperlin, Mahar, Kable, & Burgess, 2017).

The last stage of collagen maturation is carried out by lysyl oxidases acting on extracellular fibrillar collagen, which is resistant to most extracellular proteases

(Birkedal-Hansen et al., 1985; Onursal et al., 2021; Z. Yu et al., 2012). Inhibiting LOXL2, which happens after the spontaneous formation of fibrils, may have just a minor effect on the resolution and decrease of collagen in fibrotic regions (Steplewski & Fertala, 2012). Thus, interfering with earlier steps of collagen synthesis and processing may be advantageous (Birkedal-Hansen et al., 1985; Steplewski & Fertala, 2012; Z. Yu et al., 2012).

1.3.3.3 Targeting intracellular events of collagen biosynthesis

Targeting the pathway for collagen biosynthesis and maturation has been the subject of numerous studies. As stated before, extracellular collagen cross-linking inhibition as a therapeutic strategy for treatment of IPF (Barry-Hamilton et al., 2010a) failed in phase II studies. Thus, IPF treatment, a previous stage of collagen maturation, such as intracellular collagen biosynthesis or collagen fibril formation, can be targeted to inhibit collagen deposition.

As previously mentioned, several intracellular and extracellular modifications are required to form active collagen molecules (Kadler et al., 2007; Onursal et al., 2021). Intracellular PTMs of lysine and proline residues play critical roles in this process (Salo & Myllyharju, 2021). In the ER, prior to the collagen triple helix folding, collagen P4Hs, P3Hs, and LHs posttranslationally modify these amino acids to 4Hyp, 3Hyp, and Hyl, respectively. Further glycosylation of the Hyl residues can result in galactosyl-Hyl and glucosylgalactosyl-Hyl residues (C. Z. Chen & Raghunath, 2009; Salo & Myllyharju, 2021). In addition to these, collagen biosynthesis also requires a number of additional proteins and enzymes, such as PPIases.

PTMs such as hydroxylation of lysine or proline is required for proper stability, assembly, triple helix formation, procollagen secretion, and collagen maturation, and thus define the chemical characteristic of the cross-links between collagen molecules (Hudson & Eyre, 2013b; Ishikawa & Bächinger, 2013a; Onursal et al., 2021; Shao et al., 2018a; Yamauchi & Sricholpech, 2012). Since the hydroxylations have a significant effect on collagen synthesis, it is clear that the relevant hydroxylases could be targeted for antifibrotic therapies. For instance, since collagen LH2 and P4Hs play a crucial role in collagen biosynthesis, and they have long been thought of as promising targets for antifibrotic treatments (Piersma &

Bank, 2019; Salo & Myllyharju, 2021; Vasta & Raines, 2018). Prolyl 4-hydroxylase inhibition prevents collagen secretion through collagen instability and its internal cellular degradation (L. Chen et al., 2006; Piersma & Bank, 2019). Furthermore, TGF-β-triggered collagen production in bleomycin-induced mouse lung fibrosis and fibroblasts were both decreased by inhibiting collagen prolyl hydroxylase with pyridine-2,5-dicarboxylate (Luo et al., 2015).

In lung fibrosis, minoxidil, an anti-hypertensive drug that inhibits lysyl hydroxylase, reduced the synthesis of pyridine cross-links and collagen production and deposition; these effects may be mediated by suppression of LHs activity. As per the study's findings, lysyl hydroxylase may be a target for IPF treatment (Shao et al., 2018a). Moreover, in lung fibrosis, TGF-β1/SMAD3 signaling activated LH3 by Wnt/ β-catenin pathway(Shao et al., 2020).

3-Hyp has been shown to take part in inter-triple-helical interactions and is mostly likely involved in the supramolecular collagen formation and development of lateral fibrils (Hudson & Eyre, 2013a; Morello et al., 2006; Pokidysheva, Zientek, et al., 2013; Valli et al., 2012).

Mutations in P3H1, PPIB, and CRTAP all result in lysine over-hydroxylation in telopeptide regions, while mutations in LH2 or FKBP10 result in telopeptide lysine under-hydroxylation(Hudson et al., 2015). In the *P3h3* deficient mice, collagens had deficiency of cross-linking and under-hydroxylated lysine residues (Hudson et al., 2017a; Rappu et al., 2019). It's important to note that lysine underhydroxylation is also seen when P3H4 is deficient, similarly to P3H3 (Hudson et al., 2017a; Salo & Myllyharju, 2021). These mutations frequently resulted in altered collagen cross-linking, and these findings point to a possible interaction between the complex of prolyl 3-hydroxylation and the lysyl hydroxylation machinery in the ER (Barnes et al., 2012; Ha-Vinh et al., 2004; Hudson et al., 2015; U. Schwarze et al., 2013). Several studies indicate that LHs are components of structures that include chaperones also other proteins, suggesting that they may provide dynamic interactions to impact other than lysine alterations. Accordingly, deficiencies of any of these chaperones or enzymes can phenocopy each other, as was observed with LH2 and FKBP10, and LH1 and FKBP22 (Ishikawa et al., 2020; Salo & Myllyharju, 2021; Steinlein et al., 2011).

As previously stated, LH1 forms a complex with P3H4 and P3H3, and primarily drives the hydroxylation of lysine residues in the collagenous triple-helical regions of collagen molecule. In contrary, LH2, that is associated with FKBP10, mediates hydroxylation of lysine in the non-collagenous telopeptide regions. P3H4 and FKBP10 loss resulted in unstable collagen with reduced extracellular cross-linking due to decreased lysyl hydroxylation by affecting LH1 and LH2 activity, respectively (Duran et al., 2017b; Onursal et al., 2021). The cis-trans isomerization of proline residues, one of the rate-limiting processes in the formation of procollagen into triple helices, is promoted by rER localized peptidyl-prolyl isomerases including FKBP10 (Ishikawa & Bächinger, 2013a, 2014).

Interestingly, unpublished data from our laboratory show that FKBP10 (Claudia A. Staab-Weijnitz et al., 2015a) deficiency resulted in decreased mRNA levels of P3H4 in phLFs, indicating FKBP10 as a potential indirect modulator of lysine hydroxylation of helical regions by LH1 and telopeptide regions by LH2. FKBP10 may indirectly affect LH1 activity in addition to LH2 activity.

An anti-fibrotic therapeutic approach based on inhibiting the self-assembly of collagen molecules into fibrils has previously been proposed (Chung et al., 2008). This concept is supported by the discovery that both potent IPF drugs function on this level. Nintedanib and Pirfenidone function on critical regulatory levels in collagen synthesis and processing in addition to dose-dependently delaying the type I collagen fibril formation in IPF fibroblasts. Importantly, collagen I fibril synthesis was inhibited by both drugs, and this led to a decrease in collagen fibril bundles and an alteration in their appearance. Both drugs reduced collagen V expression, which is essential for the development of extracellular fibrillogenesis. Therefore, these findings support the concept of targeting collagen synthesis and extracellular fibril formation is a promising therapeutic strategy for IPF treatment (Knüppel et al., 2017).

Prolyl-3-hydroxylase family member 4 (P3H4), which contributes to the production of collagen and deficiency of which induces connective tissue defects due to decreased collagen lysyl hydroxylation by affecting LH1 activity, can be a promising drug target for limiting this positive feedback mechanism. The role of P3H4 in this context and its potential as a therapeutic target, however, is unknown.

1.3.4 FK506 binding proteins (FKBPs) and FKBP10

Cyclophilins and FKBPs are representatives of one the rER-associated proteins that have peptidyl-prolyl cis-trans isomerase activity (Gruenwald et al., 2014). FK506 binding proteins (FKBPs) are intracellular proteins that function as peptidyl-prolyl-isomerases (PPIs), catalyzing the *cis*/*trans* isomerization of proline, and are participated in several cellular processes such as receptor signaling and protein folding (Kang et al., 2008; Tong & Jiang, 2015). FKBPs are molecular chaperones that belong to the immunophilin family and are known to bind to FK506 (tacrolimus), an immunosuppressive drug that inhibits cis/trans isomerase (PPIase) activity (Ghartey-Kwansah et al., 2018; Kang et al., 2008). Despite the presence of a PPIase domain, not all members of the FKBP family have PPIase activity or can bind to FK506. Nevertheless, the PPI domain seems to be required for their function (Tong & Jiang, 2015).

In addition to PPIase domain, the tetratricopeptide repeat receptor (TPR) domain has been identified in larger molecular weight FKBPs involved in transcription and protein transportation (Ghartey-Kwansah et al., 2018).

The smallest member of the FKBPs is FKBP12, a peptide of 108 amino acids that has the essential PPIase sequence, whereas larger FKBPs are identified by comparing their sequences to FKBP12 and are composed of functionally independent domains (Ghartey-Kwansah et al., 2018; Tong & Jiang, 2015).

1.3.4.1 FKBP10

FKBP10 (FKBP65), a large member of the FKBPs, is an ER localized PPIase consisting of four PPIase domains **(Figure 9)** (Tong & Jiang, 2015).

FKBP10 functions as a collagen chaperone, which is critical for the maturation and stabilization of collagen. It regulates the folding of collagen and interacts with tropoelastin, both of which are proline-rich proteins in the ECM of tissue (Ishikawa et al., 2008; Lietman et al., 2014; Tong & Jiang, 2015). Following ER stress, FKBP10 is degraded together with the Ca^{2+} release from ER. The stability of FKBP10 is controlled by its EF-hand Ca^{2+} binding domain (Tong & Jiang, 2015).

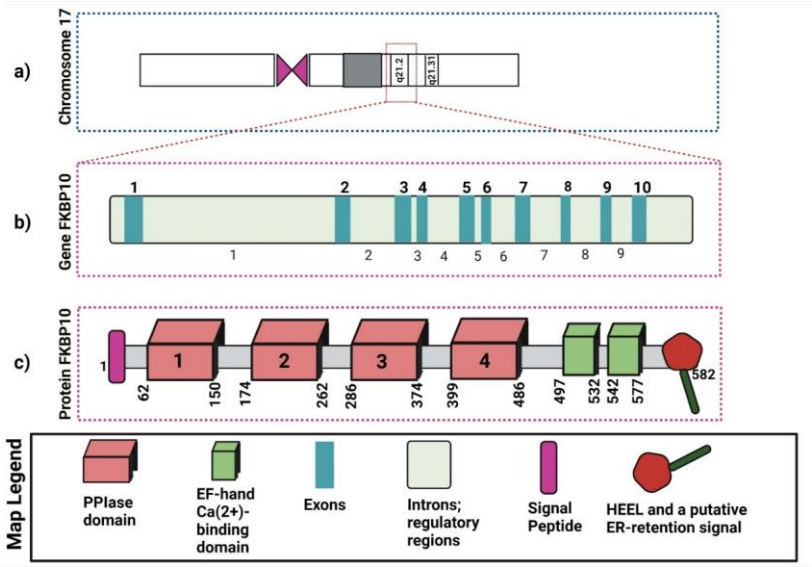

Figure 9: The FKBP10 protein is shown graphically as containing four PPIase domains, a signal peptide, an EF/Hand binding domain, a HEEL domain, and a potential ER-retention sequence. a) Location of the *FKBP10* gene on a chromosome. **b)** Exonic and intronic domains of the gene *FKBP10.* **c)** Encoded protein FKBP10 (the numbers below show where the amino acids are located in different protein domains). Figure created using BioRender (https://biorender.com/) and adapted from (D'Arrigo et al., 2016; Umair et al., 2016).

FKBP10 mutations have been linked to diseases that affect collagen such as recessive *osteogenesis imperfecta*, a genetic disorder of connective tissue characterized by alteration in the synthesis and type I collagen PTM and bone fragility and (Gruenwald et al., 2014; Kelley et al., 2011; Lietman et al., 2014, 2017). FKBP10 null mouse embryos are postnatally lethal and have been shown to decreased cross-linking of collagen in calvarial bone (Lietman et al., 2014). FKBP10 has been identified to modulate collagen LH2 activity and be critical for the activity of lysyl hydroxylase (Barnes et al., 2012; Y. Chen et al., 2017). The quantity and stability of the extracellular collagen cross-links produced by LOX family enzymes are thus affected by FKBP10 indirectly through the formation of collagen hydroxylysines (Duran et al., 2017b).

FKBP10 inhibits the type I collagen fibrils formation *in vitro*, confirming the concept that FKBP10 interacts with triple helical collagen, and acts as a collagen chaperone (Ishikawa et al., 2008; Tong & Jiang, 2015). FKBP10 also interacts

with collagen VI, and its deficiency decreases phLFs migration mainly *via* inhibiting collagen VI synthesis (Knüppel et al., 2018a). Moreover, silencing FKBP10 inhibited total collagen secretion with efficiency comparable to Nintedanib (Claudia A. Staab-Weijnitz et al., 2015a). FKBP10 has been considered as a novel therapeutic target for IPF (Claudia A. Staab-Weijnitz et al., 2015b).

1.3.5 Prolyl 3-hydroxylase family member 4 (P3H4)

P3H4 (also known as SC65 or LEPREL4) was initially discovered to be a protein linked to the synaptonemal complex (SC), an important formation that involves the matching of homologous chromosomes during the initial meiotic prophase. However, while P3H4 knockout mice were fertile, most mice with essential synaptonemal complex components were infertile, and studies have identified additional functions for P3H4. P3H4 and its mutations are linked to human disease, and collagen alterations seem to be the primary underlying cause (Heard et al., 2016a; Zimmerman et al., 2018).

P3H4 is a non-enzymatic protein from the rER-associated protein family, known as Leprecans (Leucine Proline-Enriched Proteoglycans) or family of prolyl-3-hydroxylases, which includes CRTAP, P3H1, P3H2, P3H3, and P3H4 (Gruenwald et al., 2014; Heard et al., 2016b; W.-K. Yu et al., 2022).

Prolyl 3-hydroxylase enzymes P3H3, P3H2, and P3H1/Leprecan contain a carboxyl-terminal domain that corresponds to the 2-oxo-glutarate, Fe(II)- and ascorbate- dependent dioxygenase domains. These enzymes can hydroxylate particular proline residues in the triple helical domain of fibrillar collagen. Although CRTAP and P3H4 lack the enzymatic domain, their N-terminal regions have similarities to those of the P3Hs, such as the existence of the tetratricopeptide repeat (TPR) domain, which is presumed to be the protein-protein interaction domain. There are two CXXXC sequences between two tetratricopeptide repeat domains, and this sub-domain appears twice in the amino-terminal domain. This domain's function, however, is unknown **(Figure 10)** (Gruenwald et al., 2014; Heard et al., 2016b; Ishikawa et al., 2017; Ishikawa & Bächinger, 2013a; M. Zimmerman et al., 2018). Understanding the function of these motifs may help to better understand the function of P3H4 (Ishikawa & Bächinger, 2013b).

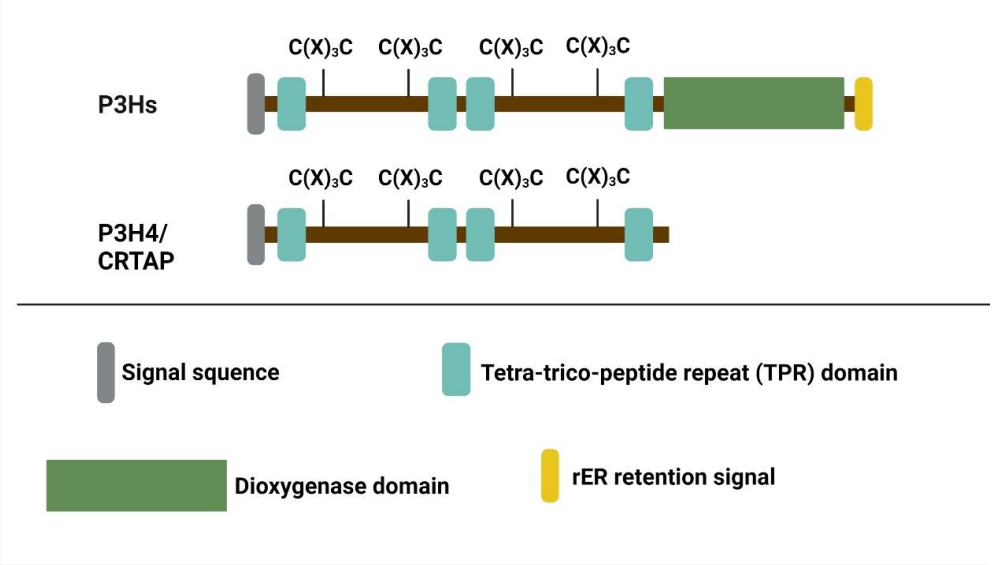

Figure 10: Schematic representation of the P3Hs structures. The domain structures of P3Hs and P3H4/CRTAP are shown. Figure *created using* BioRender (https://biorender.com/) and *adapted from* (Ishikawa & Bächinger, 2013b)

In the ER, P3H4 interacts with LH1 and P3H3 in the ER, where they form a stable complex (Hao et al., 2020; M. Zimmerman et al., 2018). P3H4 is an essential component of this ER-localized complex that facilitates the activity of LH1 during collagen biosynthesis at helical region cross-linking sites, likely through interactions with the enzymes and/or PPBI **(Figure 11)** (Hao et al., 2020).

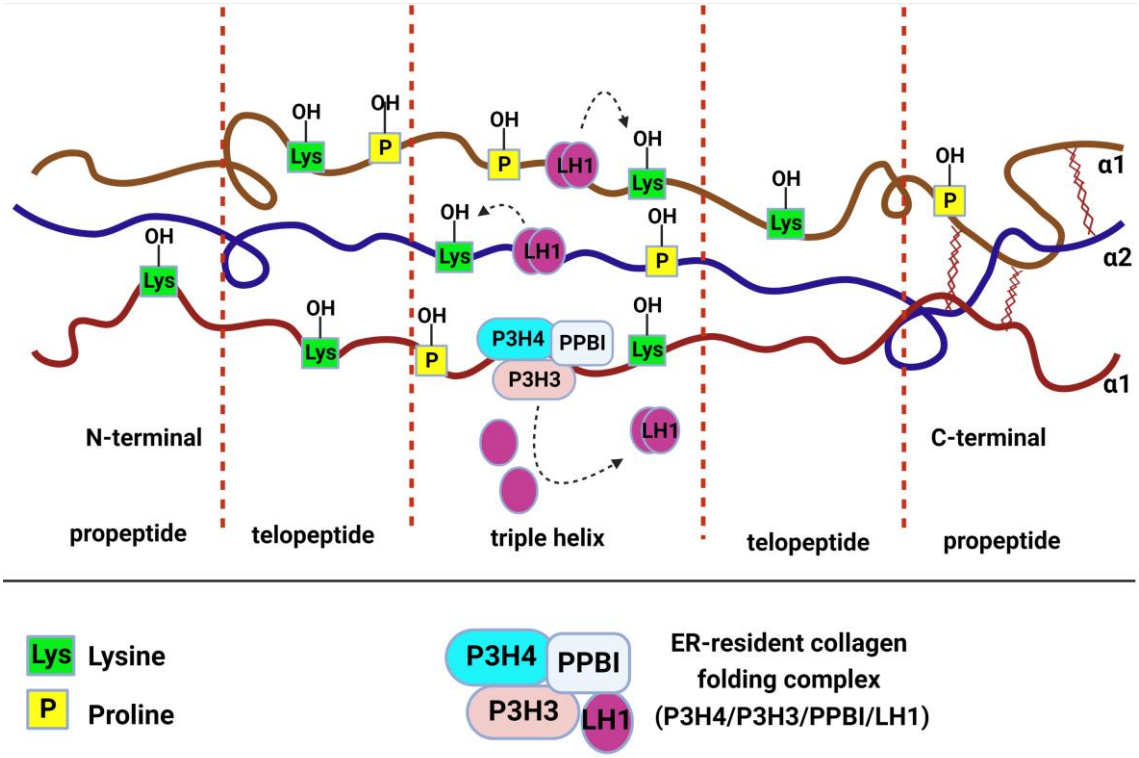

Figure 11: Schematic representation of 5-hydroxylation of lysine residues in the fibrillar collagen helical region. LH1 dimerization is driven by the P3H4/P3H3/PPBI complex in the helical domain of the α-chains. Figure created using BioRender (https://biorender.com/) and modified from (Gjaltema & Bank, 2017; Heard et al., 2016a)

In the mouse model, P3H4 deficiency induced ER complex instability, altered collagen lysine hydroxylation and cross-linking, and disrupted collagen fibrillogenesis in the ECM, which led to major connective tissue disorders such as skin fragility and low bone mass in osteoblasts or fibroblasts (Heard et al., 2016b). However, prolyl 3-hydroxylation was unaffected. The altered collagen cross-linking chemistry caused by all of these mutations suggests that the lysyl hydroxylation machinery and the prolyl 3-hydroxylation complex interact in the ER(Hudson et al., 2017a). The significant decrease in lysine hydroxylation in triple helical collagen detected by mass spectrometry implies that P3H4 protein is essential for LH1 activity, however, not for LH2 (Heard et al., 2016a; Zimmerman et al., 2018). LH1 can only function as a dimer, therefore either the P3H4/P3H3/PPBI complex as a trimeric structure or the P3H4 helps LH1 dimerize, as was previously shown for FKBP10 in LH2 dimerization (Gjaltema & Bank, 2017; Heard et al., 2016a).

Mouse cartilage, bone, and skin showed high levels of *P3h4* expression, whereas brain and kidney and a few other tissues showed lower levels (Heard et al., 2016a; M. Zimmerman et al., 2018). P3H4 was found to be an autoantigen in interstitial cystitis (Fang et al., 2022; Hao et al., 2020). P3H4 is associated with development and poor prognosis of a range of cancers, such as lung and bladder cancer (Fang et al., 2022; Hao et al., 2020; Li et al., 2018; J. Zhang et al., 2022). Based on studies into the molecular and clinical functions of P3H4 in LUAD, it was suggested that P3H4 may enhance the progression of LUAD by altering pathways related to the tumor microenvironment (X. Jin et al., 2021). Thus, P3H4 is implicated in a variety of pathological and physiological processes, including connective tissue abnormalities (Fang et al., 2022; Hao et al., 2020; Li et al., 2018). However, the function and regulation of P3H4 in lung fibrosis are unknown.

As previously mentioned, FKBP10, a collagen chaperone, has been considered as a therapeutic drug target for IPF (Claudia A. Staab-Weijnitz et al., 2015a). Interestingly, the gene encoding P3H4, is located on mouse chromosome 11 and human chromosome 17 directly adjacent to *FKBP10*, and both genes are controlled by the same bidirectional promoter in opposite directions and share common regulatory elements (**Figure 12**) (Heard et al., 2016b).

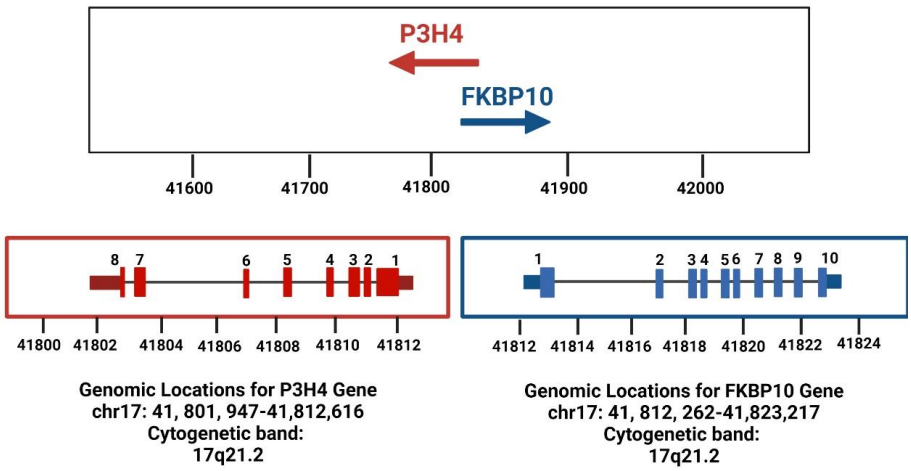

Figure 12: Genomic localization of FKBP10 and P3H4 on human chromosome 17. The gene encoding P3H4 is located directly adjacent to *FKBP10* and both genes are controlled by the same bidirectional promoter in opposite directions. *FKBP10* gene is located less than 900bp from *P3H4* exon 1. *Figure generated using BioRender* (https://biorender.com/)

2. Aims of this thesis

Currently, the only FDA-approved drugs for IPF treatment are Pirfenidone and Nintedanib. These two treatments only reduce disease progression, but do not halt let alone revert the pathological lung remodeling. Therefore, there is an urgent need for IPF-specific antifibrotic therapeutic targets. Targeting the collagen biosynthesis pathway has been put forward as a potential strategy in this context. For instance, FKBP10 has previously been proposed as a novel drug target for IPF treatment (Claudia A. Staab-Weijnitz et al., 2015a). Similar to FKBP10, also upregulation of P3H1 (encoded by *LEPRE1*) has been observed in human lung fibrosis (Schiller et al., 2017). Finally, P3H4 and FKBP10 share regulatory elements in a bidirectional promoter, which suggested some kind of functional overlap between FKBP10 and P3H4. However, the function and regulation of P3H4 in lung fibrosis and effects of P3H1 on components of the collagen biosynthesis pathway had not been assessed.

Hence, we hypothesized that P3H4 localized to ECM-producing myofibroblasts in lung fibrosis and that targeting P3H4 attenuates profibrotic gene expression, collagen biosynthesis, and collagen secretion. We furthermore hypothesized that targeting P3H1 equally blocks collagen biosynthesis.

Therefore, this study aimed to decipher the function and regulation of P3H4 in lung fibrosis, as well as the effect of P3H1 deficiency on type I collagen PTMs and the expression of proteins involved in collagen biosynthesis. First, following our discovery of downregulation of P3H4 as a result of FKBP10 deficiency in mouse lungs, I sought to examine this effect in phLFs. Next, the expression level of P3H4 was investigated in an *in vitro* lung fibrosis model, as well as in fibrotic lung sections from an *in vivo* mouse lung fibrosis model and from IPF patients. In addition, the effect of P3H4 deficiency on the FKBP10 expression, collagen I and profibrotic markers was further examined in phLFs. Finally, we performed amino acid analysis to detect the level of prolyl and lysyl hydroxylation of collagen isolated from P3H1 null mice tail tendon, as well as a gene expression analysis of components of the collagen biosynthetic machinery in P3H1 null tenocytes.

3. Results

3.1 Chapter 1: Expression profiling and functional analysis of P3H4 as a novel modulator of lung fibrosis

3.1.1 Knockout of FKBP10 downregulates the expression of *P3H4* in mouse lung

We received mouse embryonic lungs from our collaborators Caressa D. Lietman and Brendan Lee of Baylor College of Medicine, Texas, Houston, USA. The mouse embryonic lungs were harvested from FKBP10 heterozygote, homozygote, and WT mice at embryonic stage 18.5 (E18.5). We first performed transcriptomic analysis to identify differentially expressed genes using embryonic lungs from global FKBP10 knockout mice and littermate controls. Transcriptomic data, assessing the expression levels of over 10,000 genes, revealed that, aside from *Fkbp10*, only *P3h4* expression was decreased in FKBP10 knockout mice ($p<0.1$) (**Figure 13A**). Knockout of *Fkbp10* and downregulation of *P3h4* by knockout of FKBP10 were validated at the transcript level by qRT-PCR in embryonic mouse lungs. As shown in **Figure 13B**, qRT-PCR analysis confirmed the successful gene knockout of *Fkbp10* and significantly decreased expression of *P3h4* in FKBP10 knockout embryonic mouse lungs.

Mass spectrometry-based proteomic analysis was then performed to identify differentially expressed proteins using the same embryonic lungs from global FKBP10 knockout mice and littermate controls. In these experiments, protein quantification was performed by adding the abundances of each distinct peptide (identification based on 2 unique peptides) per protein following total protein normalization. The normalized protein abundances obtained have been used to calculate fold-changes between conditions and statistical parameters using the Student's t-test. We identified the top 10 significantly downregulated proteins from over 4500 detected proteins based on a fold change of more than 1.5. Proteomic analysis indicated that P3H4 is the most downregulated protein by knockout of FKBP10. Moreover, we observed that YAP1 (Yes-associated protein 1), a key effector in the Hippo pathway, and P3H3 were also significantly downregulated

in FKBP10-deficient mice (**Figure 13C**). Western blot (WB) analysis further confirmed that P3H4 was significantly decreased in FKBP10 knockout embryonic mouse lungs at the protein level. Quantitative densitometric analysis showing normalized band intensity of P3H4/β-actin in FKBP10 homozygote, WT, and heterozygote mice (**Figure 13D**).

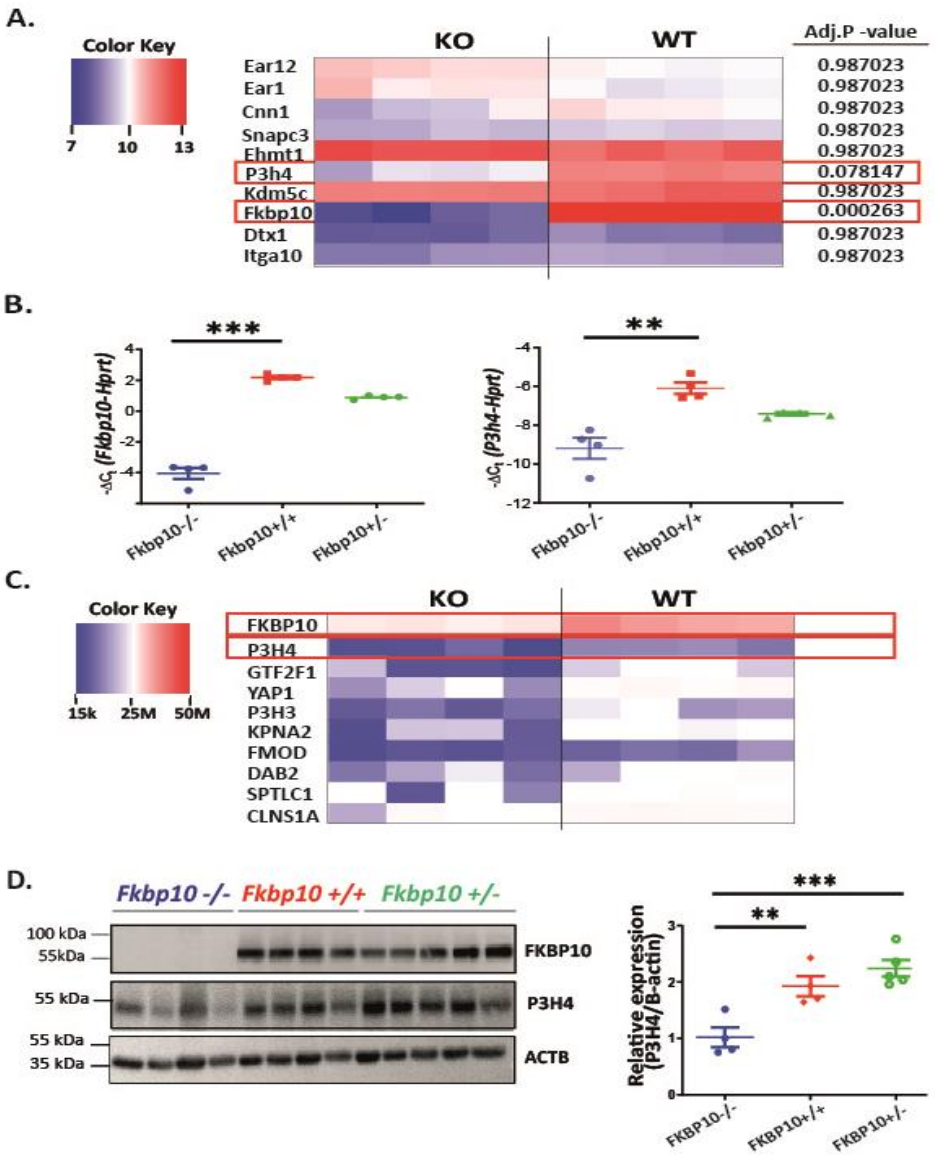

Figure 13: Down-regulation of P3H4 in FKBP10 knockout mouse embryonic lung (A) Heat map shows the top ten differently expressed genes between wild-type (WT) and FKBP10 knock-out mice (n=4);Transcript abundances are depicted according to the given color code from low abundance (blue) to high abundance (red) and indicate specific downregulation of P3H4 in the global FKBP10 knockout mice **(B)** qRT-PCR analysis of FKBP10 knockout mouse lung fibroblasts confirms successful knockout FKBP10 and significant downregulation of P3H4 with the knockout of FKBP10. *Hprt* was used as a housekeeper gene **(C)** Heat map shows the top ten differentially expressed proteins between FKBP10 knockout (n=4) and WT FKBP10 (n=4); Protein abundances are depicted according to the given color code from low abundance (blue) to high abundance (red) and show that, besides FKBP10, several proteins are differentially expressed in the FKBP10 knockout mice, but P3H4 is the most downregulated protein. **(D)** WB analysis of lung fibroblasts confirmed downregulation of P3H4 in FKBP10 knockout mouse lung fibroblasts. Quantitative densitometric analysis showing P3H4/ACTB normalized band intensity in FKBP10 homozygote, WT, and heterozygote mice (Fold Change>1.5, $p < 0.05$). Data shown are mean ± SEM. A paired two-tailed t-test was used for statistical analysis. **P<0.05, **P<0.01, ***P < 0.001.*

3.1.2 Deficiency of FKBP10 reduces the P3H4 expression in phLFs

Having identified P3H4 to be the most significantly downregulated gene in FKBP10 knockout mice, it was of interest to assess whether FKBP10 deficiency affected *P3H4* expression also in human samples. To investigate this, FKBP10 knockdown using siRNA was performed in phLFs. Following knockdown of FKBP10, we examined the gene expression of *P3H4* in phLFs. Strikingly, P3H4 mRNA expression was significantly reduced with knockdown of FKBP10 in the absence and presence of TGF-β1 (2 ng/mL). Moreover, qRT-PCR results showed significant upregulation of *P3H4* with TGF-β1 treatment after 48 hours in phLFs. Importantly, since TGF-β1 is the major pro-fibrotic cytokine, this finding shows the upregulation of P3H4 in TGF-β1 induced lung fibrosis (**Figure 14A**). The efficient FKBP10 knockdown in phLFs resulted in significant downregulation of P3H4 protein levels in absence of TGF-β1. Interestingly, the effect of FKBP10 silencing on P3H4 expression in protein level was partly counteracted following TGF-β1 treatment(48h). Densitometric quantification of FKBP10 showed successful knockdown of FKBP10 in both the presence and absence of TGF-β1. Consistent with WB analysis, downregulation of P3H4 following FKBP10 knockdown was less pronounced, not clearly after treatment with TGF-β1 as in absence of TGF-β1 in phLFs (**Figures 14B and 14C**). We further confirmed the knockdown of FKBP10 in phLF and the downregulation of P3H4 with FKBP10 knockdown by immunofluorescence staining of P3H4 and FKBP10 in phLFs in presence and absence TGF-β1.

P3H4 was detected in the nucleus and cytoplasm of phLFs. FKBP10 immunofluorescence staining in phLFs also revealed that FKBP10 was mainly detected in ER. Consistent with WB analysis, downregulation of P3H4 following FKBP10 knockdown was not clearly after treatment with TGF-β1 as observed with the absence of TGF-β1 **(Figure 14D).**

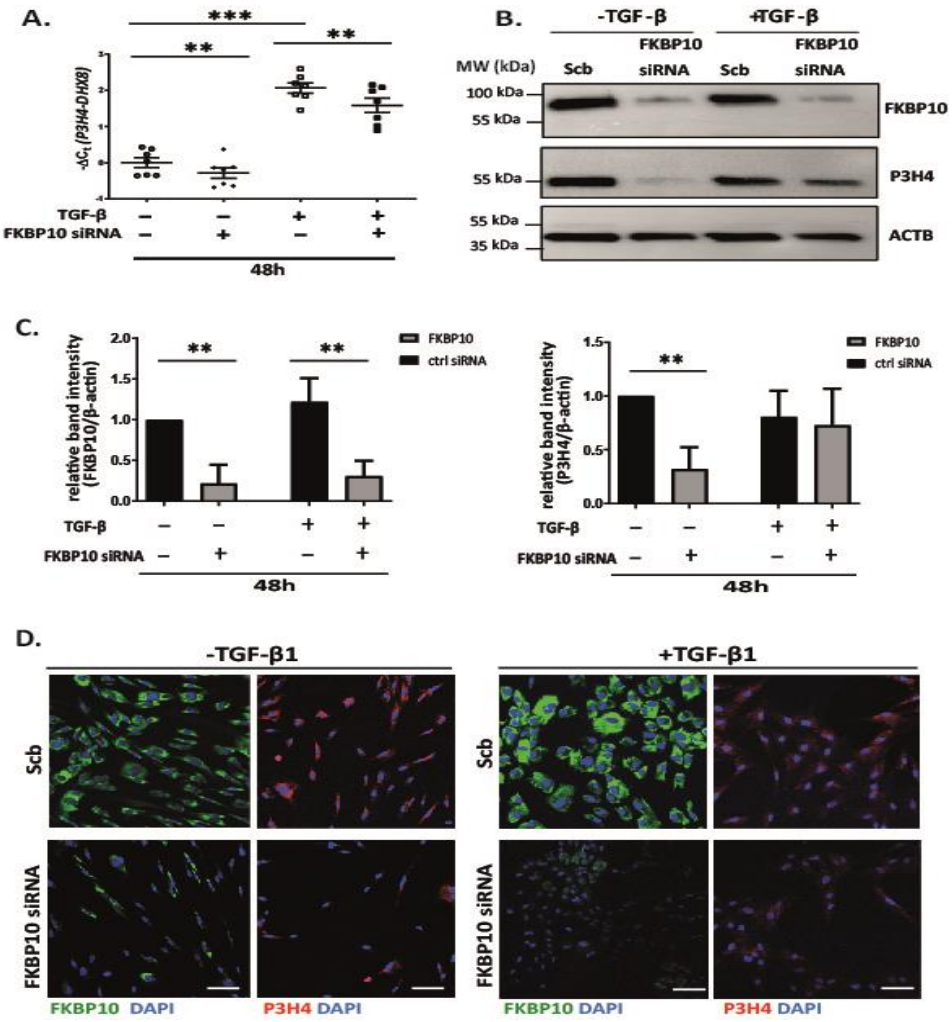

Figure 14: Downregulation of P3H4 with FKBP10 knockdown in phLFs. (A) qRT-PCR analysis of transcript levels of P3H4 after knockdown of FKBP10 in combination with TGF-β1 treatment (48h). **(B)** Effects of FKBP10 silencing using siRNA in phLFs with TGF- β1 treatment (48h). A representative WB analysis for the determination of FKBP10 and P3H4 is shown. WB analysis of lung fibroblasts showed down-regulation of P3H4 with FKBP10 knockdown in phLFs. **(C)** Densitometric quantification of FKBP10 and P3H4 protein levels in the absence and presence of TGF-β1 (48h). As a loading control, ACTB was used. Data presented as mean ± SEM and are based on four(n=4) independent experiments. The statistical analysis of FKBP10 siRNA vs. scrambled siRNA control was carried out using the paired two-tailed t-test. ctrl = control.**,** **P< 0.05*, ***P< 0.01, ***P < 0.001.* **(D)** Immunofluorescence staining of FKBP10 and P3H4 in phLFs confirms downregulation of P3H4 with knockdown of FKBP10 in absence and presence of TGF-β1 (48h) (n=1). The immunostaining for FKBP10 is shown in ***green***, and for P3H4 in ***red.*** 4′,6-diamidino-2-phenylindole (DAPI) staining is shown in ***blue***. Images were obtained by confocal microscopy (20X). Scale bar: 50 µm.

3.1.3 *P3H4* is expressed in interstitial fibroblasts and colocalizes with α-SMA in bleomycin-induced lung fibrosis in mice

As we showed significant upregulation of P3H4 on transcript level in the *in vitro* model of TGF-β1 (2 ng/ml) induced lung fibrosis, we next studied *P3h4* expression in the bleomycin-induced lung fibrosis, which is the best-studied and the most commonly used mouse model of lung fibrosis. Immunofluorescent stainings of formalin-fixed paraffin-embedded (FFPE) from human lung tissue sections, mouse lung tissue sections, both from PBS-instilled control mice and bleomycin-treated mice (day 14), were performed to characterize *P3h4* expression. The specificity of the primary antibody was examined using a negative control that was followed the identical staining protocol but without the addition of the primary antibody. As shown, expression of *P3h4* was determined to be increased in mouse fibrotic lungs with low expression of *P3h4* in PBS–instilled control mouse lungs **(Figure 15A).** Furthermore, IPF, as explained previously, is characterized by scar tissue of the lung induced by an accumulation of α-SMA positive myofibroblasts in fibrotic foci. *P3h4* expression in fibrotic regions of mouse lungs was therefore investigated using immunofluorescence co-staining of P3H4 and α-SMA on FFPE sections of bleomycin-treated mouse lungs (day 14) and PBS-instilled mouse lungs. α-SMA levels were found to be increased in mouse fibrotic lungs, but not in PBS-instilled control mice lungs. P3H4 was commonly detected in interstitial fibroblasts, including α-SMA-positive myofibroblasts in fibrotic mouse lung sections compared to PBS-instilled lung sections **(Figure 15B).**

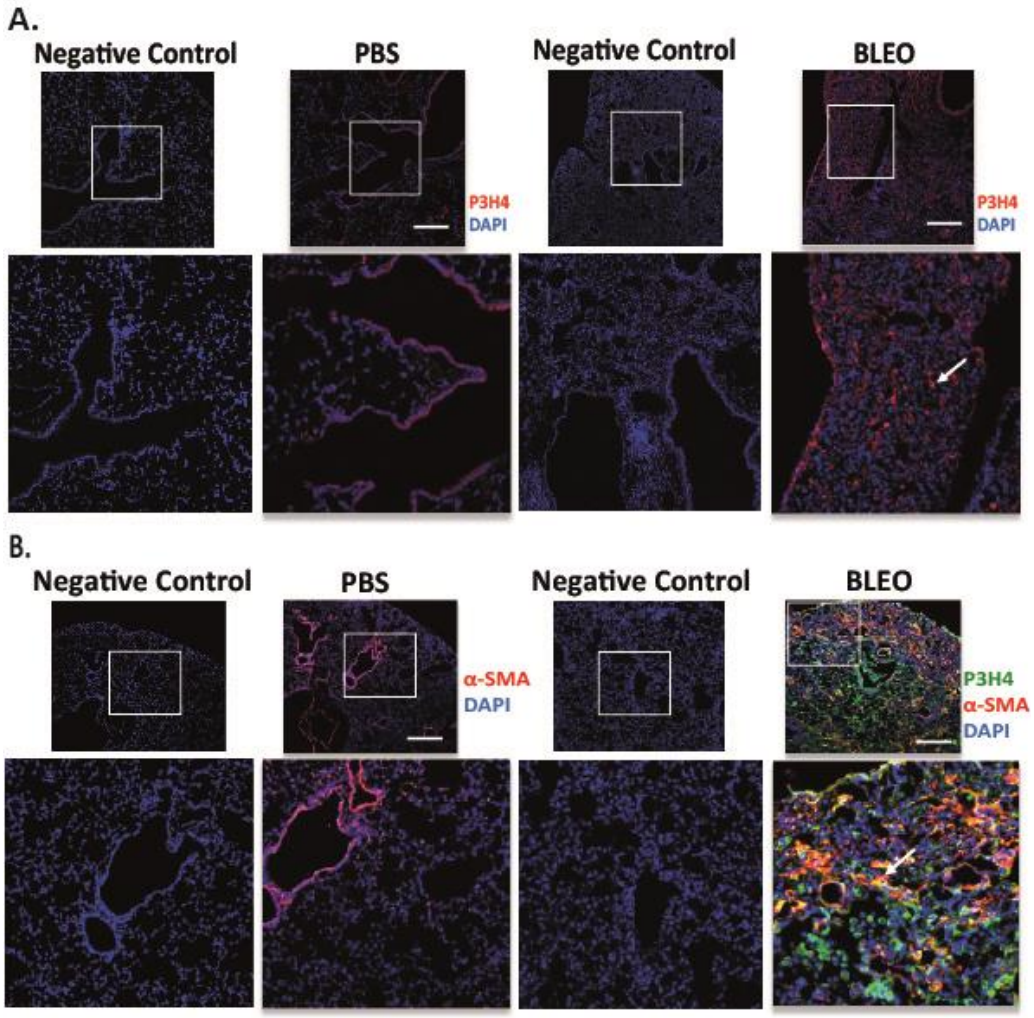

Figure 15: Expression of *P3h4* in interstitial fibroblasts, together with myofibroblasts and colocalization with α-SMA in bleomycin-treated mouse fibrotic tissue sections. Immunofluorescent stainings of FFPE lung tissue sections from PBS-instilled control mice and bleomycin-treated mice at day 14 following bleomycin administration. **A)** Representative images from immunofluorescence staining of P3H4 in mouse lung tissue sections from PBS and bleomycin-treated mice at day 14 (n=3). The white square represents the area of interest, which was then magnified at the bottom of each image. Examples of *P3h4* expression are shown by arrows in the area of interest. P3H4 immunostaining is shown in ***red***. **B)** Representative images of P3H4 and α-SMA immunofluorescence staining in FFPE lung tissue sections from PBS-instilled and bleomycin-treated mouse lungs. An example of colocalization of P3H4 and α-SMA in fibrotic region of the bleomycin-induced mouse lungs is depicted by a white arrow. Representative P3H4 immunostaining is shown in ***green*****,** α-SMA in ***red***. The white square represents the area of interest, which was then magnified at the bottom of each image. Negative controls were carried out by using the identical staining protocol without adding the primary antibody. Representative DAPI immunostaining is shown in ***blue***. Images were acquired by confocal microscopy (20X). Scale bar: 50 µm.

3.1.4 P3H4 colocalizes and interacts with FKBP10 in bleomycin-induced lung fibrosis in mice

We then evaluated the P3H4 and FKBP10 localization in the bleomycin-induced pulmonary fibrosis in mice. For that, immunofluorescence staining of FFPE lung sections from PBS-instilled and bleomycin-treated (at day 14) mouse lungs was performed. P3H4 and FKBP10 colocalized in bleomycin-treated fibrotic mouse lungs mainly in the fibrotic regions. Furthermore, P3H4 was found to be expressed alone in some regions without colocalization with FKBP10 **(Figure 16A).** Furthermore, we confirm direct interaction and colocalization of P3H4 and FKBP10 by performing proximity ligation assay (PLA) in FFPE tissue section from PBS-instilled and bleomycin-treated mouse lungs. Images from PLA showed *in situ* FKBP10 and P3H4 interaction localization in fibrotic mouse lungs. PLA signal (red dots) was abundant in fibrotic mouse lungs but not in PBS-instilled controls lungs **(Figure 16B).**

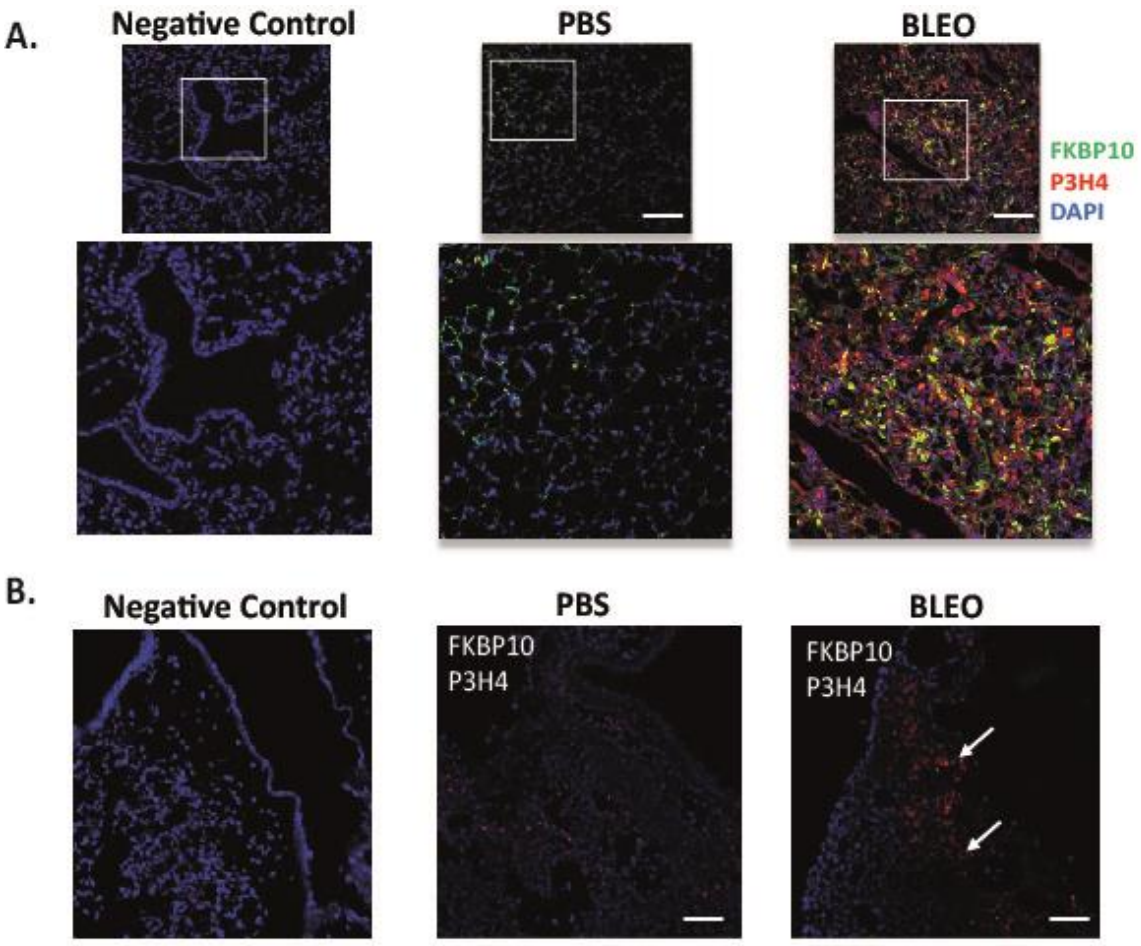

Figure 16: *In situ* localization of FKBP10-P3H4 interaction in bleomycin-treated mouse fibrotic tissue sections. A) Immunofluorescent stainings of FFPE sections from bleomycin-treated fibrotic mouse lungs at day 14 upon bleomycin instillation and control PBS-instilled mouse lungs. FKBP10 immunostaining is shown in ***green***, and P3H4 in ***red***. Examples of colocalization of P3H4 and FKBP10 in fibrotic mouse lung sections are depicted by the white arrow in the region of interest (n=3). The white square represents the area of interest, which was then magnified at the bottom of each image. **B)** The images represent *in situ* localization of FKBP10 and P3H4 interaction in bleomycin-treated and PBS-instilled mouse lung tissue sections were assessed by PLA (n=1). In fibrotic mouse lung sections, white arrows indicate examples of P3H4 and FKBP10 positive interactions, which are represented by ***red*** dots. Negative controls were carried out by using the identical staining protocol without adding the primary antibody. Representative DAPI immunostaining is shown in ***blue***. Images were acquired by confocal microscopy (20X). Scale bar: 50 µm.

3.1.5 *P3H4* expression is upregulated in IPF

To evaluate the expression of P3H4 in lung fibrosis, lung tissue from 7 healthy donors and 5 IPF patients were obtained from the UGMLC Giessen Biobank, a member of the DZL platform biobanking, and the CPC-M bioArchive at Comprehensive Pneumology Center (CPC). Lung tissue from IPF patients and healthy donors were homogenized and WB analyses were performed to assess protein levels of P3H4. Normalizing P3H4 protein expression with levels of β-actin confirmed a significant increase in *P3H4* expression in the patients with IPF compared to healthy donors. Because β-actin was unequal on the WB, probably due to a biological effect of donor and IPF samples, the Ponceau S stained blot was used as loading control (Sander et al., 2019) **(Figure 17A)**. Furthermore, immunofluorescent stainings of FFPE human lung tissue sections from IPF patients and healthy donors were performed to characterize P3H4 expression. As shown, *P3H4* expression was observed to be increased in human fibrotic lungs with little expression of *P3H4* in donor lungs. Overall, *P3H4* expression in fibrotic sections was higher than expression of *P3H4* in healthy donor tissue under identical staining and imaging circumstances (**Figure 17B**).

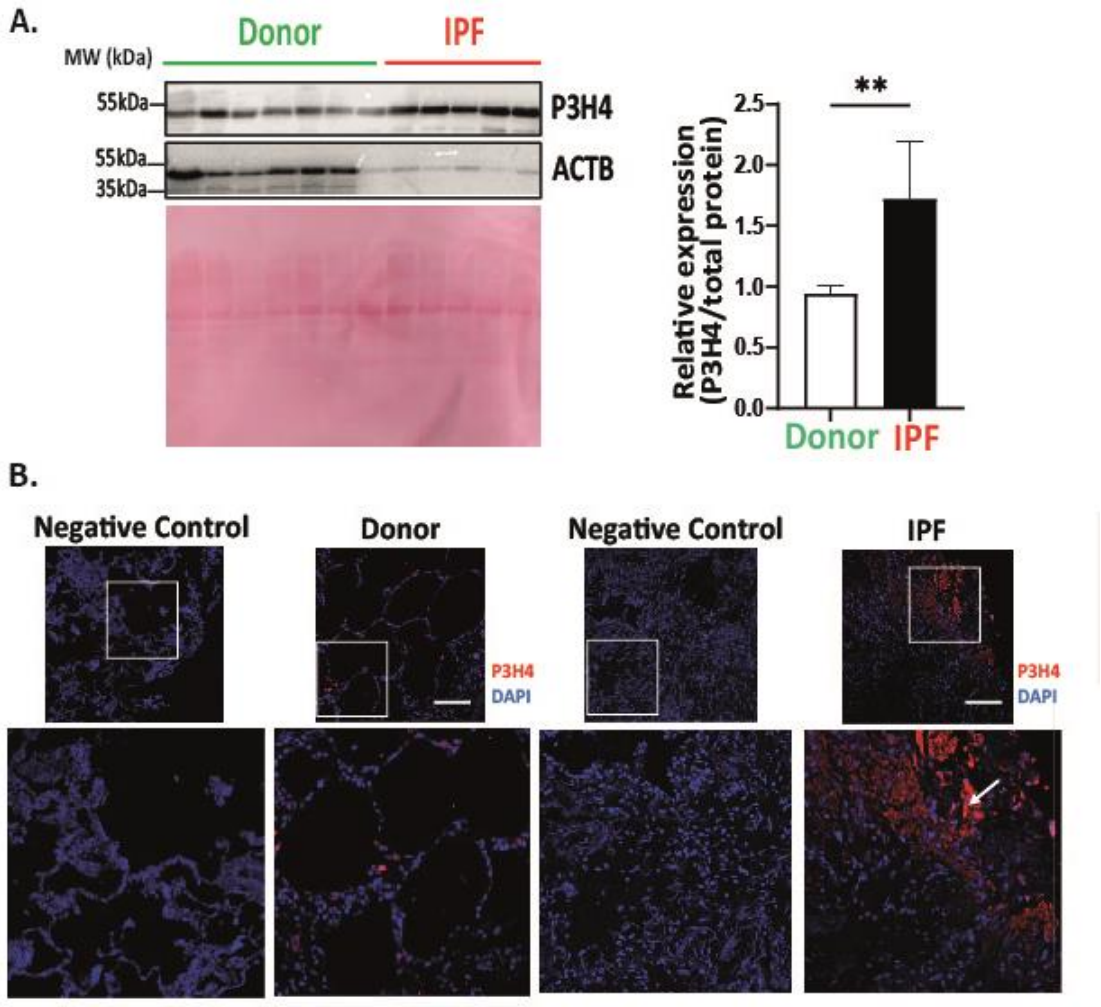

Figure 17: Expression of *P3H4* in total lung tissue homogenate and in lung tissue sections from IPF patients and donor lungs. A) WB analysis of whole lung tissue homogenate revealed an increase in P3H4 levels in IPF patients compared to donor samples, in an independent cohort. Ponceau S stained blot is shown for loading control. Quantitative densitometric analysis showing normalized band intensity of P3H4/total protein. Data presented as mean ± SEM, the Mann-Whitney test, **P,0.05, **P,0.01*. **B)** Images represent immunofluorescence staining of FFPE sections of healthy donor and human fibrotic lung tissue from patients with IPF display the *P3H4* expression(n=4). The white square represents the area of interest, which was then magnified at the bottom of each image. White arrows in the area of interest indicate examples of expression of *P3H4.* Negative controls were carried out by using the identical staining protocol without adding the primary antibody. Images were acquired by confocal microscopy. Representative DAPI immunostaining is shown in ***blue***. P3H4 immunostaining is shown in ***red***. Scale bar: 50 µm.

3.1.6 *P3H4* is expressed in interstitial fibroblasts and colocalizes with FKBP10 in IPF

Next, to investigate localization of P3H4 and FKBP10 in IPF lung tissue sections, FFPE sections from patients with IPF and healthy donors were co-stained for FKBP10 and P3H4. As reported above, in contrast to healthy donors, increased *P3H4* expression was found in the IPF FFPE tissue sections. Furthermore, colocalization of P3H4 and FKBP10 in fibrotic regions, as identified by increased FKBP10 staining, was observed in FFPE lung tissue sections from IPF patients **(Figure 18A and 18B).** Interestingly, P3H4 was also detected in epithelial cells at the surface of the fibroblast foci in FFPE lung tissue sections from IPF patients **(Figure 18B).** As shown in **Figure 18C**, immunofluorescence staining of FFPE tissue sections from IPF lung demonstrated expression of P3H4 also in interstitial macrophages and colocalization of P3H4 with FKBP10 (shown in white arrows).

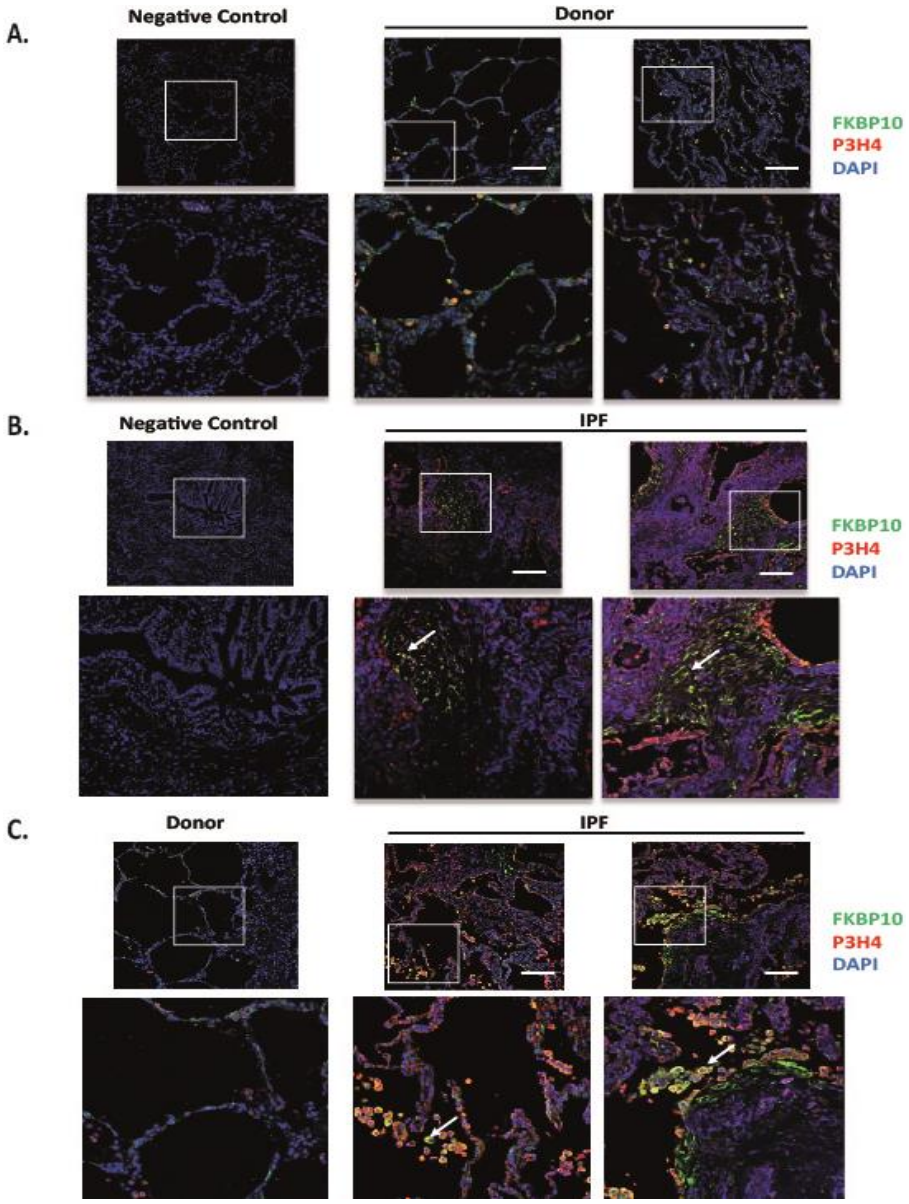

Figure 18: Expression of *P3H4* in interstitial fibroblasts, including interstitial macrophages and colocalization with FKBP10 in human fibrotic tissue sections from IPF. A) Representative immunofluorescence staining of FFPE tissue sections from healthy donor lung co-stained for FKBP10 and P3H4. **B)** Representative images of P3H4 and FKBP10 immunofluorescence double staining in lung tissue FFPE sections from patients with IPF. Examples of P3H4 and FKBP10 colocalization in human lungs with IPF are shown by white arrows in the area of interest **C)** Representative images of P3H4 and FKBP10 immunofluorescence staining in FFPE lung tissue sections from IPF patients and healthy donor shows colocalization of P3H4 and FKBP10 in interstitial macrophages (demonstrated by white arrows). The white square represents the area of interest, which was then magnified at the bottom of each image. Negative controls were carried out by using the identical staining protocol without adding the primary antibody. Representative images were chosen from four(n=4) independent experiments. The immunostaining for FKBP10 is shown in ***green***, P3H4 in ***red***, and DAPI in ***blue***. Images were acquired by confocal microscopy(20X). Scale bar: 50 µm.

3.1.7 ScRNA-seq analysis reveals *P3H4* and *FKBP10* expression in HAS1 high fibroblasts

We used a publicly accessible data set of scRNA-seq provided by Banovich and Kropski, which also includes data on the expression of *P3H4* and *FKBP10* in different cell types from 10 nonfibrotic control and 20 pulmonary fibrosis (PF) lungs (Habermann et al., 2020) (http://www.ipfcellatlas.com/). The data comprehensively defines the cell types driving fibrotic remodeling in lungs with PF. Several different mesenchymal and epithelial progenitors that contributed in the formation of the ECM in PF lungs were also discovered. Multiple previously undiscovered epithelial cell types were discovered, as well as a KRT5-/KRT17+ epithelial cell population that expressed ECM proteins, including collagen, and was significantly abundant in lungs with PF. Together with myofibroblasts, they identified multiple fibroblast phenotypes expressing pathologic ECM including $PLIN2^{+}$ fibroblasts, and $HAS1^{high}$ fibroblasts, a unique fibroblast fibroblast population that is significantly increased in lungs from patients with IPF and localizes to peripheral and subpleural regions. These findings indicate that, in addition to activated myofibroblasts, which are major producers of ECM components including collagen, other transcriptionally different fibroblast groups may be critical. Therefore, understanding the functional activities and gene expression profiles of these diverse populations may enable the discovery of new IPF treatment targets. As shown in **Figure 19A,** *P3H4* is mainly expressed in mesenchymal cells including fibroblasts, $PLIN2^{+}$ fibroblasts, myofibroblasts, mesothelial cells and $HAS1^{high}$ fibroblasts. *P3H4* is also expressed in $KRT5^{-}$/$KRT17^{+}$ epithelial cells and its expression increased in ILD. Importantly, *P3H4* is highly expressed in $HAS1^{high}$ fibroblasts, newly emerging fibroblast population in ILD. The data also shows the increased expression of *P3H4* in myofibroblasts and $MUC5AC^{high}$ epithelial cells in ILD, and, interestingly, less expression of *P3H4* in macrophages both in ILD and control. Furthermore, according to the same scRNA-seq dataset, *FKBP10* is also mainly expressed in mesenchymal cells including fibroblasts, PLIN2+ fibroblasts, smooth muscle cells, myofibroblasts, mesothelial cells and $HAS1^{high}$ fibroblasts. Most importantly, *FKBP10* is highly expressed in $HAS1^{high}$ fibroblasts in ILD. Interestingly, the data shows the expression of *FKBP10* in macrophages both in ILD and control (**Figure 19B)**.

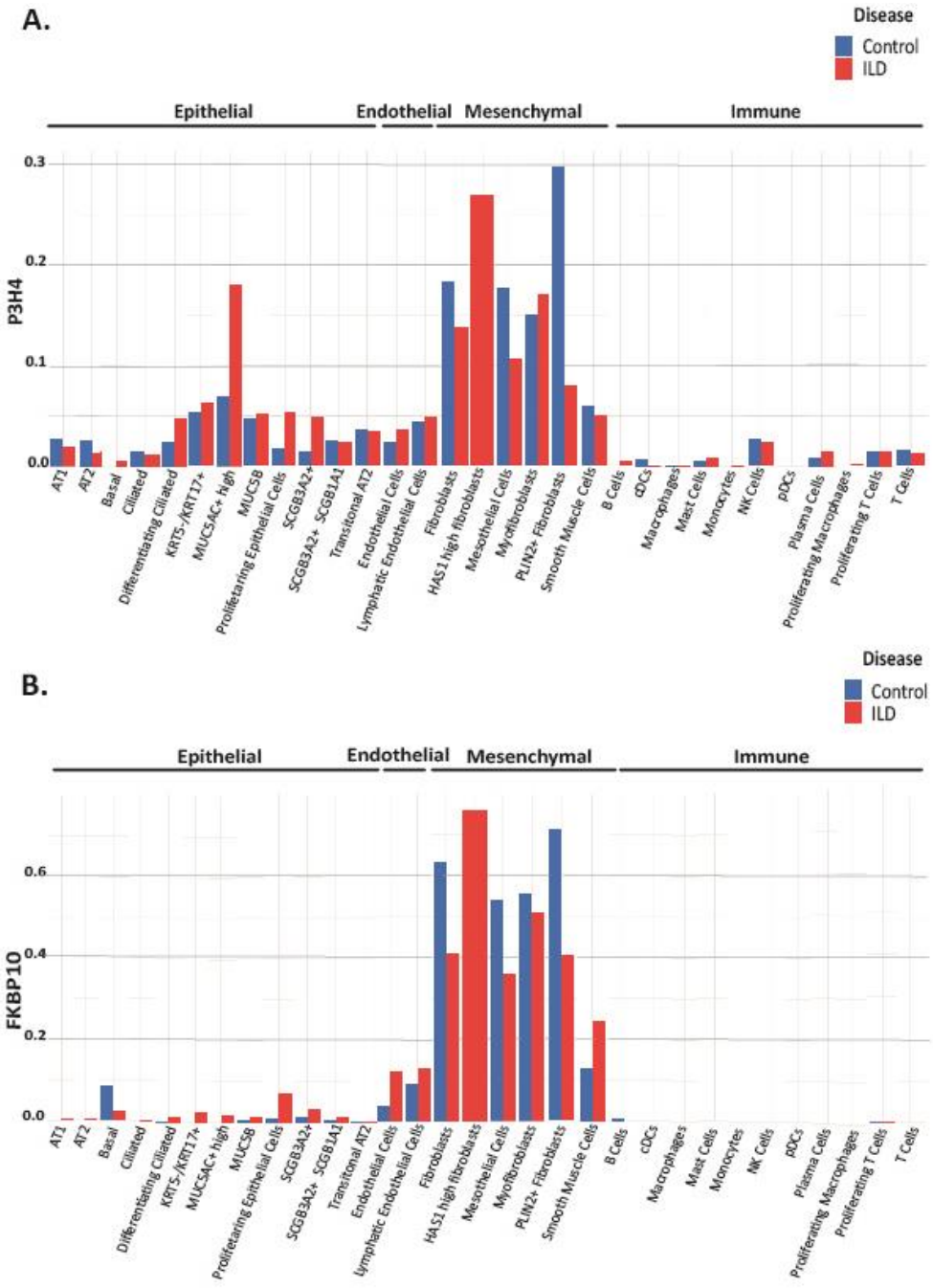

Figure 19: ScRNA-seq analysis of PF and control lung samples shows the gene expression of *P3H4* and *FKBP10* among different cell clusters. A) Gene expression of *P3H4* across different cell types in control and PF lungs. **B)** Gene expression of *FKBP10* across various cell types in control and PF lungs. Gene expression of *FKBP10* and *P3H4* has been visualized in the form of bar graph. Each bar is split by disease status; IPF and control. y-axis indicates normalized gene expression. The figure has been modified from IPF Cell atlas (http://www.ipfcellatlas.com/) using Banovich and Kropski's dataset by clustering cells into cell types such as endothelial, epithelial, mesenchymal, immune cells.

3.1.8 FKBP10 and P3H4 colocalize with HAS1 in phLFs

Based on the publicly available dataset provided by Banovich and Kropski, we further investigated the colocalization of P3H4 and FKBP10 with HAS1 in phLFs by immunofluorescence staining in the absence and presence of TGF-β1(2 ng/ml) (48h). TGF-β1 treatment strongly induced *HAS1* expression in phLFs. As shown in **Figure 20A**, HAS1 colocalized with α-SMA in some sub-population of phLFs and the expression of *HAS1* and *α-SMA* was found to be upregulated in presence of TGF-β1 with little expression in absence of TGF-β1. Next, the colocalization of P3H4 and HAS1 was assessed by immunofluorescence staining in phLFs. Images by immunofluorescence staining of phLFs showed the colocalization of P3H4 and HAS1, as well as increased expression of *HAS1* in presence of TGF-β1(**Figure 20B**). We further assessed the colocalization of FKBP10 and HAS1 by immunofluorescence staining in phLFs. Images by immunofluorescence staining of phLFs showed colocalization of FKBP10 and HAS1, as well as, as previously shown, the increased expression of *HAS1* in presence of TGF-β1 (Figure 19B). The immunofluorescence staining of phLFs performed following the identical staining protocol without adding the primary antibody served as a negative control in this experiment (**Figure 20A, 20B and 20C**).

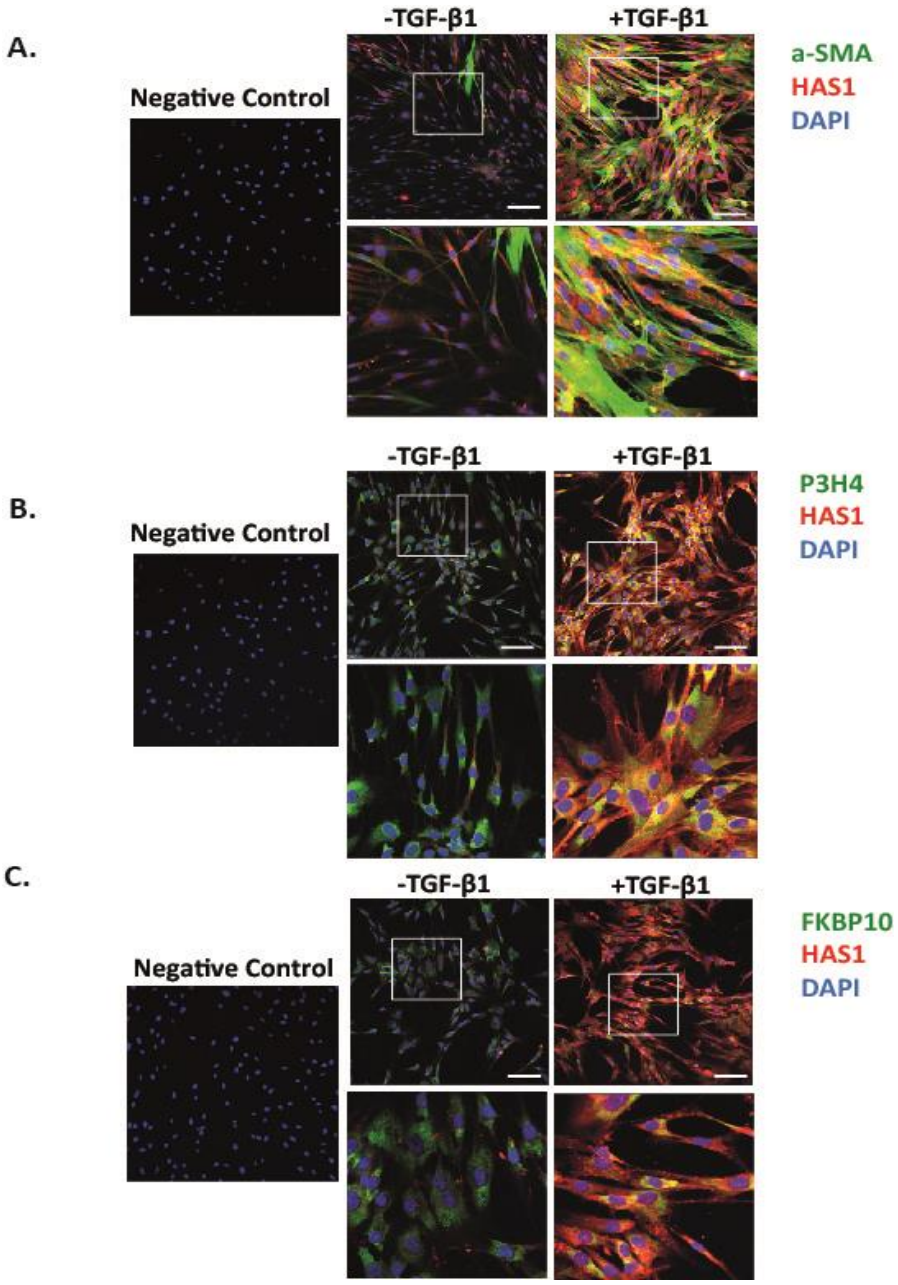

Figure 20: Colocalization of P3H4, FKBP10 and α-SMA with HAS1 in phLFs. A) Immunofluorescence staining of HAS1 and α-SMA in phLFs in the absence and presence of TGF-β1(2 ng/mL) **B)** Immunofluorescence staining of HAS1 and P3H4 in phLFs in absence and presence of TGF-β1 **C)** Immunofluorescence staining of HAS1 and FKBP10 in phLFs in absence and presence of TGF-β1 (n=1). The white square represents the area of interest, which was then magnified at the bottom of each image. Representative FKBP10, P3H4 and α-SMA immunostaining are shown in ***green***, and HAS1 in ***red***. DAPI staining is shown in ***blue***. Negative controls were carried out by using the identical staining protocol without adding the primary antibody. Images were acquired using confocal microscopy(20X). Scale bar: 50 µm.

3.1.9 P3H4 colocalizes and interacts with FKBP10 in phLFs

We further investigated the colocalization of P3H4 and FKBP10 in phLFs by immunofluorescence staining in the presence and absence of TGF-β1(2 ng/ml.) (48h). P3H4 was detected in the nucleus and cytoplasm of phLFs. It also colocalized with FKBP10, mainly in the cytoplasm. Treatment of TGF-β1 did not affect this colocalization **(Figure 21A and 21B).** Furthermore, direct interaction and colocalization of P3H4 and FKBP10 were assessed by PLA in phLFs. Images from PLA showed *in situ* localization of FKBP10 and P3H4 interaction in phLFs. Detected PLA signal for P3H4 is representing the close proximity to FKBP10. The interaction between the two proteins is indicated by red fluorescence. The previously reported positive interaction of ER protein 57 (ERp57), COL6A1 and COL6A3 with FKBP10, was used as a positive control in this experiment (Knüppel et al., 2018b). Golgin97, that has previously been shown not to interact with FKBP10, was used as a negative control **(Figure 21C).**

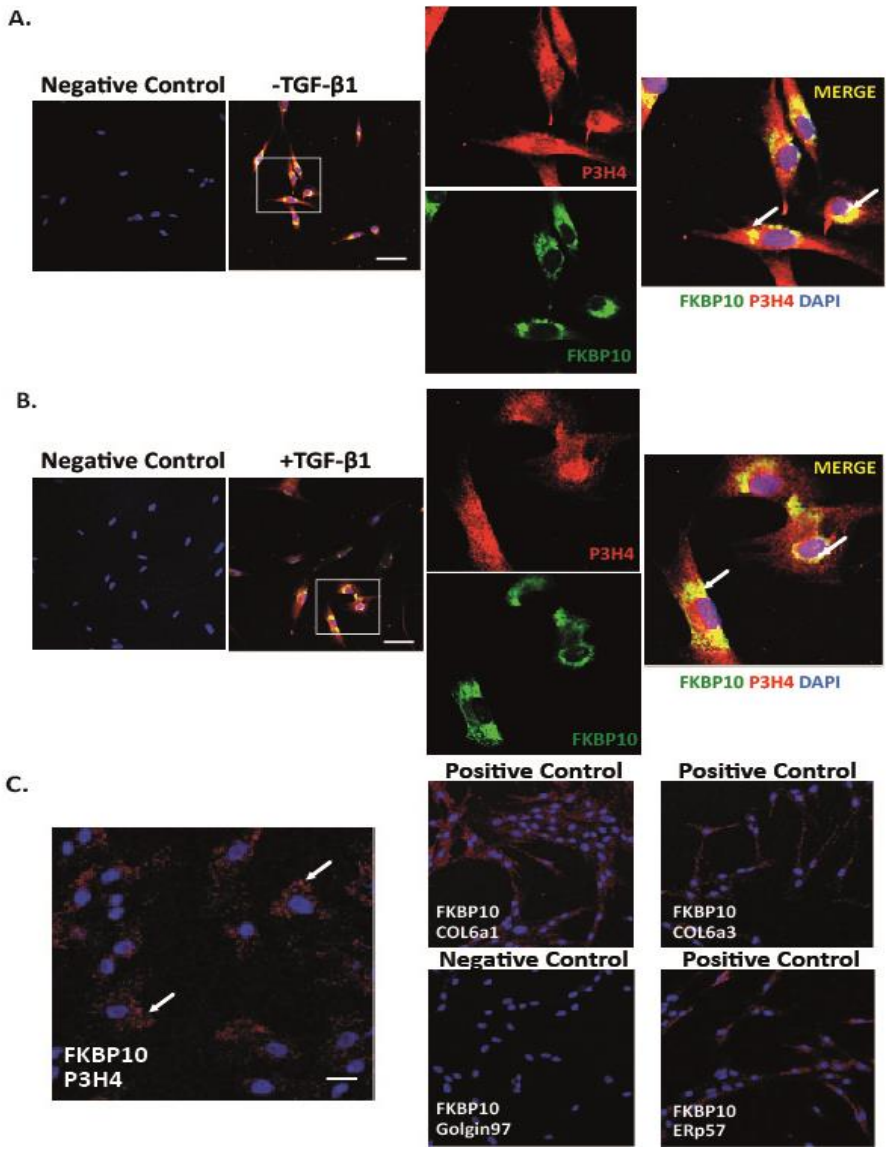

Figure 21: Colocalization and direct interaction of P3H4 with FKBP10 in phLFs. A) Immunofluorescent staining of FKBP10 and P3H4 in phLFs in absence of TGF-β1 **B)** Immunofluorescent staining of FKBP10 and P3H4 in phLFs in presence of TGF-β1. White arrows specify examples of colocalization of P3H4 with FKBP10 (n=4). The white square represents the area of interest, which was then magnified at the bottom of each image. FKBP10 immunostaining is shown in ***green***, and P3H4 in ***red***. Negative controls were carried out by using the identical staining protocol without adding the primary antibody. **C)** Representative images of *in situ* localization of FKBP10 and P3H4 interaction, COL6A1 (positive control), COL6A3 (positive control), ERp57 (positive control) and Golgin97 (negative control) and was investigated by PLA. White arrows specify examples of positive interaction of FKBP10 with P3H4. The interaction between the two proteins is indicated by ***red*** fluorescence (n=3). DAPI staining is shown in ***blue***. Images were obtained by confocal microscopy (20X). Scale bar: 50 µm.

3.1.10 Knockdown of P3H4 decreases the expression of *FKBP10* in phLFs

We further determined the effect of the P3H4 knockdown, by using siRNA, on the expression of *FKBP10* in phLFs in absence and presence of TGF-β1 (2 ng/mL) (48h) **(Figure 22A).** Densitometric quantification of P3H4 protein levels revealed that P3H4 was significantly downregulated after silencing by using siRNA in the absence and presence of TGF-β1 **(Figure 22B).** Surprisingly, WB analysis of P3H4 knockdown in phLFs showed significant downregulation of FKBP10 in presence of TGF-β1. Expression of *FKBP10* in absence of TGF-β1 appeared to be less affected by the knockdown of P3H4 in phLFs **(Figure 22A and 22B).** In addition, upon P3H4 knockdown and 48 hours of TGFβ-1 treatment, the transcript levels of FKBP10 were then assessed in phLFs. Interestingly, qRT-PCR did not reveal significant *FKBP10* gene expression changes with P3H4 knockdown neither in absence nor in presence of TGFβ-1 **(Figure 22C).**

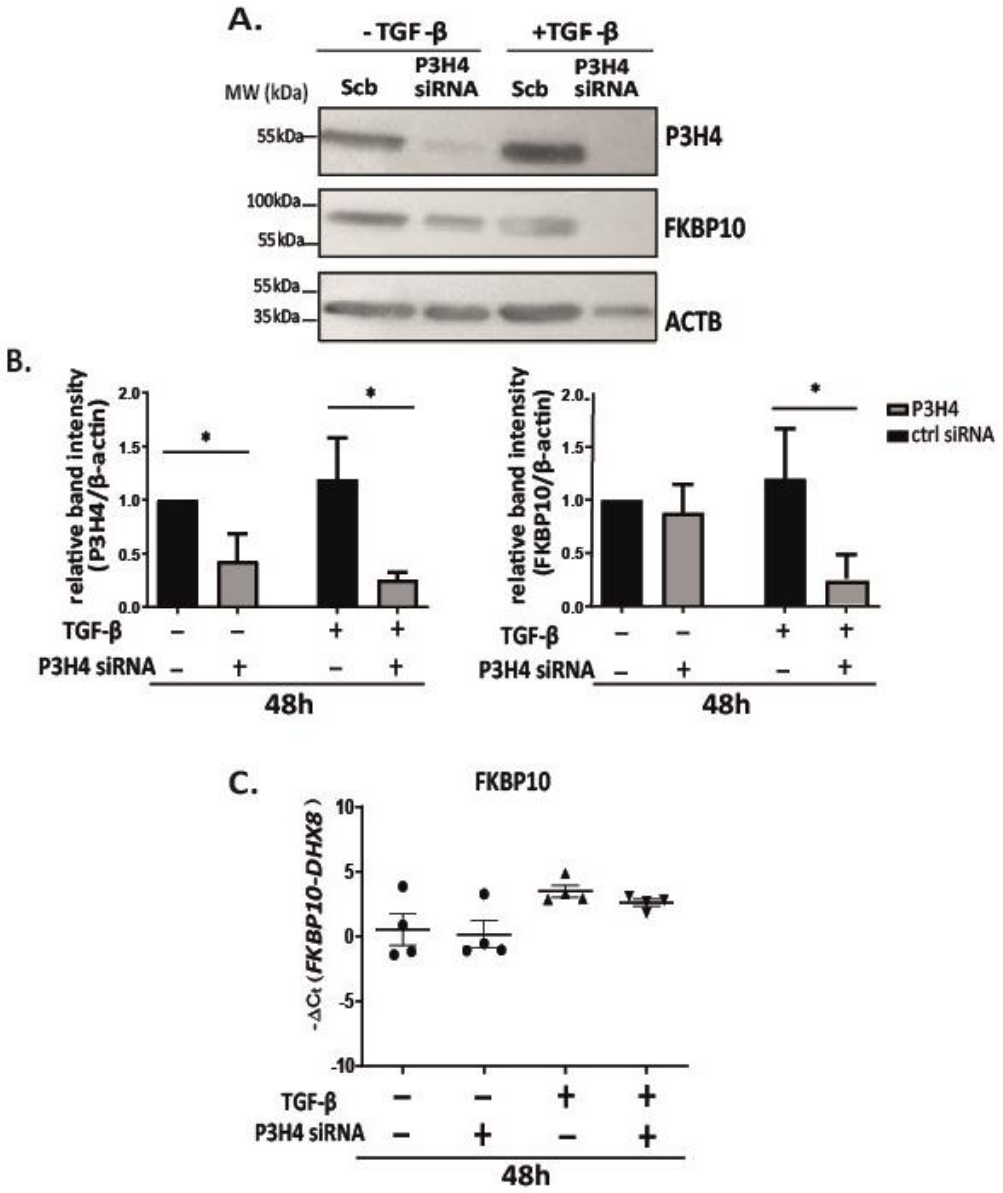

Figure 22: Downregulation of FKBP10 following P3H4 knockdown in phLFs. A) Effect of P3H4 knockdown in phLFs treated with TGF-β (2.0 ng/ml) (48h). A representative WB analysis for identification of P3H4 and FKBP10 is shown. WB analysis showed downregulation of FKBP10 with P3H4 knockdown in phLFs. One of the representative blots from completely independent experiments is shown here(n=4). As a loading control, β-actin (ACTB) was used. **B)** Densitometric quantification of protein levels of P3H4 and FKBP10 in the absence and presence of TGF-β1. The paired two-tailed t-test was used for statistical analysis. **C)** qRT-PCR analysis shows transcript levels of FKBP10 after knockdown of P3H4 with TGF-β1 treatment (48h) in phLFs. The data shown are based on four(n=4) independent experiments. One-way ANOVA with Tukey's multiple comparison test was used for statistical analysis. Scrambled siRNA was used as a control. The data are presented as mean ± SEM. **P < 0.05, **P < 0.01, ***P, < 0.001.* ctrl = control.

3.1.11 Knockdown of P3H4 reduces the secretion and expression of collagen in phLFs

Here, we examined the effect of the knockdown of P3H4, by using siRNA, on the expression of collagen I, as well as on the total collagen secretion in phLFs in absence and presence of TGF-β1 (2 ng/mL). Surprisingly, WB analysis of P3H4 knockdown in phLFs showed downregulation of collagen I protein levels in absence and presence of TGF-β1 **(Figure 23A).** Densitometric quantification of collagen I protein levels revealed that collagen I was significantly downregulated after P3H4 knockdown using siRNA in the absence and presence of TGF-β1 **(Figure 23B).** Moreover, upon P3H4 knockdown and 48 hours of TGFβ-1 treatment, the transcript levels of collagen I were then assessed in phLFs. qRT-PCR analysis showed significant downregulation of collagen I with knockdown of P3H4 after 48h TGF-β1 treatment in phLFs. Interestingly, qRT-PCR did not reveal significant changes in collagen I gene expression with P3H4 knockdown in the absence of TGFβ-1 **(Figure 23C).** Lastly, we determined levels of secreted collagen in this experiment. To quantify the total secreted collagen in phLFs, we performed the Sircol assay after knockdown of P3H4. Interestingly, P3H4 deficiency significantly reduced the collagen secretion in phLFs in both the absence and presence of TGF-β1 **(Figure 23D).**

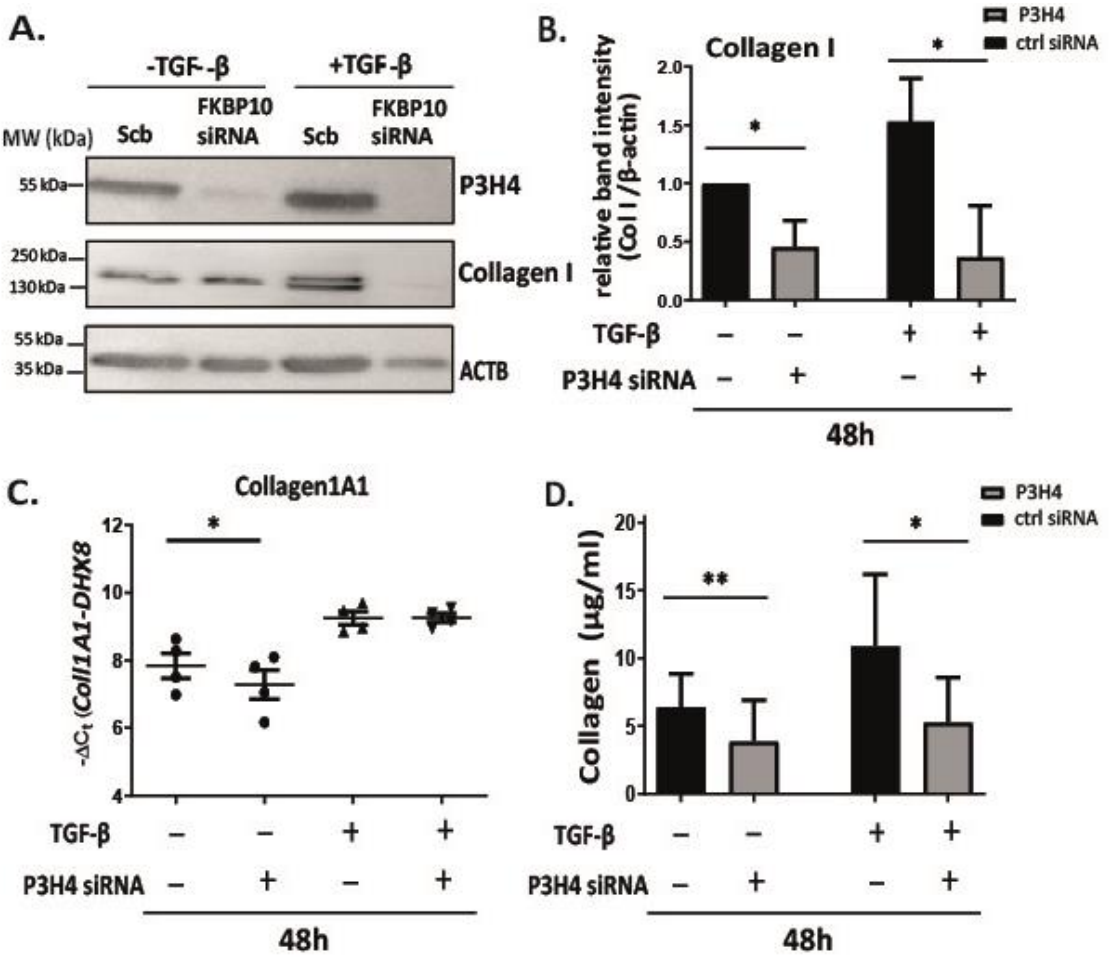

Figure 23: Down-regulation of collagen I and decreased total collagen secretion following P3H4 knockdown in phLFs. A) Effect of P3H4 knockdown in phLFs treated with TGF-β1. A representative WB analysis for identification of P3H4 and collagen I is shown. WB analysis showed down-regulation of collagen I with P3H4 knockdown in phLFs. One of four (n=4) representative blots from completely independent experiments is shown here. The same blots for P3H4 and ACTB are used in this figure and Figure 22A, and the results shown are from the same experiment. As a loading control, β -actin (ACTB) was used. **B)** Densitometric quantification of collagen I protein levels in the absence and presence of TGF-β1. For statistical analysis, the paired two-tailed t-test was used **C)** qRT-PCR analysis shows transcript levels of collagen 1A1. After knockdown of P3H4 with TGF-β1 treatment(48h) in phLFs. The data presented are based on four(n=4) independent experiments. One-way ANOVA with Tukey's multiple comparison test was used for statistical analysis **D)** Sircol assay results for determining total released collagen in cell culture supernatant following P3H4 knockdown with treatment of TGF-β1 (48h). The data presented are based on four(n=4) independent experiments. Scrambled siRNA was used as a control. Data are presented as mean ± SEM. **P < 0.05, **P < 0.01, ***P, < 0.001.* ctrl = control.

3.1.12 Knockdown of P3H4 reduces the expression of profibrotic markers in phLFs

We further determined the effect of the P3H4 knockdown, by using siRNA, on the expression of profibrotic mediators, including α-SMA and FN, as well as CTHRC1, a marker for pathologic fibroblasts in pulmonary fibrosis (J. Jin et al., 2019; Tsukui et al., 2020b) *w*ere determined in phLFs in absence and presence of TGF-β1 (2 ng/mL) **(Figure 24A).** *CTHRC1* gene expression has been shown to be upregulated in IPF lung tissues relative to control lung tissues and regulated collagen deposition (J. Jin et al., 2019; Leclère et al., 2020). In addition, CTHRC1 contains a collagen-like domain which sparked our interest in the first place.
As FKBP10 interacts with collagen I (Ishikawa et al., 2008), we hypothesized that FKBP10 may affect *CTHRC1* expression. However, we did not identify any major changes in expression of *CTHRC1* following knockdown of FKBP10. But, surprisingly, WB analysis of P3H4 knockdown in phLFs showed significant downregulation of CTHRC1 in presence of TGF-β1. *CTHRC1* expression in absence of TGF-β1 appeared to be less affected by the knockdown of P3H4 in phLFs. Moreover, densitometric quantification and WB analysis of α-SMA showed significant downregulation of α-SMA protein levels with knockdown of P3H4 in presence of TGF-β1. In addition, WB analysis of lung fibroblasts revealed downregulation of FN protein levels with knockdown of P3H4 in both the absence and presence of TGF-β1 (n=2) **(Figure 24A and 24B).** In addition, upon P3H4 knockdown and 48 hours of TGFβ-1 treatment, the transcript levels of *α-SMA, FN,* and *CTHRC1* were then assessed in phLFs. However, the gene expression of *α-SMA, FN,* and *CTHRC1* was not changed significantly following P3H4 knockdown neither in absence nor in presence of TGFβ-1 in phLFs **(Figure 24C).**

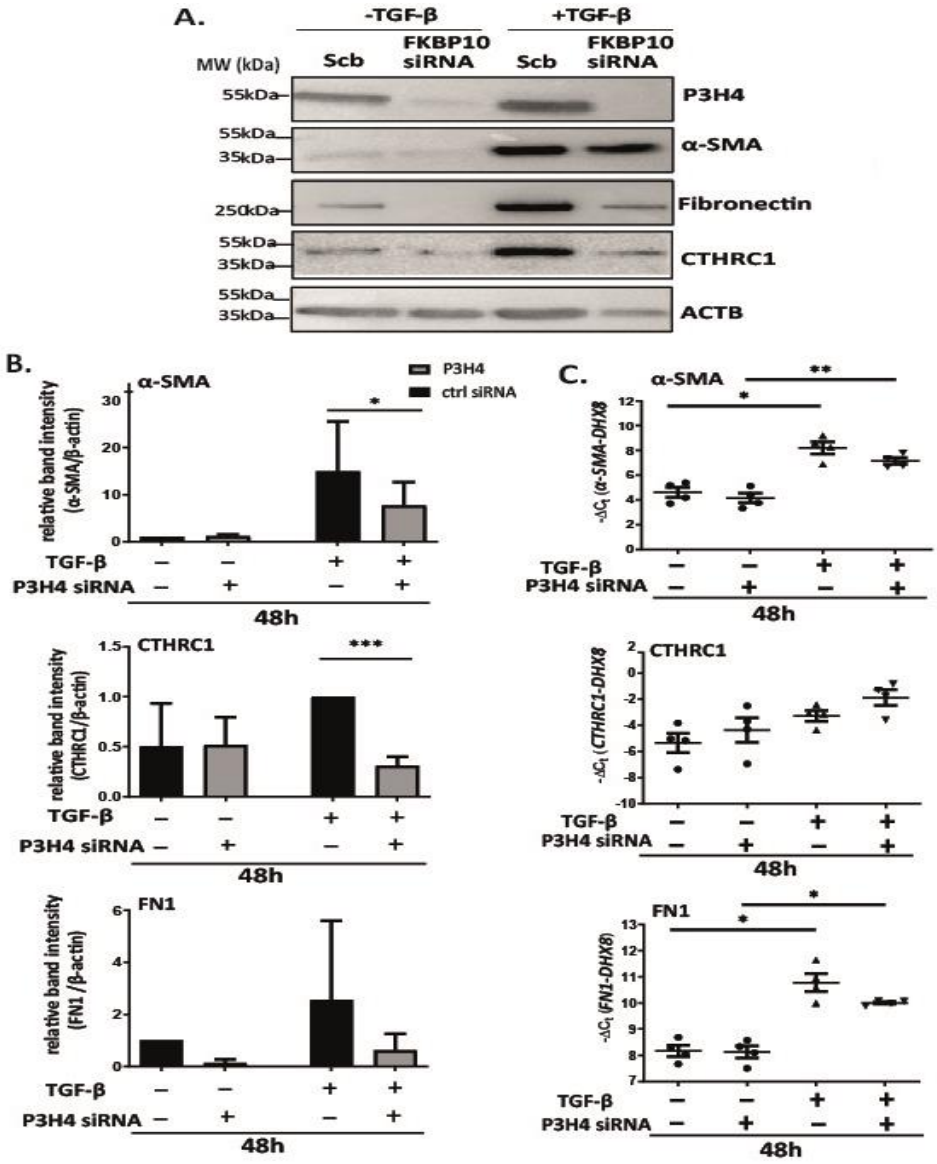

Figure 24: Downregulation of α-SMA, CTHRC1, and FN following P3H4 knockdown in phLFs. A) P3H4 knockdown effects in phLFs treated with TGF-β (2.0 ng/ml)(48h). A representative WB analysis for identification of P3H4, α-SMA, CTHRC1, and FN is shown. WB analysis showed downregulation of α-SMA, FN, and CTHRC1 in protein levels with P3H4 knockdown in phLFs. One of the representative blots from independent biological experiments is shown here(n=4), except for FN (n=2). The same blots for P3H4 and ACTB are used in this figure, Figure 22A and Figure 23A, and the results shown are from the same experiment. As a loading control, β-actin (ACTB) was used. **B)** Densitometric quantification of α-SMA, CTHRC1, and FN protein levels in the absence and presence of TGF-β1. **C)** qRT-PCR results shows transcript levels of α-SMA, CTHRC1, and FN after knockdown of P3H4 with TGF-β1 treatment in phLFs. The data presented are based on four(n=4) independent experiments. Scrambled siRNA was used as a control. One-way ANOVA with Tukey's multiple comparison test was used for statistical analysis. Data are presented as mean ± SEM. **P < 0.05, **P < 0.01, ***P, < 0.001. ctrl = control.*

3.2 Chapter 2: Effect of P3H1 deficiency on the expression of collagen biosynthetic enzymes and on type I collagen PTMs

3.2.1 Type I collagen isolated from WT and P3H1 null mouse tail tendon is >99% pure and yields similar chain stoichiometries

We first isolated collagen Type I from P3H1 null and WT mouse tail tendon to identify and characterize it. Next, we compared commercially available rat tail collagen with internally extracted mouse collagen type I. The coomassie staining of purified collagen type I from mouse and rat tail tendon was done by loading decreasing concentrations of the same sample for each. As shown in **Figure 25A**, the extracted collagen from the described internal procedure was as pure as commercially available rat tail collagen (obtained by iBAQ) **(Figure 25A)**. Equivalent amounts of type I collagen were then resolved on a 7.5% SDS-PAGE gel. After that, SDS-polyacrylamide gel electrophoresis was used to analyze and Coomassie blue was used to stain the purified type I collagen. Coomassie staining revealed several chains, and the band pattern for P3H1 null and WT mice was comparable **(Figure 25B).** By using tandem mass (MS/MS) spectrometry, we further examined the stoichiometry of alpha chains and the composition of type I collagen **(Figure 25C).** MS/MS and SDS-PAGE analysis did not reveal differences in overall composition of type I collagen. Intensity-based absolute quantification of all proteins detected in purified type I collagen by label-free MS/MS spectrometry showed that the resulting type I collagen consisted of more than 99% of the collagen chains α1(I) and α2(I) **(Figure 25C).** Chain stoichiometries given as α1(I): α2(I) obtained by iBAQ were 1.0: 0.90±0.02 for P3H1 null mice and 1.0: 0.91±0.05 for WT mice, which were very similar, but far from the expected chain stoichiometry of 1: 0.5 (Merl-Pham et al., 2019).

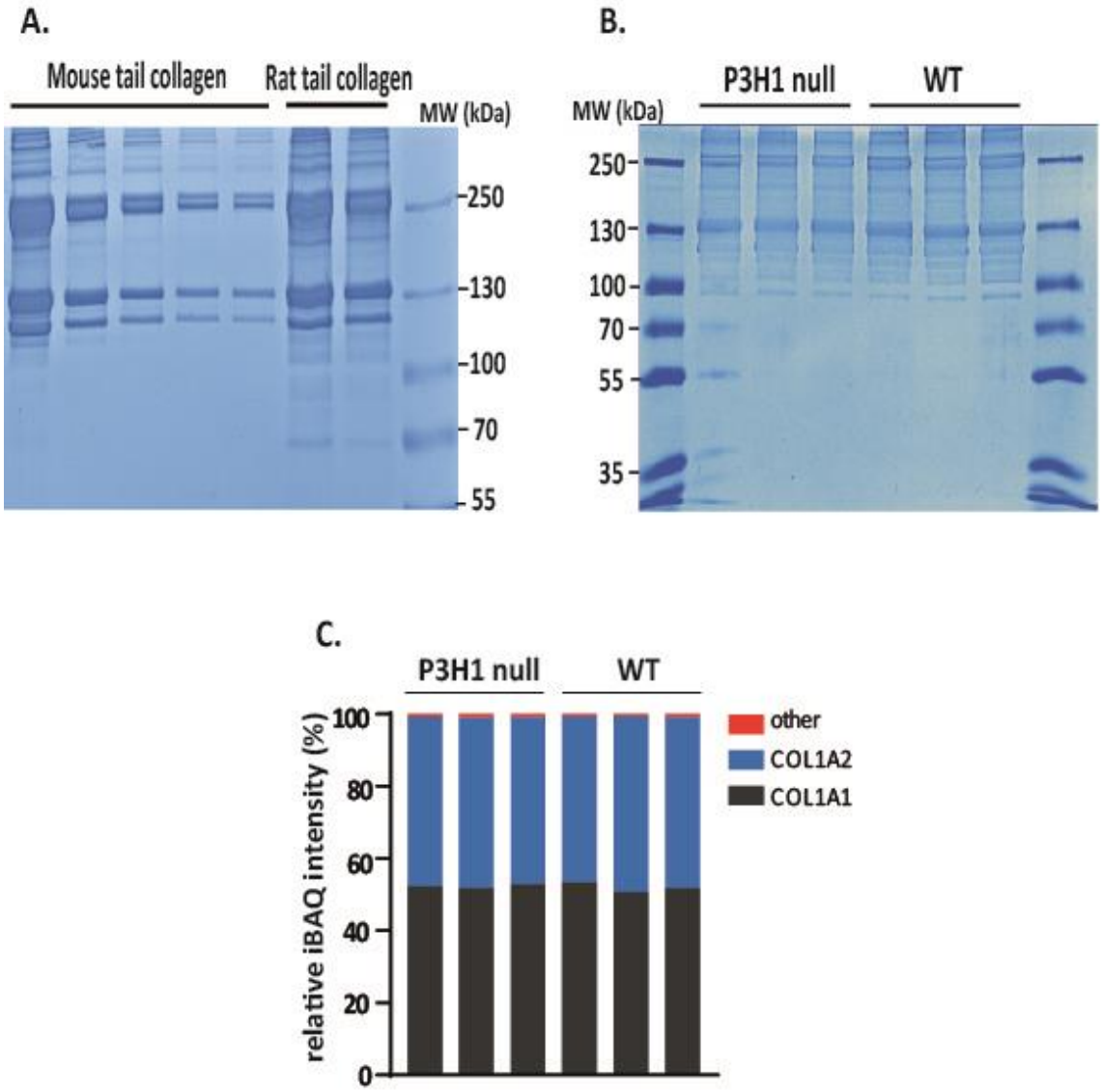

Figure 25: Identification of type I collagen from mouse tail cartilage of P3H1 null and WT mice. A) Direct comparison of commercial rat tail collagen with internally produced mouse type I collagen. Coomassie staining of purified collagen type I from rat tail tendon and mouse tail tendon (decreasing concentrations of the same sample for each). **B)** Coomassie staining of purified collagen type I from tail tendon of P3H1 null mice and WT controls. **C)** Intensity-based absolute quantification of all proteins detected in purified type I collagen by label-free MS/MS spectrometry reveals high purity of collagen type I (>99%) consisting of α1 and α2 chains.

3.2.2 Collagen type I isolated from WT and P3H1 null mouse tail tendon displays increased proline and lysine hydroxylation levels

Furthermore, we quantified Pro, 4-Hyp, 3-Hyp, Lys, and HyL relative to the total amount of Pro (Pro + 3-Hyp + 4-Hyp) or Lys (HyL+ Lys) residues in order to better characterize collagen type I from P3H1 null and WT mouse tail tendon. Surprisingly, P3H1 null mice had higher levels of the rare collagen PTM 3-Hyp, which increased from 1.5% of total proline count in WT mice to 1.9% in P3H1 null mice **(Figure 26A)**. Similarly, we identified a slight but significant increase in 4-Hyp in P3H1 null **(Figure 26A)** relative to WT mice. Lastly, we also observed increased levels of HyL in P3H1 null mice **(Figure 26B).** Thus, P3H1 deficiency increased overall collagen modification, including prolyl-3, prolyl-4, and lysyl hydroxylation.

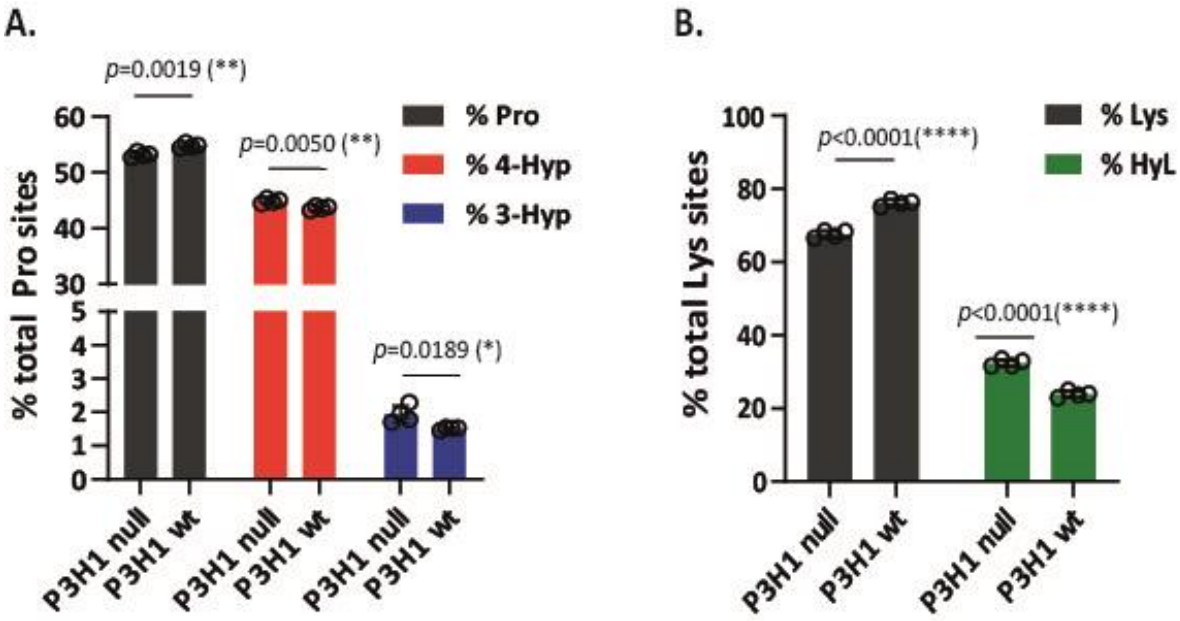

Figure 26: Amino acid analysis of collagen type I from P3H1 null and WT mouse tail tendon
A) Amino acid analysis-based quantification of Pro, 4-Hyp and 3-Hyp. **B)** Amino acid analysis-based quantification of Lys and HyL. Unpaired t-test was used for statistical analysis (n=4). *, p<0.05; **, p<0.01; ****, p<0.0001.

3.2.3 P3H1 deficiency increases expression of collagen type I and induces compensatory expression of collagen biosynthetic proteins

Considering the numerous quantitative changes in levels of multiple collagen PTMs, we hypothesized that these effects could be explained by compensatory gene expression of collagen biosynthetic enzymes. Although it is critical to better understand the magnitude, impact, and complexity of molecular collagen changes induced by P3H1 deficiency, no comprehensive analysis of potential compensatory gene expression of collagen biosynthetic enzymes has been performed until now.

For this, we started by isolating tenocytes from P3H1 null mice and WT littermates. The expression of genes encoding type I collagen, lysyl hydroxylases (LH1, LH2, and LH3), prolyl-3- hydroxylase (P3H1, P3H2, P3H3, P3H4), and prolyl-4-hydroxylase (P4HA1, P4HA2, P4HA3) family members, glycosyl transferases (GLT25D1 and GLT25D2), the collagen chaperone FKBP10, CRTAP, and PPIB was then investigated.

We confirmed *P3h1* deletion on transcript levels in P3H1 null mice. *Col1a1, P4ha2,* and *Lh2* showed significantly higher expression, while all other genes except *P3h2, Lh1,* and *P4ha3* showed a trend for higher transcript levels ($p<0.1$) **(Figure 27A).** As shown in **Figure 27B,** the deletion of P3H1 was also confirmed by WB analysis. Moreover, WB analysis showed that type I collagen, P3H3, and FKBP10 were upregulated at the protein level. Also, in contrast to unaltered P3h2 transcript levels, a strong upregulation of P3H2 on the protein level was observed. PPIB protein levels, however, remained unchanged. Overall, significant compensatory upregulation of collagen biosynthetic machinery components was observed in tenocytes from P3H1 null mice.

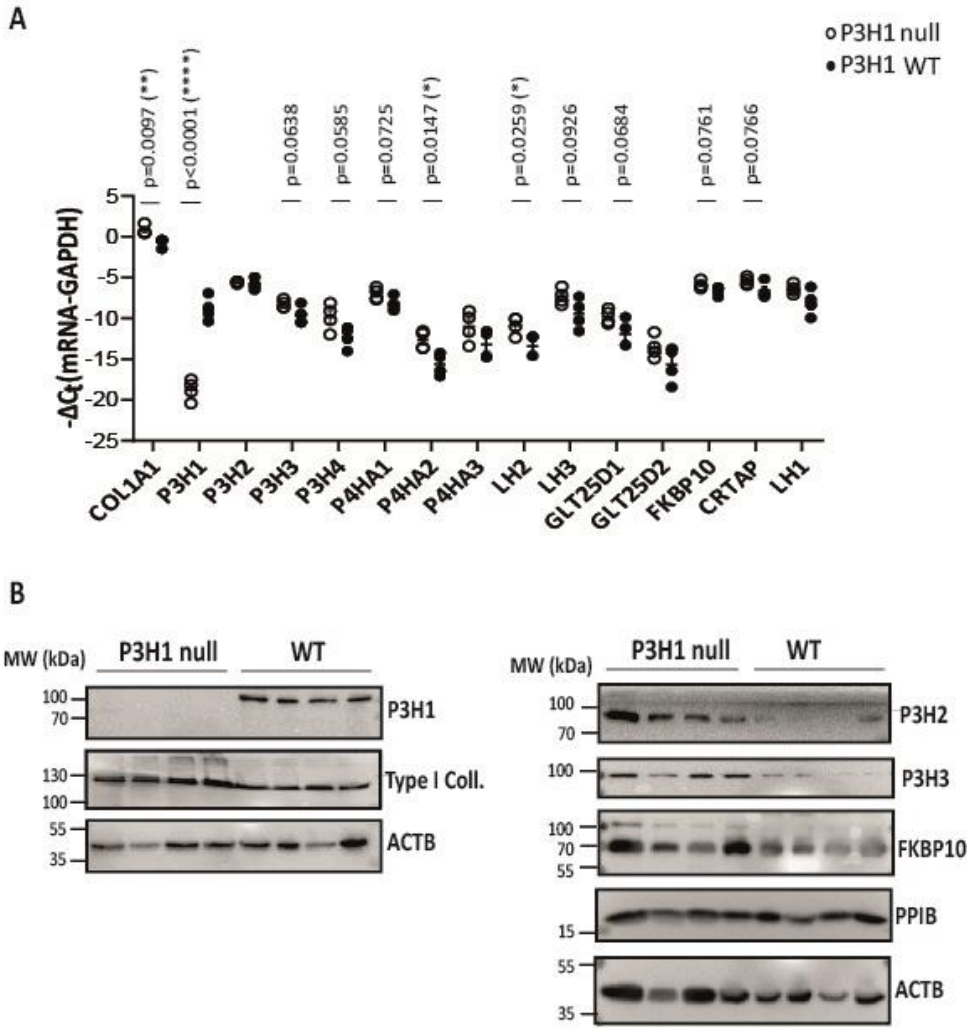

Figure 27: Analysis of gene expression of collagen biosynthetic enzymes in tail tendon from P3H1 null and WT mice. A) qRT-PCR analysis shows relative abundance as well as changes in transcript levels of Collagen 1a1, P3H1, P3H2, P3H3, P3H4, P4HA1, P4HA2, P4HA3, LH1, LH2, LH3, GLT25D1, GLT25D2, FKBP10 and CRTAP in P3H1 null and WT mice tenocytes. Data is given as $-\Delta C_t$ normalized to levels of *Gapdh* mRNA. Unpaired *t-test* was used for statistical analysis and absolute *p*-values are given, when *P<0.1. *, P<0.05; **, P<0.01; ****, P<0.0001.* **B)** Representative WB analyses for detection of type I collagen and selected collagen biosynthetic enzymes (P3H2, P3H3, FKBP10, PPIB) in P3H1 null and WT mice tenocytes are shown. As a loading control, β –actin(ACTB) was used.

4. Discussion

In the present study, we showed that P3H4, a critical component of the ER resident complex, was strongly downregulated as a result of FKBP10 deficiency in mouse embryonic lungs. Similarly, the knockdown of FKBP10 resulted in the downregulation of P3H4 in phLFs and *vice versa*. Importantly, TGF-β1 induced *P3H4* expression in phLFs. *P3H4* expression was increased in fibrotic mouse lungs, in IPF lung extracts, as well as in lung tissue from IPF patients. This is the first study showing that P3H4 is upregulated in IPF. P3H4 was mainly expressed in interstitial fibroblasts, as well as in epithelial cells and alveolar macrophages. Interestingly, FKBP10 and P3H4 colocalized and interacted in phLFs, as well as in fibrotic tissue sections from IPF patients and bleomycin-treated mice. Furthermore, P3H4 and FKBP10 colocalized with HAS1, which was induced by TGF-β1 in phLFs. P3H4 and FKBP10 colocalized in bleomycin-treated fibrotic mouse lungs mainly in the fibrotic regions, and, additionally, P3H4 was found to be expressed alone in some regions without colocalization with FKBP10. More importantly, the knockdown of P3H4 in phLFs decreased the synthesis and secretion of collagen and decreased the expression of profibrotic mediators and effectors.

In contrast, the results from P3H1 null and WT mouse tail tendon experiments revealed an increase in type I collagen expression, compensatory induction of several genes with P3H1 deficiency, as well as numerous changes in type I collagen PTMs, including an increase in overall proline and lysine hydroxylation. Importantly, upregulation of type I collagen, P3H2, P3H3, and FKBP10 was also observed on the protein level. Therefore, this study indicated very different outcomes regarding collagen biosynthesis when blocking expression of *P3H1* versus *P3H4*. These findings show, for the first time, the investigation of P3H4 regulation and function in lung fibrosis, the critical role of P3H4 in collagen biosynthesis and secretion in lung fibroblasts, as well as highlight inhibition of P3H4 as a potential novel therapeutic strategy in pulmonary fibrosis. Targeting P3H1, in contrast, may promote collagen biosynthesis and lead to a disadvantageous collagen PTM profile. The study thus emphasizes the importance of selective inhibition of specific collagen biosynthetic enzymes.

Similar to all other fibrotic diseases, IPF is characterized by increased ECM deposition and tissue remodeling. Although there is multiple evidence of changed ECM composition in IPF, the structural and molecular changes that occur in collagens during collagen biosynthesis in this disease are not well known. The deposited collagen also demonstrates qualitative post-translational changes such as cross-linking, prolyl and lysyl hydroxylation (Booth et al., 2012; Kristensen et al., 2014; C.A. Staab-Weijnitz et al., 2019; Tjin, White, Faiz, Sicard, Tschumperlin, Mahar, Kable, & Burgess, 2017; van der Slot et al., 2003). The enzymes, chaperones, and many other proteins responsible for these modifications are abnormally regulated during the development of pulmonary fibrosis (Booth et al., 2012; Organ et al., 2019; Piersma & Bank, 2019; Shao et al., 2020; X. Zhang et al., 2021). Several types of collagen are identified as playing critical roles in IPF pathogenesis. Ultimately, targeting pathological collagen biosynthesis and deposition is a promising treatment strategy for pulmonary fibrosis (Jessen et al., 2021; Lei et al., 2016; L. Liu et al., 2021; Claudia A. Staab-Weijnitz, 2022; Yang et al., 2022), but it remains unclear which components of the collagen biosynthetic machinery can be safely targeted.

4.1 Interaction and reciprocal regulation of P3H4 and FKBP10 in the lung

FKBP10, a collagen chaperone and peptidyl-prolyl-isomerase, has previously been described as a novel therapeutic target for IPF. In the same study, FKBP10 knockdown was shown to inhibit collagen secretion with the same efficiency as Nintedanib (Claudia A. Staab-Weijnitz et al., 2015a). The transcriptomic and proteomic analysis from global FKBP10 knockout embryonic mouse lung, kindly provided by Caressa D. Lietman and Brendan Lee (Lietman et al., 2014), showed strong downregulation of P3H4 with FKBP10 deficiency in both protein and transcript levels.

Mutations in *FKBP10 and P3H4* have been linked to collagen-related disease and the *FKBP10* gene is located less than 900 base pairs from *P3H4* exon 1. This strongly suggests that both genes share common regulatory elements. In

this knockout mouse model, to avoid the risk of impacting *P3H4* expression, rather than targeting exon 1, LoxP sites were introduced to flank the 2-6 exons of FKBP10 (Heard et al., 2016b; Lietman et al., 2014). In a study carried out using this FKBP10 knockout mouse model, FKBP10 deficiency resulted in alteration in collagen cross-linking and synthesis and PTM of collagen type I, and led to recessive *osteogenesis imperfecta*, a genetic connective tissue disorder (Lietman et al., 2014, 2017). In agreement, FKBP10 has been shown to complex with LH2, which facilitates the activity of lysine hydroxylation in the non-collagenous telopeptide regions of collagen and promotes its activity. FKBP10 deficiency results in altered collagen cross-linking (Duran et al., 2017b; Onursal et al., 2021; Ulrike Schwarze et al., 2013). Similar to FKBP10, previous studies showed that loss of P3H4 leads to the instability of the ER complex (P3H4/P3H3/LH1/PPIB) and results in unstable collagen with reduced extracellular cross-linking due to decreased lysyl hydroxylation, by affecting LH1 in the triple-helical collagenous regions during collagen biosynthesis (Duran et al., 2017b; Onursal et al., 2021). Another study showed that P3H4 protein is essential for LH1 activity, but, not for LH2 (Heard et al., 2016a; Zimmerman et al., 2018). Our results indicate FKBP10 as a potential indirect modulator of lysine hydroxylation of helical regions by LH1 in addition to telopeptide regions by LH2, as FKBP10 may indirectly affect LH1 activity by leading to downregulation of P3H4.

We further confirmed the downregulation of P3H4 with FKBP10 deficiency in phLFs. Similar to P3H4 downregulation in FKBP10-deficient mice, FKBP10 knockdown in phLFs resulted in P3H4 downregulation in both protein and transcript levels in absence of TGF-β1. These findings demonstrate that this coregulation is also relevant in human samples. Interestingly, the effect of FKBP10 knockdown on *P3H4* expression on protein level was partly counteracted by TGF-β1 treatment. The findings support the idea that TGF-β1 may regulate *P3H4* expression. TGF-β1, the main mediator of fibrogenesis, is upregulated in all types of fibrosis, and its role in modulating fibroblast function and myofibroblast transdifferentiation is well established (Biernacka et al., 2011; Meng et al., 2016).

We have investigated *in situ* localization of FKBP10 and P3H4 interaction in phLFs and in fibrotic mouse lungs from human and mouse. In recent scRNA-seq studies, the accumulation of profibrotic fibroblast populations, including Axin^{high},

PDGFR^{high}, CTHRC1^{high}, PDGFRb^{high}, and HAS1^{high} in IPF fibrotic lesions was investigated(Gajjala et al., 2023; Habermann et al., 2020; Tsukui et al., 2020a; Zepp et al., 2017; M. Zhao et al., 2018). These scRNA-seq studies in both humans and mice have demonstrated that the fibroblasts populations in IPF differ from healthy lungs in terms of morphology and function. These findings suggest that the excessive ECM accumulation seen in fibrosis may be mediated by any or all sub-populations (Habermann et al., 2020; Nemeth et al., 2020). As mentioned previously, Habermann *et al.* reported multiple fibroblast subtypes, including a unique HAS1^{high} ECM-producing fibroblast population, in addition to myofibroblasts, which is highly enriched in lungs from IPF patients. This new fibroblasts population seemed to be localized to the nearby subpleural areas, where fibrotic foci are typically identified first (Habermann et al., 2020). Moreover, it has been shown that HAS1^{high} fibroblasts express *FKBP10* and *P3H4* (Habermann et al., 2020). In agreement, we have shown the colocalization of FKBP10 and P3H4 with HAS1 in phLFs. These findings imply that targeting P3H4 may be promising strategy for treatment of IPF. In addition, the effects of FKBP10 on ECM regulation may require P3H4. Therefore, the interaction may be part of the collagen biosynthetic machinery and thus targetable.

Furthermore, the colocalization of P3H4 and FKBP10 in phLFs in both presence and absence of TGF-β1 was confirmed by immunofluorescent staining. FKBP10 has previously been identified as an ER localized protein that was weakly detected in both the nuclear and cytosolic extracts of phLFs (Claudia A. Staab-Weijnitz et al., 2015a), while P3H4 was detected in the cytoplasm, where it partially colocalized with FKBP10, and in the nucleus of phLFs. P3H4 localization proposed in the literature to date, however, includes either only the nucleus or, in some studies, only the ER. P3H4 has originally been identified as localized to the nucleolus (Ochs et al., 1996). In contrast, a previous study identified P3H4 as an ER localized protein that does not reside in the nucleus (Gruenwald et al., 2014). In our study, the immunofluorescent staining provided important novel evidence for P3H4 localization in phLFs, namely that P3H4 may shuttle between the cytoplasm and the nucleus. Since TGF-β1 treatment had no remarkable effect on the colocalization of FKBP10 and P3H4, our findings suggest that the interaction is not affected by pathological profibrotic conditions. Furthermore, as FKBPs are

known to bind nuclear receptors in the cytoplasm, delaying their nuclear translocation (Tatro et al., 2009), future work should assess whether FKBP10 sequesters P3H4 in the cytoplasm, preventing its translocation to the nucleus.

Knockdown of P3H4 in phLFs decreased FKBP10 levels on both protein and transcript level. Changes in FKBP10 transcript level, however, were not as significant as changes in protein level, implying that P3H4 regulates *FKBP10* expression mainly on the protein level, and that FKBP10 protein stability is regulated by P3H4.

Our findings indicate the possibility of reciprocal regulation of P3H4 and FKBP10 in the lung. Therefore, P3H4 may mediate some of the previously identified FKBP10-regulating effects on the ECM, and downregulating P3H4 may enhance the antifibrotic effects of FKBP10 inhibition in lung fibroblasts.

Furthermore, as previously stated, FKBP10 has four PPIase domains and only one of those four PPIase domains can be inhibited by FK506 (Zeng et al., 1998). This raises the question of whether FK506 can inhibit FKBP10 and thus exhibit antifibrotic effects. It also suggests that inhibiting FKBP10 may be more challenging. Moreover, prior studies have revealed that FKBP10 deficiency results in a severe form of *osteogenesis imperfecta* (Barnes et al., 2012; Steinlein et al., 2011; Tong & Jiang, 2015). However, P3H4 is consisting of one tetratricopeptide repeat (TPR) domain, which is presumed to be the protein-protein interaction domain (Gruenwald et al., 2014; Heard et al., 2016b; Ishikawa et al., 2017; Ishikawa & Bächinger, 2013a; M. Zimmerman et al., 2018). Importantly, P3H4 deficiency in mice exhibited a reduced bone mass phenotype that affected both the cortical and trabecular compartments, but it was not associated with *osteogenesis imperfecta*, at least not with the severe form (Forlino et al., 2011; Gruenwald et al., 2014; Heard et al., 2016b). In light of the available studies and our findings, targeting P3H4 may have less severe side effects, therefore be a more promising approach to prevent the progression of IPF disease since it would have a milder effect on bone synthesis.

4.2 Role of P3H4 as a novel modulator of collagen biosynthesis in lung fibroblasts and an important regulator of the ECM in the lung

P3H4 is mainly associated with post-transcriptional collagen modification of collagen chains in the ER (Gjaltema & Bank, 2017; Heard et al., 2016b). Earlier studies demonstrated that P3H4 deficiency promotes a partial loss of LH1 protein and function, under-hydroxylation of helical lysine residues, and a reduction in collagen lysine hydroxylation resulting in defective collagen cross-linking (Gruenwald et al., 2014; Heard et al., 2016b; Onursal et al., 2021), that can be altered independently of collagen secretion or synthesis. Importantly, we showed that knockdown of P3H4 in phLFs decreased collagen levels both on protein and transcript levels. Moreover, we further demonstrated that knockdown of P3H4 in phLFs reduced total collagen secretion in cell culture supernatant.

In a recent study it was shown that P3H4 knockdown reduced N-cadherin protein levels (a marker of ongoing epithelial-to-mesenchymal transition) and Vimentin, inhibited bladder cancer cell invasion and migration by blocking the EMT process, and increased the E-cadherin protein levels in bladder cancer cells (Hao et al., 2020). Since EMT plays a critical role in IPF development (Di Gregorio et al., 2020; Hill et al., 2019; Salton et al., 2019; Zhou et al., 2016) and the most important sign of EMT is decreased expression of E-cadherin, as well as an increase N-cadherin, vimentin, and FN expression, these findings may indirectly point to the involvement of P3H4 in lung fibrosis (Chilosi et al., 2017; Hao et al., 2020; Hill et al., 2019; Salton et al., 2019; B. C. Willis, 2006; Brigham C. Willis et al., 2005). ETV4, which also transcriptionally regulates some of the MMPs, has been demonstrated to specifically binds to the *P3H4* promoter and activates the transcription of P3H4 (Hao et al., 2020; X. Jin et al., 2021), may suggest that ETV4 transcriptionally regulates the expression of *P3H4* in lung fibrosis. In line with this hypothesis, P3H4 was initially identified as a nucleolar protein and an autoantigen in interstitial cystitis cases, a condition that is also characterized by fibrosis and profibrotic changes that are linked to the positive regulation of genes *collagen I* and *III*, as well as *FN* in smooth muscle cells, which is mediated by TGF-β1 (Brossard et al., 2022; Ochs et al., 1996). Interestingly, we observed that deficiency of P3H4 decreased the expression of the TGF-β-induced proteins FN

and α-SMA. The molecules localizing to the ECM and basement membrane including PDGFRα and ITGA11 have been shown to coexpress with P3H4 and suggested to be the direct target of P3H4 (X. Jin et al., 2021). Interestingly, PDGFR+ and SMA+ cells have been shown to contribute to lung fibrosis by producing collagen, as well as ITGA11 knockdown significantly reduced the contractility of collagen I matrices (Bansal et al., 2017; Barkauskas et al., 2013; Biasin et al., 2020). We have demonstrated that ECM proteins including FN and Collagen I are decreased upon P3H4 deficiency. Overall, these findings are consistent with our findings and might indicate that P3H4 contributes to the deposition of the ECM by increasing collagen and other ECM protein production and that P3H4 deficiency changes ECM topography.

Moreover, we showed that knockdown of P3H4 in phLFs reduced the TGF-β1-induced protein expression of profibrotic mediator CTHRC1. Prior studies showed that CTHRC1 functions as a cell type-specific inhibitor of TGF-β1, which in turn affects the deposition of types I and III collagen, and the dedifferentiation of smooth muscle cells (Binks et al., 2017; LeClair et al., 2007)**.** Recent studies, however, found that TGF-β1 induced CTHRC1 expression in phLFs, which was then inhibited by Pirfenidone (J. Jin et al., 2019; Leclère et al., 2020). CTHRC1, which contains a collagen-like domain, has been shown to be upregulated in IPF lung relative to control lung tissue and regulated collagen deposition. Thus, CTHRC1 has been suggested to be used for developing new therapeutic targets for IPF (J. Jin et al., 2019; Leclère et al., 2020). Moreover, using scRNA-Seq, researchers discovered collagen-producing cell subpopulations that are concentrated within fibroblastic foci and are characterized by *CTHRC1* expression in fibrotic lungs (Tsukui et al., 2020b). Another study found that fibrosis in both COVID-19 and IPF can be triggered by activated fibroblasts, which are identified by the specific expression of several genes, such as *CTHRC1*, *COL3A1*, and COL1A1. Besides the fact that the expression levels in normal control lungs was negligible, CTHRC1-positive cells have been shown to contribute to tissue fibrosis by producing excessive amount of ECM (Pérez-Mies et al., 2022).

TGF-β is known to activate receptor-associated SMAD proteins (SMAD2 and SMAD3), which in turn stimulate collagen expression in a wide range of cells.

SMAD4 forms an oligomer with activated SMAD2/3. When the complex translocates to the nucleus, it regulates the expression of TGF-β induced genes, also including CTHRC1. Interestingly, it has been demonstrated that increased CTHRC1 levels eventually reduce TGF-β signaling by inhibiting SMAD2/3 phosphorylation, that might result in SMAD2/3 degradation (Binks et al., 2017; Myngbay et al., 2021). In another study, CTHRC1 has been shown to promote the degradation of phospho-SMAD3, but had no effect on the induction of phospho-SMAD2 or phospho-SMAD3 (Bian et al., 2015). A recent study suggested that CTHRC1 may have a synergistic effect with TGF-β in the early activation of fibroblasts. In the same study, CTHRC1 overexpression in keloid fibroblasts inhibited YAP nucleus translocation and promoted its cytoplasm translation, as well as downregulated TGF-β signaling by increasing the degradation of phospho-Smad2/3 (M. Zhao et al., 2018). Interestingly, YAP was found to be one of the most downregulated proteins with FKBP10 deficiency in our proteomic analysis. Overall, these findings point to a crucial negative feedback regulatory loop in which TGF-β induces CTHRC1, which can reduce fibrosis by speeding up the degradation of phospho-Smad3. Moreover, the data may suggest the ability of CTHRC1 to inhibit phosphorylation of SMAD2 and SMAD3 gives it the potential to reduce gene expression, including *P3H4*, by this pathway. Given that we only demonstrated changes in *CTHRC1* expression on the protein level, a degradation mechanism may be involved in the regulation of CTHRC1 with P3H4 knockdown, and thus it could be a protein stability issue. Furthermore, CTHRC1 contains a collagen-like domain that may provide insights into this regulation of expression. However, a deeper understanding of the molecular mechanisms of these proteins will contribute to the ongoing development of novel treatments for this otherwise progressive and irreversible disease.

4.3 Expression and distribution of P3H4 in lung fibrosis

P3H4 has mostly been studied in the context of bone and previous research on P3H4 has shown that P3H4 is involved in a wide range of pathological and physiological processes including connective tissue defects (Fang et al., 2022; Hao et al., 2020; Li et al., 2018). An earlier study showed that P3H4 is expressed and functional during skeletal development, and P3H4 deficiency leads to progressive

osteopenia (Gruenwald et al., 2014). *P3H4* is mainly expressed in bone, and cartilage (Heard et al., 2016b; M. Zimmerman et al., 2018)**.**

Furthermore, in one study, it was found that the proteins that were upregulated in response to P3H4 overexpression were primarily enriched in pathways that regulate the tumor microenvironment, including focal adhesion, phagosome, and ECM-receptor interactions, as well as pathways associated with cancer, including the bladder cancer pathway and the hippo signaling pathway (X. Jin et al., 2021). Others discovered that P3H4 is overexpressed in bladder cancer tissues and that P3H4 knockdown suppressed the proliferation, migration, cell cycle, and invasion of bladder cancer cells (Hao et al., 2020). *P3H4* expression in lung fibrosis, however, has not been studied. Importantly, we showed that TGF-β1 induced *P3H4* gene expression in phLFs**,** as previously demonstrated for the FKBP10 (Claudia A. Staab-Weijnitz et al., 2015a). This finding supports the application of this cell culture method for *in vitro* functional analysis of P3H4 as it demonstrates that adult phLFs have the ability to increase *P3H4* expression under fibrotic conditions.

Studies in lung fibroblasts and bleomycin-induced lung fibrosis in mice revealed that increased collagen prolyl hydroxylation expression and activity is one of the critical processes effecting TGF-β-mediated profibrotic mechanisms, and Luo *et al.* proposed inhibition of collagen prolyl-4-hydroxylase as a new promising drug target in pulmonary fibrosis (Luo et al., 2015).

Furthermore, we showed that *P3H4* expression was increased in IPF lung extracts. Subsequently, IF stainings of P3H4 in fibrotic lung tissue from human and mouse confirmed increased expression of *P3H4***.** This effect is similar to that of FKBP10, which has been identified as a novel therapeutic target for IPF (Claudia A. Staab-Weijnitz et al., 2015b) and is controlled by the same promoter and likely shares the same regulatory elements. *P3H4* expression was shown to be increased in human and mouse fibrotic lungs, while *P3H4* expression was low in control mice treated with PBS or donor lungs. In agreement, *P3H4* expression has been found to be lower in alveolar cells and fibroblasts under normal conditions (http://ipfcellatlas.cm/,https://www.proteinatlas.org/).

Studies have demonstrated different subpopulations of fibroblasts contribute to lung fibrosis by producing matrix (Habermann et al., 2020; Winters et al., 2020). In the lungs from IPF patients, a unique subpleural fibroblast population with a specific expression pattern of growth factors and ECM modulators, which support ECM expansion, has been identified (Winters et al., 2020). Moreover, a unique HAS1^{high} ECM-producing population was discovered, which localizes to peripheral and subpleural regions and colocalizes with *COL1A1* expression. This population is highly enriched in lungs from patients with IPF. ECM genes, which encode ECM components and are increased in IPF lungs, were found to be highly expressed in newly identified fibroblast subpopulations (Habermann et al., 2020). We discovered that P3H4 is mainly expressed in interstitial fibroblasts, as previously demonstrated for the FKBP10 (Claudia A. Staab-Weijnitz et al., 2015a). Increased *FKBP10* expression in interstitial fibroblasts and localization in fibrotic foci, which consist of aggregates of fibroblasts and myofibroblasts surrounded by epithelial cells, regions have previously been demonstrated by immunofluorescence stainings, as evidenced by colocalization with α-SMA (Claudia A. Staab-Weijnitz et al., 2015a)**.** In agreement, as previously mentioned these genes are also co-expressed in interstitial lung disease, according to previous scRNA-Seq data (Habermann et al., 2020). In the corresponding study, HAS1^{high} fibroblasts ECM-producing population expresses *FKBP10* and *P3H4.*

P3H4 was commonly detected in fibrotic regions of bleomycin-treated mouse lungs, as proven by colocalization with α-SMA. In agreement, increased *FKBP10* expression in interstitial fibroblasts and localization in fibrotic foci regions have previously been demonstrated by immunofluorescence stainings (Staab-Weijnitz et al., 2015a). Moreover, P3H4 and FKBP10 colocalized in bleomycin-treated fibrotic mouse lungs in these fibrotic regions. However, P3H4 was observed to be expressed independent of FKBP10 in lung epithelial cells without colocalizing with FKBP10. In the mouse model and the IPF lung sections, these regions were only P3H4 positive. This data suggests that, despite their commonalities and bidirectional promoter, FKBP10 and P3H4 do not always coexpress in all cell types, indicating that different regulatory mechanisms exist. However, further research is required to establish mechanisms of co-expression and co-regulation of two

proteins during the fibrotic process. These findings may imply that P3H4 upregulation appears to be associated with the lung function and fibrotic phase, which are important for applying these findings to IPF. Our study suggests that P3H4 may have a role in synthesis of ECM proteins in phLFs and demonstrates that P3H4 is expressed by fibroblasts, making it a relevant cell type for further investigations.

In our study, we discovered the expression of *P3H4* in myofibroblasts as well, as evidenced by colocalization with α-SMA. Myofibroblasts are commonly identified by expression of a-SMA, and various studies have associated fibrosis with an increase in collagen secretion of myofibroblasts and a-SMA+ cells in the fibrotic lung (X. Liu et al., 2021; K.-H. Sun et al., 2016; Tomasek et al., 2005; Zepp et al., 2021).

As previously mentioned, macrophages, a major source of TGF-β, promote fibroblast proliferation and collagen synthesis by producing growth factors(Guoxiu Liu et al., 2019; Lucas et al., 2010; Ogawa et al., 2021). Growth factors secreted by alveolar macrophages can enhance fibroblast accumulation, proliferation, and activation, resulting in increased extracellular matrix synthesis in the lung. Emerging evidences indicating pro-fibrotic role of macrophages and their involvement in fibrosis (Guoxiu Liu et al., 2019; Lucas et al., 2010; Sim et al., 2022). Interestingly, tissue sections from IPF lung demonstrated expression of *P3H4* also in interstitial macrophages and colocalization of P3H4 with FKBP10. In agreement, a subset of FKBP10-expressing cells was found to be interstitial macrophages, as proven by colocalization with CD68 (Claudia A. Staab-Weijnitz et al., 2015a). These findings support the hypothesis that P3H4 and FKBP10 co-express in lung fibrosis.

Since ER stress is a pathological factor in IPF (A. C.-H. Chen et al., 2018; Lawson et al., 2011) and P3H4 localizes to the ER, the hypothesis that P3H4 promotes ER stress or that a response to unfolded proteins is reduced in its absence was feasible. However, it has been reported that induction of ER stress using tunicamycin did not affect the expression of endogenous *P3H4* (Gruenwald et al., 2014). This data showed that *P3H4* is not modulated during ER stress; thus, the unfolded protein response is unlikely to contribute to P3H4 up-regulation in IPF.

Moreover, direct interaction of P3H3 with P3H4 and significantly decreased protein levels of P3H3 in P3H4 knockout samples were reported (Heard et al., 2016b; Hudson et al., 2017a). And, the total amount of hydroxylysine in P3H3 knockout mouse tissues was found to be decreased, which results in aberrant cross-link formations (Heard et al., 2016b; Ishikawa et al., 2021). Furthermore, only P3H3 and P3H4, two of the collagen lysyl-hydroxylation complex components, are expressed at considerably lower levels and their expression tends to decrease with age, resulting in protein levels in testis that are undetectable after 4 weeks of age. Up until 4 weeks of age, *P3H4* is expressed in the peritubular cells of the testis, but not in the germ cells within the seminiferous tubules or in mature sperm. The fact that P3H4 and P3H3 are significantly downregulated in adults relative to 4-week-old testis and ovary suggests that they are postnatally regulated (Zimmerman et al., 2018). More interestingly, our proteomic data indicated that besides P3H4, P3H3 is also one of the most downregulated proteins with FKBP10 deficiency. Thus, the hypothesis that P3H3 deficiency in lung fibroblasts reverses the fibrotic phenotype and that this phenomenon can be also correlated with the levels of P3H4, as well as a potential interaction between FKBP10 and P3H3, is plausible.

4.4 Targeting Collagen Biosynthesis and Maturation as Therapeutic Strategy in IPF

4.4.1 Prolyl- and lysyl hydroxylases

As previously mentioned, collagen is posttranslationally modified in the ER, by glycosyl transferases and prolyl and lysyl hydroxylases which typically assemble in complexes with collagen chaperones and peptidyl-prolyl isomerases. Lack of PTMs including hydroxylation of specific lysine and proline residues, results in abnormal collagen fibril formation, defective collagen cross-linking, and eventually, an altered ECM architecture.

The quality and function of collagens are altered by different PTMs during the progression of IPF, which affects ECM quality and quantity in the lung and is responsible for the crucial processes that lead to IPF (Kristensen et al., 2014).

ECM remodeling induces distinct alterations in collagen turnover. Increased type I and III collagen turnover has been linked to disease progression in patients with IPF (Hoyer et al., 2021; Jenkins et al., 2015). In IPF, the ECM may promote pathological cross-linking, which increases fibroblast proliferation, limits normal ECM turnover, and enhances collagen accumulation(Kristensen et al., 2014; Mutsaers et al., 1998; Philp et al., 2018; Q. Wang et al., 1999).

Several studies targeting the collagen biosynthesis and maturation pathway have already been performed. Interestingly, a previous study showed that prolyl-3-hydroxylation can be regulated by TGF-β1 in a site-specific manner. Surprisingly, the findings from this study demonstrate that collagen PTMs are modulated by TGF-β1 (Merl-Pham et al., 2019). Moreover, inhibition of collagen prolyl hydroxylase by pyridine-2,5-dicarboxylate has been demonstrated to reduce collagen production, stimulated by TGF-β, bleomycin-induced mouse lung fibrosis and in cultured fibroblasts, suggesting prolyl hydroxylase inhibition as a promising strategy for preventing pulmonary fibrosis (Luo et al., 2015).

Prolyl 3-hydroxylation is a rare but essential PTM of collagens that is introduced by one of three collagen prolyl-3-hydroxylases; P3H3, P3H2, and P3H1 (Hudson & Eyre, 2013a; Ishikawa & Bächinger, 2013a; Pokidysheva et al., 2014). P3H1 is the enzyme that converts proline to 3-Hyp in collagen type I (Homan et al., 2014; Hudson & Eyre, 2013a; Pokidysheva, Zientek, et al., 2013; Vranka et al., 2010). P3H2 primarily facilitates the 3-hydroxyproline formation in type IV collagen subchains (Aypek et al., 2022; Hudson et al., 2015; Pignata et al., 2021; Pokidysheva et al., 2014). However, P3H3-dependent prolyl-3-hydroxylations have not yet been defined.

P3H1 is found in fibrillar collagen-rich tissues including skin, bone, and tendon. P3H1 is required for helix formation of collagen and bone development, and its absence altered collagen fiber architecture in these tissues (Cabral et al., 2007; Gjaltema & Bank, 2017; Vranka et al., 2010).

P3H1 and CRTAP stabilize each other and form a collagen-modifying complex with PPIB that 3-hydroxylates the a1(I) Pro986 residue of a1(I) and a1(II) fibrillar collagen chains and has PPIase activity required for proper collagen folding. In

the absence of this post-translational modification, protein-protein interactions essential for proper collagen folding may be interrupted, leading to over-modification of the helical region of collagen (Homan et al., 2014). CRTAP and P3H1 mutations lead to osteogenesis imperfecta with collagen over-modification (Barnes et al., 2006; Cabral et al., 2007; Marini et al., 2007). P3H1 is required for the stability and formation of this collagen-modifying ER-resident protein complex, and a deficiency in P3H1 associated with complete lack or reduced 3-hydroxylation of the a1(I) Pro986 residue, delays type I collagen folding and it might cause changes in collagen characteristics and the formation of the trimeric complex (Baldridge et al., 2008; Besio et al., 2019; Cabral et al., 2007; Chang et al., 2010; Marini et al., 2010; Pokidysheva, Zientek, et al., 2013).

In our study, we have observed an increase in proline hydroxylation, both for 3-Hyp and 4-Hyp in P3H1 null mice. P986, which is corresponding to P1153 in the full-length α1 chain (Uniprot Entry P11087-1), was completely 3-hydroxylated in WT mice, but mostly unhydroxylated in tendon, skin, and bone in P3H1 null mice (Pokidysheva, Zientek, et al., 2013; Vranka et al., 2010). However, at the A3 site Pro707 (Pro874 in Uniprot Entry P11087-1), 3-hydroxylation was found in bone and tendon of WT mice but not in the skin, and specifically in bone, hydroxylation was attenuated by the absence of P3H1 (Pokidysheva, Zientek, et al., 2013).

Interestingly, P3H1 has been discovered to be upregulated in human lung fibrosis (Schiller et al., 2017). This could indicate that P3H1 might also play a role in the increased production of collagen in fibrotic tissue. However, our study revealed significant upregulation of collagen I both in protein and transcript level, induced by P3H1 deficiency. In a different study, the total amount of collagen secreted by P3H1 null cells was 20%–55% higher than that of the identical number of control cells (Cabral et al., 2007).

Moreover, results from P3H1 null and WT mouse tail tendon experiments revealed significantly increased *P4ha2*, and *Lh2* expression, as well as a trend for increased transcript levels for all other genes assessed except for *P3h2* and *P4ha3*, and upregulation of P3H2, P3H3, and FKBP10 on the protein level. In individuals with P3H1 mutations, types I and V of collagen are over-modified, which suggests that P3H1 may directly serve as a collagen chaperone. In this

study, the absence of P3H1 resulted in an increase in the percentage of hydroxylated lysine residues(Cabral et al., 2007). In line with this result, our amino acid analysis revealed an increase in overall collagen PTM levels including prolyl-3-, prolyl-4- and lysyl hydroxylation in collagen type I isolated from P3H1 null mice, which was also consistent with the compensatory upregulation of *Lh2*, *P4ha2* and P3H2, P3H3, FKBP10. These findings are indicating that the observed compensatory upregulation of biosynthetic enzymes alters the collagen PTM pattern in absence of P3H1. The P3H1 complex also functions as a typical chaperone (Ishikawa et al., 2009), and our results indicate that its absence appears to induce compensatory gene expression of collagen biosynthetic machinery components and increased type I collagen expression. Overall, these findings indicate that P3H1 may not be a suitable target to treat lung fibrosis and that care must be taken to identify components of the collagen biosynthetic machinery can be safely targeted to prevent lung fibrosis. Targeting P3H1 may promote collagen biosynthesis and result in a negative collagen PTM profile.

The pattern and extent of lysine hydroxylation determine fibril formation, collagen cross-linking, and thus the stability of mature collagen molecules (Yamauchi & Shiiba, n.d.). To initiate the cross-linking process, telopeptidyl Lys and Hyl are converted by LOX and LOXL1-4 to Lys- and Hyl aldehydes, respectively. Thus, the stability of cross-links is determined through Lys hydroxylation by LH2 in collagen telopeptides, highlighting the significant contribution of LH2-mediated cross-linking to ECM quality in fibrosis (Piersma & Bank, 2019; Sato et al., 2021). The quantity of LH2-mediated collagen cross-links was found to significantly increase with *PLOD2* overexpression in squamous carcinoma cells(Sato et al., 2021). In addition, lysine residues hydroxylated by LH2 on fibrillar collagen resulted in stable collagen cross-links that stiffen the matrix in lung tumor cells (Y. Chen et al., 2015; Guo et al., 2021). Moreover, it has been shown that LH2 was dramatically increased in bleomycin induced lung fibrosis (Shao et al., 2018b).

LH inhibition has been proposed as an antifibrotic strategy, and the compound minoxidil has been shown to primarily inhibit *LH1* mRNA levels among other LHs (Zuurmond et al., 2005). This finding implying that minoxidil may have anti-fibrotic effects by decreasing the total hydroxylysine residues amount in the collagen and thus preventing the hydroxylysine cross-links formation(Shao et al., 2018;

Zuurmond et al., 2005). In skin fibroblasts from P3H4 null mice, collagen type I is also over-modified, with increased lysyl hydroxylation and glycosylation (Krane, 2006; Marini et al., 2010). P3H1 null mice showed an increase also in the glycosylation of hydroxylysine and galactosyl hydroxylysine (Vranka et al., 2010). Our amino acid analysis also revealed an increase in collagen lysyl hydroxylation in collagen type I isolated from P3H1 null mice. In line with this result, lysyl hydroxylation was shown to be increased in collagen type I from CRTAP-null and P3H1-null fibroblasts than in control collagen that is normally present (Barnes et al., 2006; Cabral et al., 2007). Mutations in P3H1, PPIB and CRTAP all result in telopeptide lysine over-hydroxylation, while mutations in LH2 or FKBP10 result in telopeptide lysine under-hydroxylation (Hudson et al., 2015). Moreover, in the P3H3 null mice, collagens had under-hydroxylated lysine residues and deficiency of crosslinking (Hudson et al., 2017a; Rappu et al., 2019). Importantly, lysine underhydroxylation is seen when P3H4 is deficient and loss of P3H4 leads to the instability of the ER complex and results in unstable collagen with reduced extracellular crosslinking due to decreased lysyl hydroxylation (Duran et al., 2017a; Hudson et al., 2017a; Onursal et al., 2021; Salo & Myllyharju, 2021). Finally, the alterations in gene expression and modification induced by P3H1 deficiency highlight the importance of target specificity when targeting the collagen biosynthesis pathway for antifibrotic treatment, as well as our discovery of P3H4 and FKBP10 as drug targets in pulmonary fibrosis.

Interestingly, preliminary data from our laboratory showed that Nintedanib treatment of phLFs reduced P3H4 mRNA and protein levels (Source: Larissa Knüppel). The fact that P3H4 is required for LH1 activity and hence for collagen fibril formation and stabilization provides an additional aspect of why targeting P3H4 may be beneficial for IPF treatment (Knüppel et al., 2017; Shao et al., 2018a; Yamauchi & Shiiba, n.d.).

4.4.2 Collagen Chaperones

HSP47 is an ER resident chaperone with a high collagen-binding affinity that is required for procollagen folding and function (Ito & Nagata, 2019; Köhler et al.,

2020; Tasab et al., 2000). Targeting the binding interactions of HSP47 with collagen has been considered as a promising therapeutic approach for the treatment of diseases linked with HSP47 overexpression. Therefore, various types of small compounds for inhibition of HSP47 have been developed (Katarkar et al., 2015; Okano-Kosugi et al., 2009). Recently, it was discovered that one of these molecules (COM IV) may prevent lung fibroblast migration and collagen synthesis (Miyamura et al., 2020). For example, antisense oligonucleotides (ASOs) against HSP47, reduced collagen accumulation in various fibrosis models (Miyamura et al., 2020), as well as ND-L02-s0201, which is a lipid nanoparticle encapsulating a siRNA that limits expression of *HSP47*, showed significant anti-fibrotic effects in two chronic rodent lung fibrosis models (Y. Liu et al., 2021).

Furthermore, previous research demonstrated cooperation between HSP47 and FKBP10 during the synthesis of type I procollagen (Duran et al., 2015). Mutations in the genes *HSP47* and *FKBP10*, which encode HSP47 and FKBP10, respectively, result in a severe form of *osteogenesis imperfecta* (Christiansen et al., 2010; Duran et al., 2015). HSP47 and FKBP10 are both upregulated in IPF (Okuno et al., 2021; Schiller et al., 2015; Claudia A. Staab-Weijnitz et al., 2015b). Their deficiency is associated with reduced collagen secretion, cross-linking, and fibrillogenesis. HSP47 knockdown reduced type I collagen expression in lung fibroblasts. Accordingly, the HSP47 inhibitor reduced type I collagen expression in lung fibroblasts in presence of TGF-β1 (Chu et al., 2019; Lindert et al., 2015; Miyamura et al., 2020; Claudia A. Staab-Weijnitz et al., 2015a; Taguchi & Razzaque, 2007).

However, a recent study showed that only the secretion of FN was decreased after HSP47 was silenced; in contrast, myofibroblast differentiation and the production, and deposition of collagen remained unchanged, indicating that further research is needed to discover how inhibiting HSP47 effects fibrosis (Ruigrok et al., 2021).

4.4.3 Propeptide Proteinases

Specific procollagen proteinases, such as members of the ADAMTS protease family, bone morphogenetic protein 1 (BMP1), and the meprins, cleave the N- and C-terminal propeptides after collagen secretion (Onursal et al., 2021; S.

Ricard-Blum, 2011; Sorushanova et al., 2019b). Studies revealed that ADAMTS-2-deficient mice had slower collagen deposition rates than WT mice (Kesteloot et al., 2007). However, it has been shown that even in the absence of the particular ADAMTS-2, a large percentage of the type I procollagen N-propeptides were still cleaved, and the deficiency of ADAMTS did not affect the processing of collagen I or the structure of collagen fibrils and cartilage (LI et al., 2001).

BMP1 has long been suggested as a potential therapeutic target for fibrotic disorders (Turtle & Ho, 2004). Inhibition of BMP1 by small molecules or antibodies has also been demonstrated to reduce liver fibrosis (Grgurevic et al., 2017). Although several potent small compounds containing hydroxamic acid have been found to inhibit BMP1 in the past, none of them have made it to clinical trials (Fish et al., 2007; Kallander et al., 2018).

BMP1 expression was discovered to be increased in both fibrotic mouse lungs and human IPF lungs. BMP1 deficiency, however, did not prevent mice from bleomycin-induced lung fibrosis. Furthermore, the production of C-term propeptide of type I procollagen in fibrotic mouse lungs was not significantly affected by BMP1 deficiency, implying that BMP1 is not critical for lung fibrosis in mice and may not be an efficient therapeutic target for IPF (Ma et al., 2022).

4.4.4 Lysyl oxidases

As already known, the maturity of collagen fibers is determined by the intermolecular cross-linking levels, and enzymes including lysyl oxidases are required for further cross-linking. Selective inhibition of LOXL2 activity has previously been studied as a potential treatment for IPF. However, clinical trials on simtuzumab, a monoclonal antibody against LOXL2, in phase II were terminated due to a lack of efficacy (Barry-Hamilton et al., 2010a; Ganesh Raghu et al., 2017; Tjin, White, Faiz, Sicard, Tschumperlin, Mahar, Kable, & Burgess, 2017). Although inhibition of cross-linking enzymes was found to be beneficial in fibrosis models, cross-linking occurs after the formation of collagen fibrils, and thus non-specific inhibition of several cross-linking enzymes is required for positive results, as previously reported (Aumiller et al., 2017; Knüppel et al., 2017; Tjin, White, Faiz, Sicard, Tschumperlin, Mahar, Kable, Burgess, et al., 2017).

However, in contrast to the approach mentioned previously, the method proposed in recent studies targets a particular downstream event in a fibrotic cascade. Restricting tissue fibrosis by directly targeting collagen fibril formation or intracellular collagen maturation is a novel concept that may be a more promising strategy for combating IPF disease progression than targeting extracellular collagen cross-linking. Moreover, both of the approved IPF drugs act on these levels, providing evidence in support of the concept that inhibiting the formation of collagen fibrils could be a potential antifibrotic strategy (Knüppel et al., 2017; Petrides & Brenner, 2012)**.**

4.5 Limitations

As with the majority of studies, our study also has limitations that could be addressed in future research. First, the functional analysis of P3H4 was only performed in a 2D environment using phLFs cell culture, the relevant cell type, and physiologically relevant concentrations of TGF-β1 and 2-phosphoascorbate. However, 3D *in vitro* models such as precision-cut lung slices (PCLS), hydrogels, and lung organoids have emerged as powerful methods for revealing different cellular and molecular signaling pathways activated during fibrotic processes. These systems could help us better understand the regulation and function of therapeutic targets in a 3D environment (Alsafadi et al., 2017; Nizamoglu et al., 2022; Vazquez-Armendariz et al., 2022). Our findings can be further investigated in a 3D cell culture system that mimics fibrosis *ex vivo* using a murine PCLS system. The second limitation is that the impact of P3H4 deficiency was not investigated in an *in vivo* model of lung fibrosis. P3H4 knockout mouse model of lung fibrosis would allow us to validate our findings *in vivo*. In previous studies, two strategies were used to inactivate the murine *P3H4* gene in embryonic stem cells. The first one was produced by introducing flanking loxP sites into the floxed *p3h4* gene and mating the generated mouse with a Cre-recombinase-expressing mouse. Because of the close proximity of the *Fkbp10* gene, the P3H4 knockout mouse was generated by conditionally targeting the last two exons (7 and 8) of P3H4, thereby excluding the potential impact on *FKBP10* expression (Heard et al., 2016a). Gene trap insertional mutagenesis was used to create the second

mouse model (Gruenwald et al., 2014). Each P3H4 knockout mouse model's generation and characterization have been described (Gruenwald et al., 2014; Heard et al., 2016b). Moreover, it is important to emphasize that adult P3H4 knockout mice didn't show lethality (Heard et al., 2016a), in contrast to FKBP10 knockout animals, which are embryonically lethal (Lietman, 2014, 361). However, conditional FKBP10 knockout mice have already been obtained from our collaboration partner Brendan Lee (Baylor College of Medicine,Texas), and an effort for FKBP10 knockout validation is currently underway in our laboratory (Lietman et al., 2014)**.** Thus, if an efficient FKBP10 knockout is achieved, *in vivo* validation of the effect of deficiency of FKBP10 on P3H4 expression could be possible, even in an *in vivo* fibrosis model using this mouse model.

4.6 Conclusion and future directions

In conclusion, our results showed, for the first time, that P3H4 is a novel regulator of collagen biosynthesis in lung fibroblasts and that P3H4 deficiency entails a variety of beneficial ECM-altering effects that may result in a broadly altered ECM architecture and be effective at preventing the development of IPF pathology. Moreover, our study presents multiple pieces of evidence that P3H4 and FKBP10 may reciprocally regulate each other. Therefore, P3H4 may mediate some of the previously described effects of FKBP10 on the ECM, and by decreasing P3H4 expression in lung fibroblasts, FKBP10 inhibition may also have an additional antifibrotic effect. Importantly, our findings indicate that not all components of the collagen biosynthetic machinery can be targeted to prevent lung fibrosis and that P3H4 represents a promising therapeutic target for IPF treatment. Overall, using a combination of *in vivo* and *in vitro* models as well as clinical samples, the study presents, for the first time, a thorough investigation of P3H4 localization, regulation, and function in lung fibrosis. The findings argue for a critical role of P3H4 in biosynthesis and secretion of collagen in lung fibroblasts in the context of lung fibrosis.

Several inhibitors against intracellular and extracellular components involved in collagen biosynthesis and maturation have been developed and studied previously, whereas P3H4 inhibition alone may already be highly efficient in the reduction of fibrotic characteristics. P3H4 deficiency in phLFs reduced collagen I expression and secretion as well as the expression of other fibrotic markers including FN and α-SMA, as well as CTHRC1, a marker for pathologic fibroblasts in pulmonary fibrosis. As mentioned previously, P3H4 knockdown has been found to inhibit bladder cancer cell proliferation, cell cycle, invasion and migration *in vitro* (Hao et al., 2020). It is tempting to assume that lung fibroblast migration may also be impacted by P3H4 deficiency. Given that P3H4 is essential for the correct assembly and cross-linking of collagen fibrils(Heard et al., 2016a), and that this study showed its impact on collagen secretion and the expression of fibrotic markers, P3H4 may reveal to be a very effective drug target for the treatment of IPF. Importantly, deficiency of P3H1, another collagen leprecan family member which also upregulated in IPF and involved in collagen hydroxylation, resulted in significantly increased expression of collagen I in mouse tenocytes, indicating that not all the prolyl-3-hydroxylases mediating collagen biosynthesis can be targeted in IPF treatment, and highlighting P3H4 as a better drug target.

Finally, we were able to identify the interaction between FKBP10 and P3H4. However, how these two proteins interact with each other exactly, remains elusive. Given that P3H4 and FKBP10 are both regulated by a common bidirectional promoter and likely share common regulatory elements, performing promoter analysis could help us to better understand how these two genes are regulated. Therefore, future work will include promoter analysis of FKBP10 and P3H4 to gain more insight into their reciprocal regulation. *ETV4* has been found to bind specifically to the P3H4 promoter region and to activate its transcription (Hao et al., 2020). Moreover, I have performed promoter analysis by using several tools including JASPAR (https://jaspar.genereg.net/), and Swissregulon (https://swissregulon.unib s.ch/sr/swissregulon). Promoter analysis has identified two potential common transcription factors including *PATZ1* and *SP1* that regulate P3H4 and FKBP10. Therefore, a functional analysis of these transcription factors may provide a crucial hint as to how both genes are regulated.

The potential of P3H4 as a therapeutic target in IPF highlights the need for the development of effective P3H4 inhibitors, which could potentially alter the pulmonary fibrotic process, resulting in a clinically beneficial effect. Although drug-like small molecules can directly target proteins, small molecules are restricted by the necessity to interact with the active site of a druggable target, which is typically more conserved (Hughes et al., 2011). However, approaches including nuclear magnetic resonance-based screening, microarray methods, and *de novo* binding site identification have been used to discover ligands for non-enzyme targets (Makley & Gestwicki, 2013). The development and *in silico* screening of small molecule inhibitors against P3H4, which has a single domain in its structure, may thus be feasible. Furthermore, monoclonal antibodies can interact with a wider region of the target molecule's surface (Hughes et al., 2011), also, allowing them to bind intracellular proteins (intrabodies) (C. Zhang et al., 2020). In addition, the efficient delivery of siRNA targeting P3H4 to bladder cancer tumors using polyarginine nanoparticles, which effectively encapsulate siP3H4 and deliver them to tumor sites, has been reported as an alternative strategy to inhibit P3H4, thus bladder cancer therapy (Hao et al., 2022). Furthermore, an ASO-based strategy to inhibit P3H4 may have a higher success rate. HSP47 ASO has been already shown to inhibit the production of collagen chaperone HSP47 and prevent pulmonary fibrosis in rats (Hagiwara et al., 2007). Another promising finding has been archived, demonstrating lung fibroblasts as highly susceptible cells to locally administered ASOs and well aligned with ASOs as therapeutics (Shin et al., 2022).

In conclusion, although many inhibitors of intracellular and extracellular molecules involved in collagen biosynthesis and maturation have been developed and tested, targeting P3H4 alone may already be very effective in reducing fibrotic characteristics. P3H4 deficiency has a variety of ECM-altering effects that may be effective at preventing the development of IPF pathology. Our findings support the concept of interfering with collagen biosynthesis and maturation as a promising therapeutic approach for IPF, with a focus on targeting P3H4. Thus, we propose P3H4 as a novel therapeutic target for IPF treatment.

5. Material and Methods

5.1 Material

The primers listed in **Table 2** were purchased from MWG Eurofins (Ebensburg, Germany). Primary antibodies that are used in the different applications are shown in **Table 3**. Secondary antibodies that have fluorescently-labeled and HRP-linked (GE Healthcare Life Sciences, Freiburg, Germany) and are shown in **Table 4.**

5.2 Biobank and ethical guidelines for obtaining human samples

Lung tissue slides from donors and patients with IPF were retrieved from the CPC-M BioArchive at the Comprehensive Pneumology Center (CPC, Munich, Germany). Ethical approval for this study was obtained from the local ethics committee of the Ludwig-Maximilians University of Munich, Germany (Ethic vote #333-10). All human specimens used for this study were provided by the BioArchive CPC-M at the Comprehensive Pneumology Center (CPC, Munich, Germany). All of the study participants accepted to have their lung tissue used for research and gave written informed consent.

5.3 Transcriptomic Data

The SurePrint G3 Mouse GE 8x60k microarrays (AMADID 28005, Agilent Technologies) were used for gene expression microarray analysis. Total RNA (60 ng) was labeled and hybridized to the array slides according to the manufacturer's protocol by using the Low Input Quick Amp Labeling Kit (Agilent Technologies, one-colour) (Michna et al., 2016). Following scanning, the raw data text files were subjected to data analysis using the R statistical platform. Data quality assessment, filtering, preprocessing, standardization and differential analysis were carried out using the Bioconductor R-packages limma (Ritchie et al., 2015) and Agi4x44Preprocess (PreProcessing of Agilent 4x44 array data with R package

version 1.16.0., Lopez-Romero). Top differentially expressed genes were visualized using the heatmap function in Excel. Transcriptomic analysis was performed by Dr. Kristian Unger (Department of Radiation Oncology and Research Unit Radiation Cytogenetics at Helmholtz Zentrum München).

5.4 Proteomic Analysis from FKBP10 Knockout Embryonic Mice

5.4.1 Protein isolation from embryonic mouse lungs

The embryonic mouse lungs (20 mg) harvested at embryonic day 18.5 (E18.5) from FKBP10 heterozygote, homozygote and WT embryonic mouse were kindly provided by Caressa D. Lietman and Brendan Lee, from Baylor College of Medicine, Houston, TX, USA (Lietman et al., 2014). The embryonic mouse lungs were divided into two vials for protein and RNA isolation and freezed back at -80°C. Homogenization of frozen tissue with the Dismembrator and protein isolation of embryonic mouse lungs have been done by Elisabeth Hennen, a technical assistant in our lab. For isolation of protein, lung tissue frozen at -80°C was homogenized using the Micro-Dismembrator (Sartorius, Gottingen, Germany). To harvest protein lysates, 200 µl of radio-immunoprecipitation assay (RIPA) buffer containing phosphatase inhibitor cocktail (Roche, PHOSS-RO) and protease inhibitors (#05892970001, Roche, Switzerland) were added to the vials, re-suspended, then incubated for 30 minutes on ice. The suspension was put in to a 1.5 ml reaction tube, after that, the lysates were clarified with brief sonification and centrifugation for 15 minutes at 15.000 rpm at 4°C. The supernatant protein lysate was transferred to a new 1.5 ml reaction tube. Using the Pierce BCA Protein Assay Kit (#23225ö Thermo Scientific), the concentration of the supernatant was determined.

5.4.2 Proteomic analysis from embryonic mouse lungs

For each sample from FKBP10 heterozygote, homozygote, and WT embryonic mouse lungs, 10 µg of isolated proteins in a 0.8 ml collection tube were then sent to the Research Unit Protein Science (PROT) and Metabolomics and Proteomics

Core (MPC) at Helmholtz Zentrum München for proteomic analysis which was performed by Juliane Merl-Pham. Each 10 µg of protein extract sent from our laboratory was digested according to an established FASP protocol (Wiśniewski et al., 2009; Grosche et al., 2015). Dithiothreitol and iodoa-cetamide were used to reduce and alkylate proteins in solution. The denatured protein samples were then centrifuged using a 30 kDa filtration device (PALL) after being diluted to 4M urea. Using trypsin and Lys-C, proteins were digested overnight on the filter, after several rounds of washing with 8 M urea and 50 M ammonium bicarbonate. The generated peptides were centrifuged to elute them, then they were stored at -20°C after being acidified with TFA. Following preparation of sample and LC-MS/MS processing, quantitative data analysis was carried out, as previously explained, using Progenesis QI for proteomics (Nonlinear Dynamics, edition 4.1, part of Waters) for label-free protein quantification (Hauck et al., Molecular & Cellular Proteomics, 2010; Merl et al., Proteomics, 2012). All of the MSMS spectra data were saved as mgf files and the features of charges 2 - 7 were used. The version 2.6.2 of Mascot software was used to perform a peptide search against the Ensembl database of mouse proteins (54197 sequences, 24204564 residues, release 80). The following search parameters were used: oxidation of methionine and proline; allowance of 0.02 Da fragment; carbamidomethyl on cysteine as a fixed modification; allowance of one missed cleavage; deamidation of asparagine and glutamine allowed as a variable modification. Peptide false discovery rate (FDR) after using percolator algorithm (Brosch et al., Proteome Research, 2009) was 0.88%. The search results were reimported into the Progenesis QI software. Protein quantification was performed by adding the abundances of all unique peptides per protein following total protein normalization. The normalized protein abundances obtained were used to calculate fold-changes between conditions and statistical values using the Student's t-test.

5.5 Cell Culture

5.5.1 Isolation and Culture of phLFs

As previously explained, PhLFs were isolated and cultured (Staab-Weijnitz et al., 2015). For this study, phLFs were used in passages 3-6. The cells were suspended and cultured on 10 cm cell culture dishes in DMEM / F-12 (Life Technologies, USA), supplemented with Penicillin/Streptomycin (Life Technologies) and 20% FBS (Pan Biotech), and incubated under normal conditions of 37°C, 5% CO2 and 95% air humidity. The fibroblast cell culture medium was changed every other day until the cells reached 85–90% confluence. After washing with PBS, by using 2 ml of 0.25% Trypsin-EDTA (#25200056, Gibco) per dish, the cells were detached. 8 ml of DMEM / F-12 medium was added to each dish, and the cell suspensions from the dishes were combined and incubated at 37°C.

5.5.2 Transfection of phLFs

Gene silencing experiments in phLFs were carried out by using the pre-designed double-stranded silencer RNA (siRNA) and Lipofectamine RNAiMAX (Life Technologies, 13778150) as per the manufacturer's instructions. For this study, cells were seeded with a density of ~17.000 cells per cm² in 6-well plates and transfected in the presence of Lipofectamine RNAiMAX either with human P3H4 siRNA (Thermo Fisher Scientific, s20829), human FKBP10 siRNA (Thermo Fisher Scientific, s34171) or negative control siRNA (Life Technologies, 4390843) in a final concentration of 10 nM. Respective siRNAs and Lipofectamine RNAiMAX were mixed in OptiMEM I (Invitrogen, 31985047) and incubated at room temperature (RT) for 20 minutes. After adding 0.5 ml of transfection reagents mixture to 2.5 cell suspension for a total of 3 ml per well, plates were incubated under normal conditions of 37°C, 5% CO2 and 95% air humidity. Upon transfection, the medium was aspirated, cells were rinsed with PBS, and then incubated for 24 hours in starvation medium (DMEM/F12 supplemented with 0.5% FBS). 0.1 mM of 2-phospho-L-ascorbic acid (Sigma-Aldrich, St. Louis, USA) was added to the starvation medium to assess collagen secretion.

5.5.3 Treatment of phLFs with TGF-β1

After being starved in starvation medium for 24 hours, cells were treated with recombinant human TGF-β1 (R&D Systems, Minneapolis, USA) for 24 or 48 hours with a total concentration of 2 ng/ml in starvation medium containing 0.1 mM 2-Phospho-L-ascorbic acid. Following TGF-β1 treatment, cell culture supernatant was collected for total collagen secretion analysis, and before being extracted for protein and RNA analysis, cells were washed in PBS.

5.6 RNA Analysis

5.6.1 Primers

Table 2: List of primers used for qRT-PCR analysis. Primers were synthesized by MWG Eurofins (Ebersberg, Germany).

Target Gene	Species	Forward primer (5′-3′)	Reverse primer (5′-3′)
ACTA2	human	CGAGATCTCACTGACTACCTCATGA	AGAGCTACATAACACAGTTTCTCCTTGA
COL1A1	human	TACAGAACGGCCTCAGGTACCA	ACAGATCACGTCATCGCACAAC
CTHRC1	human	TAGGAGCATCACAGTCAAG	GCACATTCCATTATACTTCC
DHX8	human	TGACCCAGAGAAGTGGGAGA	ATCTCAAGGTCCTCATCTTCTTCA
FKBP10	human	CGACACCAGCTACAGTAAG	TAATCTTCCTTCTCTCTCCA
FN1	human	CCGACCAGAAGTTTGGGTTCT	CAATGCGGTACATGACCCCT
P3H4	human	AGGAGGCCATGCTCTA	TCTCCTCCAGCTCCAT
Col1a1	mouse	CCAAGAAGACATCCCTGAAGTCA	TGCACGTCATCGCACACA
CRTAP	mouse	ACTTCAAGGACTTCTACCTG	TCACAACGAATCTTACACTC
Fkbp10	mouse	GGACGTGTGGAACAAAGCAG	AGCGCACAAAGTCACTGTTC
Fkbp10	mouse	GGACGTGTGGAACAAAGCAG	AGCGCACAAAGTCACTGTTC
Glt25d1	mouse	GCACCCAATGTCAGAA	CTCATTATTCCACACAACTG
Glt25d2	mouse	GAACGAGCCAGAGTCTTAC	GGATGTAATCTGACCATTTT
Hprt	mouse	ATAGTGATAGATCCATTCCTATGACTG	TTCAACAATCAAGACATTCTTTCCA
Lh1	mouse	CTCTTCGTTGACAGTTATGA	CTTGGTATAAAAGAGCTGGT
Lh2	mouse	TTACACTGTGAAGGTTCTTG	GTAGTGCTCCATAGCTTCTT
Lh3	mouse	ATTGCTGGTGATCACTGT	AATCACGTCGTAGCTGTC
P3h1	mouse	CCATCACAGATCATTACG	CAATGTTGTAGTAGGCAAAC
P3h2	mouse	GCAATCGCAGATCACTAT	AACTGGAGGTAGTCGTAATG

P3h3	mouse	GCCTACTACCAGTTGAAGAA	GCAGACATCCTTCTGTACTTA
P3h4	mouse	ATATATGACGGTCTTTGCTC	TGTCCAGAGTTCCTGCTA
P3h4	mouse	TTTGCCTACTACAAACTGAAT	ATGTGTGTGAAGTCTAGCAA
P4ha1	mouse	AGCCGAGCTACAGTACAT	ACAGCCAAGCACTCTTAG
P4ha2	mouse	GTGAAGACTGCAGAGCTATT	AAGGGTCGCCTTGAG
P4ha3	mouse	GGAGGAATGTGGTACATAGT	CATAGGCCACCTTGC

5.6.2 RNA-extraction and cDNA synthesis

RNA extraction from cultured phLFs was performed using the peqGold Dnase I Digest Kit (#12-1091-02, Peqlab) and peqGOLD Total RNA isolation Kit (#12-6834-02, Peqlab) according to manufacturers' instructions. Using a NanoDrop 1000 spectrophotometer (NanoDrop, Wilmington, Germany), by measuring the absorbance at 260 nm, total concentration of RNA was determined. RNA was eluted by adding 35 µl RNase free water (Gibco, 10977) and incubating for 3 minutes at RT before centrifugation for 1 minute at 5000 g. RNA lysates were either used instantly for reverse transcription or stored at -80°C in 1.5 ml collection tubes.

Reverse transcription of the RNA into complementary DNA (cDNA) for qRT-PCR analysis was performed by using reverse transcriptase (#28025013, Invitrogen) and random hexamer primers (Applied Biosystems, N8080127). For each individual sample, 1 g RNA was calculated and diluted to 20µl with RNase-free water in 0.5 ml SafeSeal reaction tube (Sarstedt). The RNA samples were then denatured for 10 minutes at 70°C to remove secondary and tertiary RNA structures. 20 µl of cDNA synthesis master mix (8 µl 5x First – Strand Buffer, 4 µl 0.1 M DTT, 2 µl dNTP's (10 mM each), 2 µl 50µM Random Hexamers, 1 µl 10 U/µl Rnase Inhibitor, 0.5 µl 200U/µl MuLV Reverse Transcriptase, 2.5 µl RNase-free water) was added to all of the samples, then mixed. For cDNA synthesis, a total volume of 40µl was heated for 60 minutes at 37°C and then incubated for 10 minutes at 75°C. The synthesized cDNA was diluted in 160 µl RNase free water to reach a final concentration of 5 µg/ml and was stored at -20°C for using in qRT-PCR analysis.

5.6.3 Primer Design

Using the primer BLAST tool from NCBI, reverse and forward primers were designed for the intended target mRNAs. Primer length was determined to be between 18 and 22 base pairs, the melting temperature (Tm) between 57 and 61°C, with an optimum Tm of 60°C, and GC-% content between 40 and 55%.

5.6.4 Real-Time Quantitative Reverse Transcriptase Polymerase Chain Reaction Analysis

Using validated primer pairs, qRT-PCR analysis was carried out to amplify and identify particular mRNA-sequences that had already been converted into cDNA. The primers were diluted to 100pmol/l each with DNase/RNase free water according to the Oligonucleotide Synthase Report, and a primer mix was prepared of 10 pmol/l forward and reverse primers. For every reaction, a master mix containing 1.5 µl DNase/RNase free water, 5 µl Light Cycler 480 SYBR Green I Master (#04 887 352 001, Roche), and 1 µl of primer mix was prepared. A total of 7.5 µl of master mix and 2.5 µl of cDNA were mixed and placed in duplicates in a 96-well PCR plate (#712282, Biozym) for each target and housekeeper. The PCR plate was then sealed with adhesive Clear PCR Seal (Biozym, 600208) and centrifuged for 1 minute at 1000 rpm before running the Light Cycler 480 II's (27047, Roche) SYBR standard program. The housekeeping genes DEAH-box helicase 8 (DXH8) and hypoxanthine-guanine phosphoribosyltransferase (HPRT) were utilized to normalize the gene expression of the samples obtained during distinct conditions. For each condition, ΔCt(sample) was calculated as “Ct (target gene) - Ct (reference gene)” and data were presented as – ΔCt values.

5.7 Protein analysis

5.7.1 Protein extraction and concentration determination

Lung tissues from IPF patients and donors were retrieved from the UGMLC Giessen Biobank, a member of the DZL platform biobanking, and the CPC-M bioArchive at Comprehensive Pneumology Center (CPC). Tissue homogenization and protein extraction from total lung tissue were carried out as previously described (Claudia A. Staab-Weijnitz et al., 2015a).

For protein isolation from cultured phLFs in 6 well plates, cells were rinsed with ice-cold PBS and scraped with a cold plastic cell scraper in 80 µl ice-cold RIPA buffer (50 mM Tris-HCl, 150 mM NaCl, pH 7.6, 1% Triton X-100, 0.5% sodium deoxycholate and 0.1% SDS) included PhosSTOP phosphatase inhibitor cocktail (#4906837001, PHOSS-RO, Roche) and cOmplete™ protease inhibitor cocktail (#05892970001, Roche, Switzerland). The cell lysates were transferred to a 1.5 ml reaction tube and incubated on ice for 30 minutes before centrifugation at 15.000 rpm for 15 minutes at 4°C. Pellets were discarded and the supernatant's protein concentration was measured using the Pierce™ BCA (Bicinchoninic acid) Protein Assay (Thermo Fisher Scientific, Rockford, USA, 23225) according to the manufacturer's instructions. The supernatant then was stored at -20°C to use for SDS-PAGE and WB analysis.

5.7.2 SDS-PAGE, WB analysis and immunochemical protein detection

Protein samples were denatured at 95°C for 5 minutes in 6X laemmli buffer (100 mM DTT, 2% SDS, 65 mM Tris-HCl pH 6.8, 0.01% bromophenol blue, 10% glycerol). The samples were then loaded into the gel (%10 or %12) and separated from each other using SDS-PAGE gel electrophoresis as per their sizes. Protein samples were transferred from the gel to methanol-activated (incubated in methanol for 30 seconds) millipore polyvinylidene difluoride (PVDF) membranes by applying an electrical current (90 V for 85 minutes).To prevent nonspecific binding, the membranes were then blocked for 60 minutes at RT with shaking in a blocking buffer prepared with 5% milk in 1X TBST (0.1% Tween®20 in TBS buffer).The PVDF membranes were then rinsed and washed three times for 5 minutes with 1X TBS-T before being incubated overnight at 4°C with a primary antibody solution (diluted in BSA blocking buffer 5% in TBS with 0.02% sodium azide) specific for the target proteins of interest. The membranes were subsequently washed three times (10 minutes each) with 1X TBS-T, followed by an hour of shaking, and incubated with the appropriate secondary antibody solution at RT. The membranes were washed three times (10 minutes each) in 1X TBS-T, shaking at RT, to remove any unbound secondary antibodies.

A suitable chemiluminescent substrate working solution (SuperSignal™ West-Dura Extended Duration Substrate or Femto Maximum Sensitivity Substrate,

Thermo Fisher Scientific) was prepared, then added to the membrane and incubated for 1 minute. The proteins were then detected using the imaging system of ChemiDocXRS+ (Bio-Rad, Munich, Germany). Using the version 6.0.1 of Image Lab software (Bio-Rad, Hercules, CA), detected bands were quantified, and relative protein abundance was determined by dividing the target protein's band intensity by the band intensity of the loading control (β -actin) from the same sample. The list of primary (Table 2) and secondary (Table 3) antibodies that were used are as follows:

Table 3: Primary antibodies for WB analysis

Target Protein	Host	Cat#	Provider	Application
Collagen 1	Rabbit	ab260043	Abcam	WB
Collagen Type I	Rabbit	600-401-103-0.1	Rockland	WB
CTHRC1	Rabbit	16534-1-AP	Proteintech	WB
FKBP10	Rabbit	12172-1-AP	Proteintech	WB,IF
FN	Rabbit	ab199056	Santa Cruz	WB
P3H1	Rabbit pc	HPA012113	Atlas	WB
P3H2	Rabbit pc	HPA007890	Atlas	WB
P3H3	Rabbit pc	16023-1-AP	Proteintech	WB
P3H4	Mouse	sc-514276	Santa Cruz	IF
P3H4	Mouse	H00010609-B01P	Novus Biologicals	WB,IF
P3H4	Rabbit	15288-1-AP	Proteintech	WB,IF
PPIB	AB_2169138	PA1-027A	Invitrogen	WB
α-SMA	Mouse	A5228	Sigma Aldrich	WB,IF
β-actin	HRP-conjugated	A3854	Sigma Aldrich	WB

WB, Western Blot; IF, immunofluorescent staining.

Table 4: Secondary antibodies for IF-staining

Product	Provider	Cat#	Dilution	Application
Goat anti-Rabbit IgG- Alexa Fluor 488	Thermo Fisher Scientific	A-11008	1:500	IF
Donkey anti-Mouse IgG- Alexa Fluor 568	Thermo Fisher Scientific	A-10037	1:500	IF
Donkey anti-Mouse IgG- Alexa Fluor 488	Thermo Fisher Scientific	A-21202	1:500	IF
Goat anti-Rabbit IgG-Alexa Fluor 568	Thermo Fisher Scientific	A-11011	1:500	IF
Amersham ECL Rabbit IgG, HRP-linked $F(ab')_2$ fragment (donkey), monoclonal	GE Healthcare Chicago, USA	NA934	1:50000	WB
Amersham ECL Mouse IgG, HRP-linked whole Ab (sheep), monoclonal	GE Healthcare Chicago, USA	NA931	1:50000	WB

WB, Western Blot; IF, immunofluorescent staining.

5.7.3 Quantification of Secreted Collagen in cell culture supernatants

For each condition, 1 ml of cell culture supernatants were collected in 1.5 ml protein LoBind tubes (Eppendorf, 0030 108.116), in duplicate, and stored at -80°C. Using the Sircol Collagen Assay Kit (#S1000, Biocolor) in accordance with the manufacturers' instructions, the total amount of collagen secreted was quantified. First, standard solutions in 15 ml falcons were prepared with established collagen contents that ranged from 0 g to 30 g. As a diluent and blank solution, starvation medium was used. After thawing the supernatants, 200 µl of the kit's cold Isolation and Concentration Reagent was added to 1ml of cell supernatant, 1 ml standard dilutions, and 1ml blank solution. The mixture was then incubated overnight at 4°C on an ice-water mix. The tubes were then centrifuged at 14000 RPM for 30 minutes. The supernatant was then carefully removed by inverting the tubes. 1 ml Sircol Dye Reagent was added to each tube and was mixed by inverting. Using a thermomixer, the tubes were then gently shaken at 400 RPM for 30 minutes at RT. The tubes were centrifuged again for 30 minutes at 14000 RPM

and depleted by inverting. Without touching the pellet, a cotton bud was used to carefully remove unbound dye from the inside of the tube and cap. 750 µl ice-cold Acid-Salt Wash Reagent was slowly added to the pellet and the tubes were then centrifuged at 14000 RPM for 30 minutes. The washing step was repeated after the washing solution was removed. 250 µl of alkali reagent was added to the tubes, and the pellet was vortexed until all bound dye dissolved. After spinning down the tubes, 200 µl of each sample was loaded to a 96-well plate for measurement. The samples were measured using the Sunrise Reader (Sunrise Reader, Tecan) at a detection wavelength of 550 nm. The concentrations of collagen were calculated using reference solutions.

5.8 Immunofluorescence staining of cultured cells and lung tissues

5.8.1 Immunofluorescence staining of FFPE mouse and human lung tissue sections

FFPE lung tissue sections from Bleo and PBS treated mouse lungs were obtained from Herbert Schiller lab at Comprehensive Pneumology Center (CPC) and Institute of Lung Health and Immunity (LHI). The bleomycin treatment experiments of mouse were performed as earlier described (Strunz et al., 2020).

For deparaffinization, the FFPE lung tissue sections from Bleo and PBS treated mouse lungs, healthy donors and patients with IPF were incubated for 30 minutes at 60°C. Slides containing the tissue sections were then incubated in xylene (twice, 5 minutes each), and then transferred to 100% EtOH for 2 minutes, 100% EtOH for 2 minutes, 90% EtOH for 1 minute, 80% EtOH for 1 minute, and 70% EtOH for 1 minute at RT. The slides were then put in citrate buffer (2.94-gram sodium citrate was dissolved in 1X PBS and adjusted pH to 6.0) to enable antigen retrieval and were heated in an 80°C water bath for 30 minutes, and then taken out to cool at RT for 30 minutes. After cooling, the slides were washed with PBS three times, each time for five minutes. For permeabilization, the slides were incubated with 0.2 % Triton X-100 in PBS at RT for 5 minutes and then were

washed three times with PBS for 3 minutes each. Slides were then incubated with blocking buffer (% 5 BSA in PBS) for one hour at RT. After aspirating the blocking buffer, the primary antibodies were diluted in %1 BSA (prepared in 1X PBS) were applied to the slides and incubated overnight at 4°C. Negative controls were prepared by adding only 1% BSA in 1×PBS to the slides. The following day, the slides were rinsed three times in 1X PBS (3 minutes each), and then 1:500 dilutions of each fluorescently-labeled secondary antibody in %1 BSA was applied to the slides for 2 hours at RT by protecting samples from light. The slides were then again rinsed 3 times in 1X PBS for 3 minutes each. After washing, the slides were covered with 25-µl drop of appropriate mounting medium with DAPI and then with a glass plate. The slides were placed in an incubator chamber, and stored in dark at 4°C until ready to image. Images were obtained with an LSM 710 Confocal Microscope using a 20X objective.

5.8.2 Cell Fixation and Immunofluorescent Staining

PhLFs were seeded on sterilized coverslips coated with poly-lysine for 30 mins, and treated before fixation and immunostaining. After aspiration cell culture medium and washing the cells with 1X PBS, the cell fixation was performed using 4% paraformaldehyde (PFA) for 10 minutes at RT. The cells were then rinsed with 1X PBS three times for 3 minutes each. For permeabilization, the cells were incubated with 0.2 % Triton X-100/1X PBS for 5 minutes at RT and then they were washed three times with 1X PBS. The cells were then blocked using % 5 BSA/1X PBS for 1 hour at RT. After 1 hour, the blocking buffer was aspirated, primary antibody diluted in %1 BSA/1X PBS was added to the cells and incubated overnight at 4°C. The following day, the cells were washed three times with 1X PBS and the secondary antibodies diluted in %1 BSA (1:500) were added to the cells for 1 hour at RT in darkness. After washing again three times with 1X PBS, the cells were mounted in mounting media with DAPI (Invitrogen, 15596276) by inverting the coverslips over the appropriate 25 µl drop of mounting media with facing down the side with cells and then slides were stored at 4°C until ready to image. Imaging was performed using LSM 710 Confocal Microscope using a 20X objective.

5.9 Proximity Ligation Assay (PLA)

PLA was performed for protein-protein interactions detection *in situ* at endogenous protein levels using Duolink® PLA kit according to the manufacturer`s instructions. PLA was carried out on phLFs and PBS/BLEO-treated mouse lung tissue sections on glass slides using immunofluorescence. Before starting, the cells were seeded on 8 well-chambered coverslips (µ-Slide, Ibidi, #80826) and fixation and permeabilization of cells were performed. For PLA on f FFPE tissue sections, deparaffinization, antigen retrieval and permeabilization were performed previously. After that, the following PLA protocol was performed for a 1 cm2 sample on a slide, using 40 µl of solution for sufficient coverage. According to reaction area and number of samples, the volume was adjusted.

After fixation/permeabilization of cells or deparaffinization/retrieval/permeabilization of tissue sections, the samples were blocked using Duolink blocking solution (Sigma) and incubated at 37°C for 60 minutes. After aspirated blocking solution, samples were incubated with FKBP10 (rabbit) (1:50) and P3H4 (mouse) (1:50) primary antibody diluted in Duolink Antibody Diluent. The samples were then incubated in a humidity chamber for 60 minutes at 37°C. Followed by two washings with 1X wash buffer A (5 minutes each) at RT, the samples were incubated with specific Duolink PLA probes Anti-Mouse MINUS (#DUO92004-30RXN) and Anti-Rabbit PLUS (#DUO92002-30RXN), diluted 1:5 Duolink Antibody Diluent for 1 hour in humidity chamber for at 37°C. The samples were again washed with 1X wash buffer A (5 minutes each) at RT and incubated with 1X Duolink Ligation buffer in a humidity chamber at 37°C for 30 minutes. After ligation step, the samples were washed once again using 1X wash buffer A and incubated with 1x Amplification buffer in humidity chamber at 37°C in dark for 100 minutes. The samples were then washed with 1X wash buffer B twice (10 minutes each) and using 0.01X wash buffer B (1 min each) at RT. For preparation of imaging, the samples were mounted using an optimum volume of Duolink *in situ* mounting medium with DAPI and incubated for 15 minutes before being analyzed with LSM 710 Confocal Microscope using 20X objective. Following imaging, the slides were stored in the dark at 4°C.

5.10 Mouse tail tendon experiments using P3H1 Null and WT mice

P3H1 null mice were provided on a C57B6 background by the Bächinger lab (Biochemistry and Molecular Biology Department, University of Oregon Health & Science, Portland) and have been described in detail in Vranka *et al* and Pokidysheva *et al* (Pokidysheva, Mizuno, et al., 2013; Pokidysheva, Tufa, et al., 2013; Vranka et al., 2010). Mouse housing and breeding was according to international standards for the use and care of experimental animals and approved by the Upper Bavarian government (ROB-55.2-2532.Vet_02-20-62).

5.10.1 Isolation of type I collagen from mouse tail tendon

Collagen Type I was extracted from tail tendon of P3H1 null and WT adult mice using procedures adapted from Rajan *et al* and Vranka *et al* (Pokidysheva, Tufa, et al., 2013; Rajan et al., 2006). Briefly, tail tendons were rinsed with PBS, chopped and digested with 0.25 mg/mL pepsin (Fisher Chemical, P/1120/46) in 0.1 M acetic acid at 4°C overnight. Undigested tendon was removed by centrifugation at 4.500 rpm for 10 minutes, followed by addition of NaCl to the supernatant up to a final concentration of 0.7 M and incubation for 24 to 72 h. Precipitated type I collagen was centrifuged at 13 000 rpm for 30 minutes and the pellet resolved in 0.05 M acetic acid. The resulting solution was dialyzed to 0.05 M acetic acid at 4°C overnight, and protein concentration estimated by measuring absorbance at 280 nm in a Nanodrop 1000 Spectrophotometer (ThermoFisher) using known concentrations of rat tail collagen (Sigma Aldrich, C3867) as standard. By using sodium dodecyl sulfate polyacrylamide gel electrophoresis(SDS-PAGE), similar amounts of type I collagen were resolved on a 7.5% gel, and identified with Coomassie Brilliant Blue (R-250, Bio Rad, #161-0436).

The described in-house procedure yields collagen of superior purity as compared to commercially available rat tail collagen (Sigma Aldrich, C3867, see Figure 26), but with a α1(I): α2(I) chain stoichiometry of 1:0.94 for mouse type I collagen as compared to 1:0.55 for rat type I collagen (obtained by iBAQ).

5.10.2 Proteomic Analysis from P3H1 Null Mice

Per sample each 10 µg of purified mouse tail collagen were reduced by adding dithiothreitol to a final concentration of 2 mM and incubating at 60°C for 10 minutes. After equilibration to RT, iodoacetamide was added to a total concentration of 6 mM and incubated for 30 minutes at RT in the dark, followed by tryptic digest (Promega, VA1060) at ratio of 1:20 overnight at 37°C for 18h. Before the mass spectrometry analysis, samples were trifluoroacetylated and stored at 20 °C.

As described previously, the LC-MS/MS analysis was carried out on a Q-Exactive HF mass spectrometer digitally paired to an UltiMate 3000 RSLCnano System (Thermo Scientific) (Merl-Pham et al., 2019; Philipp et al., 2017). 0.3 µg of purified collagen protein were briefly loaded into the trap column, then eluted and separated on the C18 analytical column after 5 minutes (nanoEase M/Z HSS T3 Column, 75 µm I.D. X 250 mm length, 100Å pore size, 1.8 µm particles, Waters) *via* a non-linear acetonitrile gradient for 90 minutes. MS and MSMS spectra have been recorded as described (Merl-Pham et al., 2019).

The acquired spectra were analyzed in the MaxQuant software (version 2.3.0.1, MPI Biochemistry Martinsried) applying default settings (Tyanova et al., 2016). Searches were performed within the MaxQuant software using the Andromeda search tool (Jürgen Cox et al., 2011) against the Swissprot mouse protein database (Release 2020_02, 17061 sequences) additionally allowing for oxidation of proline and lysine as variable modifications. LFQ (ratio count 1,(Jürgen Cox et al., 2014)), iBAQ (Schwanhäusser et al., 2013), and TOP3 (Silva et al., 2006) quantification based on unique peptides were included. Identifications were filtered for a peptide-spectrum-match and 1% false discovery rate of protein. The resulting list of protein groups including intensities, LFQ intensities, iBAQ, and TOP3 values were used for the calculation of sample purity and chain stoichiometries.

5.10.3 Analysis of amino acids

Analysis of amino acids was carried out by the Molecular Structure Facility at UC Davis (University of California, USA). In brief, 200 µl of type I collagen solution

were transferred to a hydrolysis tube and dried, followed by liquid phase hydrolysis using 200 µl 6N HCl (1% phenol) for 24h at 110°C. The hydrolysate was dried and dissolved in 50 µl Lithium citrate buffer containing 5 nmol S-aminoethyl-cysteine (AE-Cys) as internal standard and analyzed on a Hitachi L-8800 amino acid analyzer.

5.10.4 Isolation of RNA and protein from mouse tendon of P3H1 null and WT mice

RNA and protein were simultaneously extracted from mouse tendon using protocols adapted from Grinstein et al, Vorreiter et al, and Chey et al (Chey et al., 2011; Grinstein et al., 2018) as follows: Mouse tendons were washed with sterile PBS, chopped into small pieces, and homogenized in Qiazol lysis reagent using a TissueLyser II (Qiagen) in accordance with the manufacturer's instructions. For RNA extraction, 1-bromo-3-chloropropane was added, followed by vigorous shaking for 15s, 10 minutes of incubation, and centrifugation at 15.000 x g at 4°C for 20 minutes. The lower organic phase was kept on ice for isolation of protein (see below, isolation of protein). The upper colorless aqueous phase containing the RNA was transferred into clean tubes and 0.5 ml isopropanol added per ml Qiazol. Samples were vortexed for 10s, incubated for 10 minutes, and the RNA pelleted by centrifugation for at least 1h at 4°C, at 15.000 x g, the pellet was rinsed twice with 75% ethanol, allowed to dry, and finally resuspended in 12 µl RNAse free water. The concentration of RNA was measured in a Nanodrop 1000 Spectrophotometer (ThermoFisher).

For the isolation of protein, the interphase was carefully separated from the lower phase and discarded. Approximately 2.5 volumes of 100% ethanol were added to 1 volume of protein-containing solution (organic phase). Then, approximately 1 volume of bromochloropropane was added and samples were thoroughly mixed. Approximately 2 volumes of water were added, and, after repeated mixing, samples were centrifuged for 30 minutes at 12.000xg. The colorless aqueous supernatant at the top was discarded followed by addition of approximately 3 volumes of 100% ethanol to the lower phase and the interphase, for precipitation of protein. Samples were thoroughly mixed and centrifuged for 15 minutes at 12.000x g. The occured protein pellet was rinsed once with 1 ml of 100% ethanol,

briefly left to dry at room air, followed by resuspending in 4% SDS containing 1X protease inhibitor cocktail (Roche) and quantification using the Bradford assay kit (Bio-Rad). Gene expression analysis by qRT-PCR and WB was performed as described initially. Primers were synthesized by Eurofins and are listed in table 2. Primary antibodies are given in Table 3.

5.11 Statistical analysis

GraphPad Prism v8.0 analysis (GraphPad Software, CA, San Diego, USA) was used for statistical analysis. Data were shown as mean ± standard error of mean (SEM). Paired t-test or one-way ANOVA with Tukey's multiple comparison test was used for statistical analysis. Significance is demonstrated as follows: *$p<0.05$, **$p<0.01$, ***$p<0.001$.

References

Aburto, M., Herráez, I., Iturbe, D., & Jiménez-Romero, A. (2018). Diagnosis of Idiopathic Pulmonary Fibrosis: Differential Diagnosis. *Medical Sciences*, *6*(3), 73. https://doi.org/10.3390/medsci6030073

Alsafadi, H. N., Staab-Weijnitz, C. A., Lehmann, M., Lindner, M., Peschel, B., Königshoff, M., & Wagner, D. E. (2017). An ex vivo model to induce early fibrosis-like changes in human precision-cut lung slices. *American Journal of Physiology-Lung Cellular and Molecular Physiology*, *312*(6), L896–L902. https://doi.org/10.1152/ajplung.00084.2017

Aumiller, V., Strobel, B., Romeike, M., Schuler, M., Stierstorfer, B. E., & Kreuz, S. (2017). Comparative analysis of lysyl oxidase (like) family members in pulmonary fibrosis. *Scientific Reports*, *7*(1), 149. https://doi.org/10.1038/s41598-017-00270-0

Aypek, H., Krisp, C., Lu, S., Liu, S., Kylies, D., Kretz, O., Wu, G., Moritz, M., Amann, K., Benz, K., Tong, P., Hu, Z., Alsulaiman, S. M., Khan, A. O., Grohmann, M., Wagner, T., Müller-Deile, J., Schlüter, H., Puelles, V. G., Grahammer, F. (2022). Loss of the collagen IV modifier prolyl 3-hydroxylase 2 causes thin basement membrane nephropathy. *Journal of Clinical Investigation*, *132*(9). https://doi.org/10.1172/JCI147253

Azuma, A., Inomata, M., & Nishioka, Y. (2015). Nintedanib: evidence for its therapeutic potential in idiopathic pulmonary fibrosis. *Core Evidence*, 89. https://doi.org/10.2147/CE.S82905

Baldridge, D., Schwarze, U., Morello, R., Lennington, J., Bertin, T. K., Pace, J. M., Pepin, M. G., Weis, M., Eyre, D. R., Walsh, J., Lambert, D., Green, A., Robinson, H., Michelson, M., Houge, G., Lindman, C., Martin, J., Ward, J., Lemyre, E., Lee, B. (2008). CRTAP and LEPRE1 mutations in recessive osteogenesis imperfecta. *Human Mutation*, *29*(12), 1435–1442. https://doi.org/10.1002/humu.20799

Bansal, R., Nakagawa, S., Yazdani, S., van Baarlen, J., Venkatesh, A., Koh, A. P., Song, W.-M., Goossens, N., Watanabe, H., Beasley, M. B., Powell, C. A., Storm, G., Kaminski, N., van Goor, H., Friedman, S. L., Hoshida, Y., & Prakash, J. (2017). Integrin alpha 11 in the regulation of the myofibroblast phenotype: implications for fibrotic diseases. *Experimental & Molecular Medicine*, *49*(11), e396–e396. https://doi.org/10.1038/emm.2017.213

Bardou, O., Menou, A., François, C., Duitman, J. W., von der Thüsen, J. H., Borie, R., Sales, K. U., Mutze, K., Castier, Y., Sage, E., Liu, L., Bugge, T. H., Fairlie, D. P., Königshoff, M., Crestani, B., & Borensztajn, K. S. (2016). Membrane-anchored Serine Protease Matriptase Is a Trigger of Pulmonary Fibrogenesis. *American Journal of Respiratory and Critical Care Medicine*, *193*(8), 847–860. https://doi.org/10.1164/rccm.201502-0299OC

Barkauskas, C. E., Cronce, M. J., Rackley, C. R., Bowie, E. J., Keene, D. R., Stripp, B. R., Randell, S. H., Noble, P. W., & Hogan, B. L. M. (2013). Type 2 alveolar cells are stem cells in adult lung. *Journal of Clinical Investigation*, *123*(7), 3025–3036. https://doi.org/10.1172/JCI68782

Barnes, A. M., Cabral, W. A., Weis, M., Makareeva, E., Mertz, E. L., Leikin, S., Eyre, D., Trujillo, C., & Marini, J. C. (2012). Absence of FKBP10 in recessive type XI osteogenesis imperfecta leads to diminished collagen cross-linking and reduced collagen deposition in extracellular matrix. *Human Mutation*, *33*(11), 1589–1598. https://doi.org/10.1002/humu.22139

Barnes, A. M., Chang, W., Morello, R., Cabral, W. A., Weis, M., Eyre, D. R., Leikin, S., Makareeva, E., Kuznetsova, N., Uveges, T. E., Ashok, A., Flor, A. W., Mulvihill, J. J., Wilson, P. L., Sundaram, U. T., Lee, B., & Marini, J. C. (2006). Deficiency of Cartilage-Associated Protein in Recessive Lethal Osteogenesis Imperfecta. *New England Journal of Medicine*, *355*(26), 2757–2764. https://doi.org/10.1056/NEJMoa063804

Barry-Hamilton, V., Spangler, R., Marshall, D., McCauley, S., Rodriguez, H. M., Oyasu, M., Mikels, A., Vaysberg, M., Ghermazien, H., Wai, C., Garcia, C. A., Velayo, A. C., Jorgensen, B., Biermann, D., Tsai, D., Green, J., Zaffryar-Eilot, S., Holzer, A., Ogg, S., Smith, V. (2010a). Allosteric inhibition of lysyl oxidase-like-2 impedes the development of a pathologic microenvironment. *Nature Medicine*, *16*(9), 1009–1017. https://doi.org/10.1038/nm.2208

Bernard, K. (2018). Collagen Biosynthesis in Pulmonary Fibrosis: Unraveling the Metabolic Web. *American Journal of Respiratory Cell and Molecular Biology*, *58*(5), 545–546.

https://doi.org/10.1165/rcmb.2017-0350ED

Besio, R., Garibaldi, N., Leoni, L., Cipolla, L., Sabbioneda, S., Biggiogera, M., Mottes, M., Aglan, M., Otaify, G. A., Temtamy, S. A., Rossi, A., & Forlino, A. (2019). Cellular stress due to impairment of collagen prolyl hydroxylation complex is rescued by the chaperone 4-phenylbutyrate. *Disease Models & Mechanisms*. https://doi.org/10.1242/dmm.038521

Bian, Z., Miao, Q., Zhong, W., Zhang, H., Wang, Q., Peng, Y., Chen, X., Guo, C., Shen, L., Yang, F., Xu, J., Qiu, D., Fang, J., Friedman, S., Tang, R., Gershwin, M. E., & Ma, X. (2015). Treatment of cholestatic fibrosis by altering gene expression of Cthrc1: Implications for autoimmune and non-autoimmune liver disease. *Journal of Autoimmunity*, *63*, 76–87. https://doi.org/10.1016/j.jaut.2015.07.010

Biasin, V., Crnkovic, S., Sahu-Osen, A., Birnhuber, A., El Agha, E., Sinn, K., Klepetko, W., Olschewski, A., Bellusci, S., Marsh, L. M., & Kwapiszewska, G. (2020). PDGFRα and αSMA mark two distinct mesenchymal cell populations involved in parenchymal and vascular remodeling in pulmonary fibrosis. *American Journal of Physiology-Lung Cellular and Molecular Physiology*, *318*(4), L684–L697. https://doi.org/10.1152/ajplung.00128.2019

Biernacka, A., Dobaczewski, M., & Frangogiannis, N. G. (2011). TGF-β signaling in fibrosis. *Growth Factors*, *29*(5), 196–202. https://doi.org/10.3109/08977194.2011.595714

Binks, A. P., Beyer, M., Miller, R., & LeClair, R. J. (2017). Cthrc1 lowers pulmonary collagen associated with bleomycin-induced fibrosis and protects lung function. *Physiological Reports*, *5*(5), e13115. https://doi.org/10.14814/phy2.13115

Birk, D. E., Fitch, J. M., Babiarz, J. P., Doane, K. J., & Linsenmayer, T. F. (1990). Collagen fibrillogenesis in vitro: interaction of types I and V collagen regulates fibril diameter. *Journal of Cell Science*, *95*(4), 649–657. https://doi.org/10.1242/jcs.95.4.649

Birkedal-Hansen, H., Taylor, R. E., Bhown, A. S., Katz, J., Lin, H. Y., & Wells, B. R. (1985). Cleavage of bovine skin type III collagen by proteolytic enzymes. Relative resistance of the fibrillar form. *Journal of Biological Chemistry*, *260*(30), 16411–16417. https://doi.org/10.1016/S0021-9258(17)36252-X

Blaauboer, M. E., Boeijen, F. R., Emson, C. L., Turner, S. M., Zandieh-Doulabi, B., Hanemaaijer, R., Smit, T. H., Stoop, R., & Everts, V. (2014). Extracellular matrix proteins: A positive feedback loop in lung fibrosis. *Matrix Biology*,*34*,170–178. https://doi.org/10.1016/j.matbio.2013.11.002

Blokland, K. E. C., Habibie, H., Borghuis, T., Teitsma, G. J., Schuliga, M., Melgert, B. N., Knight, D. A., Brandsma, C.-A., Pouwels, S. D., & Burgess, J. K. (2021). Regulation of Cellular Senescence Is Independent from Profibrotic Fibroblast-Deposited ECM. *Cells*, *10*(7), 1628. https://doi.org/10.3390/cells10071628

Bonnans, C., Chou, J., & Werb, Z. (2014). Remodelling the extracellular matrix in development and disease. *Nature Reviews Molecular Cell Biology*, *15*(12), 786–801. https://doi.org/10.1038/nrm3904

Booth, A. J., Hadley, R., Cornett, A. M., Dreffs, A. A., Matthes, S. A., Tsui, J. L., Weiss, K., Horowitz, J. C., Fiore, V. F., Barker, T. H., Moore, B. B., Martinez, F. J., Niklason, L. E., & White, E. S. (2012). Acellular Normal and Fibrotic Human Lung Matrices as a Culture System for In Vitro Investigation. *American Journal of Respiratory and Critical Care Medicine*, *186*(9), 866–876. https://doi.org/10.1164/rccm.201204-0754OC

Bourgot, I., Primac, I., Louis, T., Noël, A., & Maquoi, E. (2020). Reciprocal Interplay Between Fibrillar Collagens and Collagen-Binding Integrins: Implications in Cancer Progression and Metastasis. *Frontiers in Oncology*, *10*. https://doi.org/10.3389/fonc.2020.01488

Brossard, C., Lefranc, A.-C., Pouliet, A.-L., Simon, J.-M., Benderitter, M., Milliat, F., & Chapel, A. (2022). Molecular Mechanisms and Key Processes in Interstitial, Hemorrhagic and Radiation Cystitis. *Biology*, *11*(7), 972. https://doi.org/10.3390/biology11070972

Burgstaller, G., Oehrle, B., Gerckens, M., White, E. S., Schiller, H. B., & Eickelberg, O. (2017). The instructive extracellular matrix of the lung: basic composition and alterations in chronic lung disease. *European Respiratory Journal*, *50*(1),1601805.

https://doi.org/10.1183/13993003.01805-2016

Burjanadze, T. V. (1992). Thermodynamic substantiation of water-bridged collagen structure. *Biopolymers*, *32*(8), 941–949. https://doi.org/10.1002/bip.360320805

Cabral, W. A., Chang, W., Barnes, A. M., Weis, M., Scott, M. A., Leikin, S., Makareeva, E., Kuznetsova, N. V, Rosenbaum, K. N., Tifft, C. J., Bulas, D. I., Kozma, C., Smith, P. A., Eyre, D. R., & Marini, J. C. (2007). Prolyl 3-hydroxylase 1 deficiency causes a recessive metabolic bone disorder resembling lethal/severe osteogenesis imperfecta. *Nature Genetics*, *39*(3), 359–365. https://doi.org/10.1038/ng1968

Caley, M. P., Martins, V. L. C., & O'Toole, E. A. (2015). Metalloproteinases and Wound Healing. *Advances in Wound Care*, *4*(4), 225–234. https://doi.org/10.1089/wound.2014.0581

Canty, E. G., & Kadler, K. E. (2005a). Procollagen trafficking, processing and fibrillogenesis. *Journal of Cell Science*, *118*(7), 1341–1353. https://doi.org/10.1242/jcs.01731

Chakraborty, A., Mastalerz, M., Ansari, M., Schiller, H. B., & Staab-Weijnitz, C. A. (2022). Emerging Roles of Airway Epithelial Cells in Idiopathic Pulmonary Fibrosis. *Cells*, *11*(6), 1050. https://doi.org/10.3390/cells11061050

Chang, W., Barnes, A. M., Cabral, W. A., Bodurtha, J. N., & Marini, J. C. (2010). Prolyl 3-hydroxylase 1 and CRTAP are mutually stabilizing in the endoplasmic reticulum collagen prolyl 3-hydroxylation complex. *Human Molecular Genetics*, *19*(2),223–234. https://doi.org/10.1093/hmg/ddp481

Chen, A. C.-H., Burr, L., & McGuckin, M. A. (2018). Oxidative and endoplasmic reticulum stress in respiratory disease. *Clinical & Translational Immunology*, *7*(6),e1019. https://doi.org/10.1002/cti2.1019

Chen, C. Z., & Raghunath, M. (2009). Focus on collagen: in vitro systems to study fibrogenesis and antifibrosis _ state of the art. *Fibrogenesis & Tissue Repair*, *2*(1), 7. https://doi.org/10.1186/1755-1536-2-7

Chen, L., Shen, Y. H., Wang, X., Wang, J., Gan, Y., Chen, N., Wang, J., LeMaire, S. A., Coselli, J. S., & Wang, X. L. (2006). Human Prolyl-4-hydroxylase α(I) Transcription Is Mediated by Upstream Stimulatory Factors. *Journal of Biological Chemistry*, *281*(16), 10849–10855. https://doi.org/10.1074/jbc.M511237200

Chen, S., & Birk, D. E. (2013). The regulatory roles of small leucine-rich proteoglycans in extracellular matrix assembly. *FEBS Journal*, *280*(10), 2120–2137. https://doi.org/10.1111/febs.12136

Chen, Y., Terajima, M., Banerjee, P., Guo, H., Liu, X., Yu, J., Yamauchi, M., & Kurie, J. M. (2017). FKBP65-dependent peptidyl-prolyl isomerase activity potentiates the lysyl hydroxylase 2-driven collagen cross-link switch. *Scientific Reports*, *7*(1), 46021. https://doi.org/10.1038/srep46021

Chen, Y., Terajima, M., Yang, Y., Sun, L., Ahn, Y.-H., Pankova, D., Puperi, D. S., Watanabe, T., Kim, M. P., Blackmon, S. H., Rodriguez, J., Liu, H., Behrens, C., Wistuba, I. I., Minelli, R., Scott, K. L., Sanchez-Adams, J., Guilak, F., Pati, D., Kurie, J. M. (2015). Lysyl hydroxylase 2 induces a collagen cross-link switch in tumor stroma. *Journal of Clinical Investigation*, *125*(3), 1147–1162. https://doi.org/10.1172/JCI74725

Chey, S., Claus, C., & Liebert, U. G. (2011). Improved method for simultaneous isolation of proteins and nucleic acids. *Analytical Biochemistry*, *411*(1), 164–166. https://doi.org/10.1016/j.ab.2010.11.020

Chien, J. W., Richards, T. J., Gibson, K. F., Zhang, Y., Lindell, K. O., Shao, L., Lyman, S. K., Adamkewicz, J. I., Smith, V., Kaminski, N., & O'Riordan, T. (2014). Serum lysyl oxidase-like 2 levels and idiopathic pulmonary fibrosis disease progression. *European Respiratory Journal*, *43*(5), 1430–1438. https://doi.org/10.1183/09031936.00141013

Chilosi, M., Caliò, A., Rossi, A., Gilioli, E., Pedica, F., Montagna, L., Pedron, S., Confalonieri, M., Doglioni, C., Ziesche, R., Grubinger, M., Mikulits, W., & Poletti, V. (2017). Epithelial to mesenchymal transition-related proteins ZEB1, β-catenin, and β-tubulin-III in idiopathic pulmonary fibrosis. *Modern Pathology*, *30*(1), 26–38.

https://doi.org/10.1038/modpathol.2016.147

Chioccioli, M., Roy, S., Newell, R., Pestano, L., Dickinson, B., Rigby, K., Herazo-Maya, J., Jenkins, G., Ian, S., Saini, G., Johnson, S. R., Braybrooke, R., Yu, G., Sauler, M., Ahangari, F., Ding, S., DeIuliis, J., Aurelien, N., Montgomery, R. L., & Kaminski, N. (2022). A lung targeted miR-29 mimic as a therapy for pulmonary fibrosis. *EBioMedicine*, *85*, 104304. https://doi.org/10.1016/j.ebiom.2022.104304

Christiansen, H. E., Schwarze, U., Pyott, S. M., AlSwaid, A., Al Balwi, M., Alrasheed, S., Pepin, M. G., Weis, M. A., Eyre, D. R., & Byers, P. H. (2010). Homozygosity for a Missense Mutation in SERPINH1, which Encodes the Collagen Chaperone Protein HSP47, Results in Severe Recessive Osteogenesis Imperfecta. *The American Journal of Human Genetics*, *86*(3), 389–398. https://doi.org/10.1016/j.ajhg.2010.01.034

Chu, H., Jin, L., & Wang, J. (2019). *HSP47 and Its Involvement in Fibrotic Disorders* (pp. 299–312). https://doi.org/10.1007/978-3-030-02254-9_14

Chuliá-Peris, L., Carreres-Rey, C., Gabasa, M., Alcaraz, J., Carretero, J., & Pereda, J. (2022). Matrix Metalloproteinases and Their Inhibitors in Pulmonary Fibrosis: EMMPRIN/CD147 Comes into Play. *International Journal of Molecular Sciences*, *23*(13), 6894. https://doi.org/10.3390/ijms23136894

Chung, H. J., Steplewski, A., Chung, K. Y., Uitto, J., & Fertala, A. (2008). Collagen Fibril Formation. *Journal of Biological Chemistry*, *283*(38), 25879–25886. https://doi.org/10.1074/jbc.M804272200

Clarke, D. L., Carruthers, A. M., Mustelin, T., & Murray, L. A. (2013). Matrix regulation of idiopathic pulmonary fibrosis: the role of enzymes. *Fibrogenesis & Tissue Repair*, *6*(1), 20. https://doi.org/10.1186/1755-1536-6-20

Clause, K. C., & Barker, T. H. (2013). Extracellular matrix signaling in morphogenesis and repair. *Current Opinion in Biotechnology*, *24*(5), 830–833. https://doi.org/10.1016/j.copbio.2013.04.011

Confalonieri, P., Volpe, M. C., Jacob, J., Maiocchi, S., Salton, F., Ruaro, B., Confalonieri, M., & Braga, L. (2022). Regeneration or Repair? The Role of Alveolar Epithelial Cells in the Pathogenesis of Idiopathic Pulmonary Fibrosis (IPF). *Cells*, *11*(13), 2095. https://doi.org/10.3390/cells11132095

Costabel, U., Behr, J., Crestani, B., Stansen, W., Schlenker-Herceg, R., Stowasser, S., & Raghu, G. (2018). Anti-acid therapy in idiopathic pulmonary fibrosis: insights from the INPULSIS® trials. *Respiratory Research*, *19*(1), 167. https://doi.org/10.1186/s12931-018-0866-0

Coward, W. R., Saini, G., & Jenkins, G. (2010). The pathogenesis of idiopathic pulmonary fibrosis. *Therapeutic Advances in Respiratory Disease*, *4*(6), 367–388. https://doi.org/10.1177/1753465810379801

Cox, Jürgen, Hein, M. Y., Luber, C. A., Paron, I., Nagaraj, N., & Mann, M. (2014). Accurate Proteome-wide Label-free Quantification by Delayed Normalization and Maximal Peptide Ratio Extraction, Termed MaxLFQ. *Molecular & Cellular Proteomics*, *13*(9), 2513–2526. https://doi.org/10.1074/mcp.M113.031591

Cox, Jürgen, Neuhauser, N., Michalski, A., Scheltema, R. A., Olsen, J. V., & Mann, M. (2011). Andromeda: A Peptide Search Engine Integrated into the MaxQuant Environment. *Journal of Proteome Research*, *10*(4), 1794–1805. https://doi.org/10.1021/pr101065j

D'Arrigo, P., Tufano, M., Rea, A., Romano, S., & Romano, M. F. (2016). FKBP (FK506 Binding Protein). In *Encyclopedia of Signaling Molecules* (pp. 1–31). Springer New York. https://doi.org/10.1007/978-1-4614-6438-9_101769-1

Datta, A., Scotton, C. J., & Chambers, R. C. (2011). Novel therapeutic approaches for pulmonary fibrosis. *British Journal of Pharmacology*, *163*(1), 141–172. https://doi.org/10.1111/j.1476-5381.2011.01247.x

De Giorgi, F., Fumagalli, M., Scietti, L., & Forneris, F. (2021). Collagen hydroxylysine glycosylation: non-conventional substrates for atypical glycosyltransferase enzymes. *Biochemical Society Transactions*, *49*(2), 855–866. https://doi.org/10.1042/BST20200767

Decaris, M. L., Gatmaitan, M., FlorCruz, S., Luo, F., Li, K., Holmes, W. E., Hellerstein, M. K., Turner, S. M., & Emson, C. L. (2014). Proteomic Analysis of Altered Extracellular Matrix Turnover in Bleomycin-induced Pulmonary Fibrosis. *Molecular & Cellular Proteomics*, *13*(7), 1741–1752. https://doi.org/10.1074/mcp.M113.037267

Degryse, A. L., Tanjore, H., Xu, X. C., Polosukhin, V. V., Jones, B. R., Boomershine, C. S., Ortiz, C., Sherrill, T. P., McMahon, F. B., Gleaves, L. A., Blackwell, T. S., & Lawson, W. E. (2011). TGFβ signaling in lung epithelium regulates bleomycin-induced alveolar injury and fibroblast recruitment. *American Journal of Physiology-Lung Cellular and Molecular Physiology*, *300*(6), L887–L897. https://doi.org/10.1152/ajplung.00397.2010

Deng, Z., Fear, M. W., Suk Choi, Y., Wood, F. M., Allahham, A., Mutsaers, S. E., & Prêle, C. M. (2020). The extracellular matrix and mechanotransduction in pulmonary fibrosis. *The International Journal of Biochemistry & Cell Biology*, *126*, 105802. https://doi.org/10.1016/j.biocel.2020.105802

Di Gregorio, J., Robuffo, I., Spalletta, S., Giambuzzi, G., De Iuliis, V., Toniato, E., Martinotti, S., Conti, P., & Flati, V. (2020). The Epithelial-to-Mesenchymal Transition as a Possible Therapeutic Target in Fibrotic Disorders. *Frontiers in Cell and Developmental Biology*, *8*. https://doi.org/10.3389/fcell.2020.607483

Dudala, S. S., Venkateswarulu, T. C., Kancharla, S. C., Kodali, V. P., & Babu, D. J. (2021). A review on importance of bioactive compounds of medicinal plants in treating idiopathic pulmonary fibrosis (special emphasis on isoquinoline alkaloids). *Future Journal of Pharmaceutical Sciences*, *7*(1), 156. https://doi.org/10.1186/s43094-021-00304-5

Duran, I., Martin, J. H., Weis, M. A., Krejci, P., Konik, P., Li, B., Alanay, Y., Lietman, C., Lee, B., Eyre, D., Cohn, D. H., & Krakow, D. (2017b). A Chaperone Complex Formed by HSP47, FKBP65, and BiP Modulates Telopeptide Lysyl Hydroxylation of Type I Procollagen. *Journal of Bone and Mineral Research*, *32*(6), 1309–1319. https://doi.org/10.1002/jbmr.3095

Duran, I., Nevarez, L., Sarukhanov, A., Wu, S., Lee, K., Krejci, P., Weis, M., Eyre, D., Krakow, D., & Cohn, D. H. (2015). HSP47 and FKBP65 cooperate in the synthesis of type I procollagen. *Human Molecular Genetics*, *24*(7), 1918–1928. https://doi.org/10.1093/hmg/ddu608

Eyre, D. R., Weis, M., Hudson, D. M., Wu, J.-J., & Kim, L. (2011). A Novel 3-Hydroxyproline (3Hyp)-rich Motif Marks the Triple-helical C Terminus of Tendon Type I Collagen. *Journal of Biological Chemistry*, *286*(10), 7732–7736. https://doi.org/10.1074/jbc.C110.195768

Fang, C., Liang, Y., Huang, Y., Jiang, D., Li, J., Ma, H., Guo, L., Jiang, W., & Feng, Y. (2022). P3H4 Promotes Malignant Progression of Lung Adenocarcinoma via Interaction with EGFR. *Cancers*, *14*(13), 3243. https://doi.org/10.3390/cancers14133243

Fernandez, I. E., & Eickelberg, O. (2012). The Impact of TGF-β on Lung Fibrosis. *Proceedings of the American Thoracic Society*, *9*(3), 111–116. https://doi.org/10.1513/pats.201203-023AW

Fish, P. V., Allan, G. A., Bailey, S., Blagg, J., Butt, R., Collis, M. G., Greiling, D., James, K., Kendall, J., McElroy, A., McCleverty, D., Reed, C., Webster, R., & Whitlock, G. A. (2007). Potent and Selective Nonpeptidic Inhibitors of Procollagen C-Proteinase. *Journal of Medicinal Chemistry*, *50*(15), 3442–3456. https://doi.org/10.1021/jm061010z

Flaherty, K. R., Fell, C. D., Huggins, J. T., Nunes, H., Sussman, R., Valenzuela, C., Petzinger, U., Stauffer, J. L., Gilberg, F., Bengus, M., & Wijsenbeek, M. (2018). Safety of nintedanib added to pirfenidone treatment for idiopathic pulmonary fibrosis. *European Respiratory Journal*, *52*(2), 1800230. https://doi.org/10.1183/13993003.00230-2018

Flevaris, P., & Vaughan, D. (2016). The Role of Plasminogen Activator Inhibitor Type-1 in Fibrosis. *Seminars in Thrombosis and Hemostasis*, *43*(02), 169–177. https://doi.org/10.1055/s-0036-1586228

Forlino, A., Cabral, W. A., Barnes, A. M., & Marini, J. C. (2011). New perspectives on osteogenesis imperfecta. *Nature Reviews Endocrinology*, *7*(9), 540–557. https://doi.org/10.1038/nrendo.2011.81

Fujimoto, H., Kobayashi, T., & Azuma, A. (2015). Idiopathic Pulmonary Fibrosis: Treatment and

Prognosis. *Clinical Medicine Insights: Circulatory, Respiratory and Pulmonary Medicine*, *9s1*, CCRPM.S23321. https://doi.org/10.4137/CCRPM.S23321

Gajjala, P. R., Singh, P., Odayar, V., Ediga, H. H., McCormack, F. X., & Madala, S. K. (2023). Wilms Tumor 1-Driven Fibroblast Activation and Subpleural Thickening in Idiopathic Pulmonary Fibrosis. *International Journal of Molecular Sciences*, *24*(3),2850. https://doi.org/10.3390/ijms24032850

Gelse, K., Pöschl, E., & Aigner, T. (2003). Collagens - Structure, function, and biosynthesis. *Advanced Drug Delivery Reviews*, *55*(12),1531–1546. https://doi.org/10.1016/j.addr.2003.08.002

Ghartey-Kwansah, G., Li, Z., Feng, R., Wang, L., Zhou, X., Chen, F. Z., Xu, M. M., Jones, O., Mu, Y., Chen, S., Bryant, J., Isaacs, W. B., Ma, J., & Xu, X. (2018). Comparative analysis of FKBP family protein: evaluation, structure, and function in mammals and Drosophila melanogaster. *BMC Developmental Biology*, *18*(1), 7. https://doi.org/10.1186/s12861-018-0167-3

Ghumman, M., Dhamecha, D., Gonsalves, A., Fortier, L., Sorkhdini, P., Zhou, Y., & Menon, J. U. (2021). Emerging drug delivery strategies for idiopathic pulmonary fibrosis treatment. *European Journal of Pharmaceutics and Biopharmaceutics*, *164*,1–12. https://doi.org/10.1016/j.ejpb.2021.03.017

Gjaltema, R. A. F., & Bank, R. A. (2017). Molecular insights into prolyl and lysyl hydroxylation of fibrillar collagens in health and disease. *Critical Reviews in Biochemistry and Molecular Biology*, *52*(1), 74–95. https://doi.org/10.1080/10409238.2016.1269716

Glass, D. S., Grossfeld, D., Renna, H. A., Agarwala, P., Spiegler, P., DeLeon, J., & Reiss, A. B. (2022). Idiopathic pulmonary fibrosis: Current and future treatment. *The Clinical Respiratory Journal*, *16*(2), 84–96. https://doi.org/10.1111/crj.13466

Grgurevic, L., Erjavec, I., Grgurevic, I., Dumic-Cule, I., Brkljacic, J., Verbanac, D., Matijasic, M., Paljetak, H. C., Novak, R., Plecko, M., Bubic-Spoljar, J., Rogic, D., Kufner, V., Pauk, M., Bordukalo-Niksic, T., & Vukicevic, S. (2017). Systemic inhibition of BMP1-3 decreases progression of CCl 4-induced liver fibrosis in rats. *Growth Factors*, *35*(6), 201–215. https://doi.org/10.1080/08977194.2018.1428966

Grigorieva, O. A., Vigovskiy, M. A., Dyachkova, U. D., Basalova, N. A., Aleksandrushkina, N. A., Kulebyakina, M. A., Zaitsev, I. L., Popov, V. S., & Efimenko, A. Y. (2021). Mechanisms of Endothelial-to-Mesenchymal Transition Induction by Extracellular Matrix Components in Pulmonary Fibrosis. *Bulletin of Experimental Biology and Medicine*, *171*(4), 523–531. https://doi.org/10.1007/s10517-021-05264-7

Grinstein, M., Dingwall, H. L., Shah, R. R., Capellini, T. D., & Galloway, J. L. (2018). A robust method for RNA extraction and purification from a single adult mouse tendon. *PeerJ*, *6*, e4664. https://doi.org/10.7717/peerj.4664

Gruenwald, K., Castagnola, P., Besio, R., Dimori, M., Chen, Y., Akel, N. S., Swain, F. L., Skinner, R. A., Eyre, D. R., Gaddy, D., Suva, L. J., & Morello, R. (2014). Sc65 Is a Novel Endoplasmic Reticulum Protein That Regulates Bone Mass Homeostasis. *Journal of Bone and Mineral Research*, *29*(3), 666–675. https://doi.org/10.1002/jbmr.2075

Guo, H.-F., Bota-Rabassedas, N., Terajima, M., Leticia Rodriguez, B., Gibbons, D. L., Chen, Y., Banerjee, P., Tsai, C.-L., Tan, X., Liu, X., Yu, J., Tokmina-Roszyk, M., Stawikowska, R., Fields, G. B., Miller, M. D., Wang, X., Lee, J., Dalby, K. N., Creighton, C. J., … Kurie, J. M. (2021). A collagen glucosyltransferase drives lung adenocarcinoma progression in mice. *Communications Biology*, *4*(1), 482. https://doi.org/10.1038/s42003-021-01982-w

Ha-Vinh, R., Alanay, Y., Bank, R. A., Campos-Xavier, A. B., Zankl, A., Superti-Furga, A., & Bonafé, L. (2004). Phenotypic and molecular characterization of Bruck syndrome (osteogenesis imperfecta with contractures of the large joints) caused by a recessive mutation in PLOD2. *American Journal of Medical Genetics Part A*, *131A*(2), 115–120. https://doi.org/10.1002/ajmg.a.30231

Habermann, A. C., Gutierrez, A. J., Bui, L. T., Yahn, S. L., Winters, N. I., Calvi, C. L., Peter, L., Chung, M.-I., Taylor, C. J., Jetter, C., Raju, L., Roberson, J., Ding, G., Wood, L., Sucre, J.

M. S., Richmond, B. W., Serezani, A. P., McDonnell, W. J., Mallal, S. B., … Kropski, J. A. (2020). Single-cell RNA sequencing reveals profibrotic roles of distinct epithelial and mesenchymal lineages in pulmonary fibrosis. *Science Advances*, *6*(28). https://doi.org/10.1126/sciadv.aba1972

Hagiwara, S., Iwasaka, H., Matsumoto, S., & Noguchi, T. (2007). An antisense oligonucleotide to HSP47 inhibits paraquat-induced pulmonary fibrosis in rats. *Toxicology*, *236*(3), 199–207. https://doi.org/10.1016/j.tox.2007.04.013

Hao, L., Pang, K., Pang, H., Zhang, J., Zhang, Z., He, H., Zhou, R., Shi, Z., & Han, C. (2020). Knockdown of P3H4 inhibits proliferation and invasion of bladder cancer. *Aging*, *12*(3), 2156–2168. https://doi.org/10.18632/aging.102732

Hao, L., Shi, Z., Dong, Y., Chen, J., Pang, K., He, H., Zhang, S., Wu, W., Zhang, Q., & Han, C. (2022). Efficient Delivery of P3H4 siRNA and Chlorin e6 by cRGDfK-Installed Polyarginine Nanoparticles for Tumor-Targeting Therapy of Bladder Cancer. *Pharmaceutics*, *14*(10), 2149. https://doi.org/10.3390/pharmaceutics14102149

Hastings, J. F., Skhinas, J. N., Fey, D., Croucher, D. R., & Cox, T. R. (2019). The extracellular matrix as a key regulator of intracellular signalling networks. *British Journal of Pharmacology*, *176*(1), 82–92. https://doi.org/10.1111/bph.14195

Heard, M. E., Besio, R., Weis, M., Rai, J., Hudson, D. M., Dimori, M., Zimmerman, S. M., Kamykowski, J. A., Hogue, W. R., Swain, F. L., Burdine, M. S., Mackintosh, S. G., Tackett, A. J., Suva, L. J., Eyre, D. R., & Morello, R. (2016b). Sc65-Null Mice Provide Evidence for a Novel Endoplasmic Reticulum Complex Regulating Collagen Lysyl Hydroxylation. *PLOS Genetics*, *12*(4), e1006002. https://doi.org/10.1371/journal.pgen.1006002

Herrera, J. A., Dingle, L., Angeles Montero, M., Venkateswaran, R. V., Blaikley, J. F., Lawless, C., & Schwartz, M. A. (2022). The UIP/IPF fibroblastic focus is a collagen biosynthesis factory embedded in a distinct extracellular matrix. *JCI Insight*, *7*(16). https://doi.org/10.1172/jci.insight.156115

Heukels, P., Moor, C. C., von der Thüsen, J. H., Wijsenbeek, M. S., & Kool, M. (2019). Inflammation and immunity in IPF pathogenesis and treatment. *Respiratory Medicine*, *147*, 79–91. https://doi.org/10.1016/j.rmed.2018.12.015

Hewlett, J. C., Kropski, J. A., & Blackwell, T. S. (2018). Idiopathic pulmonary fibrosis: Epithelial-mesenchymal interactions and emerging therapeutic targets. *Matrix Biology*, *71–72*, 112–127. https://doi.org/10.1016/j.matbio.2018.03.021

Hill, C., Jones, M., Davies, D., & Wang, Y. (2019). Epithelial-Mesenchymal Transition Contributes to Pulmonary Fibrosis via Aberrant Epithelial/Fibroblastic Cross-Talk. *Journal of Lung Health and Diseases*, *3*(2), 31–35. https://doi.org/10.29245/2689-999X/2019/2.1149

Homan, E. P., Lietman, C., Grafe, I., Lennington, J., Morello, R., Napierala, D., Jiang, M.-M., Munivez, E. M., Dawson, B., Bertin, T. K., Chen, Y., Lua, R., Lichtarge, O., Hicks, J., Weis, M. A., Eyre, D., & Lee, B. H. L. (2014). Differential Effects of Collagen Prolyl 3-Hydroxylation on Skeletal Tissues. *PLoS Genetics*, *10*(1), e1004121. https://doi.org/10.1371/journal.pgen.1004121

Hoyer, N., Jessen, H., Prior, T. S., Sand, J. M. B., Leeming, D. J., Karsdal, M. A., Åttingsberg, E. K. A., Vangsgaard, G. K. M., Bendstrup, E., & Shaker, S. B. (2021). High turnover of types III and VI collagen in progressive idiopathic pulmonary fibrosis. *Respirology*, *26*(6), 582–589. https://doi.org/10.1111/resp.14056

Hoyer, N., Prior, T. S., Bendstrup, E., Wilcke, T., & Shaker, S. B. (2019). Risk factors for diagnostic delay in idiopathic pulmonary fibrosis. *Respiratory Research*, *20*(1), 1–9. https://doi.org/10.1186/s12931-019-1076-0

Hudson, D. M., & Eyre, D. R. (2013a). Collagen prolyl 3-hydroxylation: A major role for a minor post-translational modification? *Connective Tissue Research*, *54*(4–5), 245–251. https://doi.org/10.3109/03008207.2013.800867

Hudson, D. M., Joeng, K. S., Werther, R., Rajagopal, A., Weis, M., Lee, B. H., & Eyre, D. R. (2015). Post-translationally Abnormal Collagens of Prolyl 3-Hydroxylase-2 Null Mice Offer a

Pathobiological Mechanism for the High Myopia Linked to Human LEPREL1 Mutations. *Journal of Biological Chemistry*, *290*(13), 8613–8622. https://doi.org/10.1074/jbc.M114.634915

Hudson, D. M., Weis, M., Rai, J., Joeng, K. S., Dimori, M., Lee, B. H., Morello, R., & Eyre, D. R. (2017a). P3h3-null and Sc65-null mice phenocopy the collagen lysine under-hydroxylation and cross-linking abnormality of ehlers-danlos syndrome type VIA. *Journal of Biological Chemistry*, *292*(9), 3877–3887. https://doi.org/10.1074/jbc.M116.762245

Hudson, D. M., Weis, M., Rai, J., Joeng, K. S., Dimori, M., Lee, B. H., Morello, R., & Eyre, D. R. (2017b). P3h3-null and Sc65-null Mice Phenocopy the Collagen Lysine Under-hydroxylation and Cross-linking Abnormality of Ehlers-Danlos Syndrome Type VIA. *Journal of Biological Chemistry*, *292*(9), 3877–3887. https://doi.org/10.1074/jbc.M116.762245

Hughes, J., Rees, S., Kalindjian, S., & Philpott, K. (2011). Principles of early drug discovery. *British Journal of Pharmacology*, *162*(6), 1239–1249. https://doi.org/10.1111/j.1476-5381.2010.01127.x

Huh, J.-Y., Lee, J. H., & Song, J. W. (2021). Efficacy and safety of combined use of pirfenidone and nintedanib in patients with idiopathic pulmonary fibrosis. *Idiopathic Interstitial Pneumonias*, PA468. https://doi.org/10.1183/13993003.congress-2021.PA468

Hulmes, D. J. S. (2002). Building Collagen Molecules, Fibrils, and Suprafibrillar Structures. *Journal of Structural Biology*, *137*(1–2), 2–10. https://doi.org/10.1006/jsbi.2002.4450

Hynes, R. O. (2009). The Extracellular Matrix: Not Just Pretty Fibrils. *Science*, *326*(5957), 1216–1219. https://doi.org/10.1126/science.1176009

Ishikawa, Y., & Bächinger, H. P. (2013a). A molecular ensemble in the rER for procollagen maturation. *Biochimica et Biophysica Acta (BBA) - Molecular Cell Research*, *1833*(11), 2479–2491. https://doi.org/10.1016/j.bbamcr.2013.04.008

Ishikawa, Y., & Bächinger, H. P. (2013b). An Additional Function of the Rough Endoplasmic Reticulum Protein Complex Prolyl 3-Hydroxylase 1·Cartilage-associated Protein·Cyclophilin B. *Journal of Biological Chemistry*, *288*(44), 31437–31446. https://doi.org/10.1074/jbc.M113.498063

Ishikawa, Y., & Bächinger, H. P. (2014). A Substrate Preference for the Rough Endoplasmic Reticulum Resident Protein FKBP22 during Collagen Biosynthesis. *Journal of Biological Chemistry*, *289*(26), 18189–18201. https://doi.org/10.1074/jbc.M114.561944

Ishikawa, Y., Holden, P., & Bächinger, H. P. (2017). Heat shock protein 47 and 65-kDa FK506-binding protein weakly but synergistically interact during collagen folding in the endoplasmic reticulum. *Journal of Biological Chemistry*, *292*(42), 17216–17224. https://doi.org/10.1074/jbc.M117.802298

Ishikawa, Y., Mizuno, N., Holden, P., Lim, P. J., Gould, D. B., Rohrbach, M., Giunta, C., & Bächinger, H. P. (2020). The novel missense mutation Met48Lys in FKBP22 changes its structure and functions. *Scientific Reports*, *10*(1), 497. https://doi.org/10.1038/s41598-019-57374-y

Ishikawa, Y., Taga, Y., Zientek, K., Mizuno, N., Salo, A. M., Semenova, O., Tufa, S. F., Keene, D. R., Holden, P., Mizuno, K., Gould, D. B., Myllyharju, J., & Bächinger, H. P. (2021). Type I and type V procollagen triple helix uses different subsets of the molecular ensemble for lysine posttranslational modifications in the rER. *Journal of Biological Chemistry*, *296*, 100453. https://doi.org/10.1016/j.jbc.2021.100453

Ishikawa, Y., Vranka, J., Wirz, J., Nagata, K., & Bächinger, H. P. (2008). The Rough Endoplasmic Reticulum-resident FK506-binding Protein FKBP65 Is a Molecular Chaperone That Interacts with Collagens. *Journal of Biological Chemistry*, *283*(46), 31584–31590. https://doi.org/10.1074/jbc.M802535200

Ishikawa, Y., Wirz, J., Vranka, J. A., Nagata, K., & Bächinger, H. P. (2009). Biochemical Characterization of the Prolyl 3-Hydroxylase 1·Cartilage-associated Protein·Cyclophilin B Complex. *Journal of Biological Chemistry*, *284*(26), 17641–17647. https://doi.org/10.1074/jbc.M109.007070

Ito, S., & Nagata, K. (2019). Roles of the endoplasmic reticulum–resident, collagen-specific molecular chaperone Hsp47 in vertebrate cells and human disease. *Journal of Biological Chemistry*, *294*(6), 2133–2141. https://doi.org/10.1074/jbc.TM118.002812

Iwaki, T., Urano, T., & Umemura, K. (2012). PAI-1, progress in understanding the clinical problem and its aetiology. *British Journal of Haematology*, *157*(3), 291–298. https://doi.org/10.1111/j.1365-2141.2012.09074.x

Jenkins, R. G., Simpson, J. K., Saini, G., Bentley, J. H., Russell, A.-M., Braybrooke, R., Molyneaux, P. L., McKeever, T. M., Wells, A. U., Flynn, A., Hubbard, R. B., Leeming, D. J., Marshall, R. P., Karsdal, M. A., Lukey, P. T., & Maher, T. M. (2015). Longitudinal change in collagen degradation biomarkers in idiopathic pulmonary fibrosis: an analysis from the prospective, multicentre PROFILE study. *The Lancet Respiratory Medicine*, *3*(6), 462–472. https://doi.org/10.1016/S2213-2600(15)00048-X

Jessen, H., Hoyer, N., Prior, T. S., Frederiksen, P., Karsdal, M. A., Leeming, D. J., Bendstrup, E., Sand, J. M. B., & Shaker, S. B. (2021). Turnover of type I and III collagen predicts progression of idiopathic pulmonary fibrosis. *Respiratory Research*, *22*(1), 205. https://doi.org/10.1186/s12931-021-01801-0

Jin, J., Togo, S., Kadoya, K., Tulafu, M., Namba, Y., Iwai, M., Watanabe, J., Nagahama, K., Okabe, T., Hidayat, M., Kodama, Y., Kitamura, H., Ogura, T., Kitamura, N., Ikeo, K., Sasaki, S., Tominaga, S., & Takahashi, K. (2019). Pirfenidone attenuates lung fibrotic fibroblast responses to transforming growth factor-β1. *Respiratory Research*, *20*(1), 119. https://doi.org/10.1186/s12931-019-1093-z

Jin, X., Zhou, H., Song, J., Cui, H., Luo, Y., & Jiang, H. (2021). P3H4 Overexpression Serves as a Prognostic Factor in Lung Adenocarcinoma. *Computational and Mathematical Methods in Medicine*, *2021*, 1–9. https://doi.org/10.1155/2021/9971353

Kadler, K. E., Baldock, C., Bella, J., & Boot-Handford, R. P. (2007). Collagens at a glance. *Journal of Cell Science*, *120*(12), 1955–1958. https://doi.org/10.1242/jcs.03453

Kadler, K. E., Hill, A., & Canty-Laird, E. G. (2008). Collagen fibrillogenesis: fibronectin, integrins, and minor collagens as organizers and nucleators. *Current Opinion in Cell Biology*, *20*(5), 495–501. https://doi.org/10.1016/j.ceb.2008.06.008

Kallander, L. S., Washburn, D., Hilfiker, M. A., Eidam, H. S., Lawhorn, B. G., Prendergast, J., Fox, R., Dowdell, S., Manns, S., Hoang, T., Zhao, S., Ye, G., Hammond, M., Holt, D. A., Roethke, T., Hong, X., Reid, R. A., Gampe, R., Zhang, H., Willette, B. (2018). Reverse Hydroxamate Inhibitors of Bone Morphogenetic Protein 1. *ACS Medicinal Chemistry Letters*, *9*(7), 736–740. https://doi.org/10.1021/acsmedchemlett.8b00173

Kang, C. B., Hong, Y., Dhe-Paganon, S., & Yoon, H. S. (2008). FKBP Family Proteins: Immunophilins with Versatile Biological Functions. *Neurosignals*, *16*(4), 318–325. https://doi.org/10.1159/000123041

Karsdal, M. A. (2016). Introduction. *Biochemistry of Collagens, Laminins and Elastin: Structure, Function and Biomarkers*, xix–xxxiv. https://doi.org/10.1016/B978-0-12-809847-9.02001-8

Katarkar, A., Haldar, P. K., & Chaudhuri, K. (2015). De novo design based pharmacophore query generation and virtual screening for the discovery of Hsp-47 inhibitors. *Biochemical and Biophysical Research Communications*, *456*(3), 707–713. https://doi.org/10.1016/j.bbrc.2014.12.051

Kato, M., Sasaki, S., Nakamura, T., Kurokawa, K., Yamada, T., Ochi, Y., Ihara, H., Takahashi, F., & Takahashi, K. (2019). Gastrointestinal adverse effects of nintedanib and the associated risk factors in patients with idiopathic pulmonary fibrosis. *Scientific Reports*, *9*(1), 1–9. https://doi.org/10.1038/s41598-019-48593-4

Kay, E. J., Koulouras, G., & Zanivan, S. (2021). Regulation of Extracellular Matrix Production in Activated Fibroblasts: Roles of Amino Acid Metabolism in Collagen Synthesis. *Frontiers in Oncology*, *11*. https://doi.org/10.3389/fonc.2021.719922

Kelley, B. P., Malfait, F., Bonafe, L., Baldridge, D., Homan, E., Symoens, S., Willaert, A., Elcioglu, N., Van Maldergem, L., Verellen-Dumoulin, C., Gillerot, Y., Napierala, D., Krakow, D.,

Beighton, P., Superti-Furga, A., De Paepe, A., & Lee, B. (2011). Mutations in FKBP10 cause recessive osteogenesis imperfecta and bruck syndrome. *Journal of Bone and Mineral Research*, *26*(3), 666–672. https://doi.org/10.1002/jbmr.250

Kesteloot, F., Desmoulière, A., Leclercq, I., Thiry, M., Arrese, J. E., Prockop, D. J., Lapière, C. M., Nusgens, B. V., & Colige, A. (2007). ADAM metallopeptidase with thrombospondin type 1 motif 2 inactivation reduces the extent and stability of carbon tetrachloride-induced hepatic fibrosis in mice. *Hepatology*, *46*(5), 1620–1631. https://doi.org/10.1002/hep.21868

King, T. E., Bradford, W. Z., Castro-Bernardini, S., Fagan, E. A., Glaspole, I., Glassberg, M. K., Gorina, E., Hopkins, P. M., Kardatzke, D., Lancaster, L., Lederer, D. J., Nathan, S. D., Pereira, C. A., Sahn, S. A., Sussman, R., Swigris, J. J., & Noble, P. W. (2014). A Phase 3 Trial of Pirfenidone in Patients with Idiopathic Pulmonary Fibrosis. *New England Journal of Medicine*, *370*(22), 2083–2092. https://doi.org/10.1056/NEJMoa1402582

Kistler, K. D., Nalysnyk, L., Rotella, P., & Esser, D. (2014). Lung transplantation in idiopathic pulmonary fibrosis: a systematic review of the literature. *BMC Pulmonary Medicine*, *14*(1), 139. https://doi.org/10.1186/1471-2466-14-139

Knüppel, L., Heinzelmann, K., Lindner, M., Hatz, R., Behr, J., Eickelberg, O., & Staab-Weijnitz, C. A. (2018b). FK506-binding protein 10 (FKBP10) regulates lung fibroblast migration via collagen VI synthesis. *Respiratory Research*, *19*(1), 1–14. https://doi.org/10.1186/s12931-018-0768-1

Knüppel, L., Ishikawa, Y., Aichler, M., Heinzelmann, K., Hatz, R., Behr, J., Walch, A., Bächinger, H. P., Eickelberg, O., & Staab-Weijnitz, C. A. (2017). A Novel Antifibrotic Mechanism of Nintedanib and Pirfenidone. Inhibition of Collagen Fibril Assembly. *American Journal of Respiratory Cell and Molecular Biology*, *57*(1), 77–90. https://doi.org/10.1165/rcmb.2016-0217OC

Köhler, A., Mörgelin, M., Gebauer, J. M., Öcal, S., Imhof, T., Koch, M., Nagata, K., Paulsson, M., Aumailley, M., Baumann, U., Zaucke, F., & Sengle, G. (2020). New specific HSP47 functions in collagen subfamily chaperoning. *The FASEB Journal*, *34*(9), 12040–12052. https://doi.org/10.1096/fj.202000570R

Krane, S. M. (2006). Mutations in genes encoding components of a post-translational-modifying protein complex cause another collagen disease. *BoneKEy-Osteovision*, *3*(11), 10–13. https://doi.org/10.1138/20060236

Kreuter, M., Bonella, F., Wijsenbeek, M., Maher, T. M., & Spagnolo, P. (2015). Pharmacological Treatment of Idiopathic Pulmonary Fibrosis: Current Approaches, Unsolved Issues, and Future Perspectives. *BioMed Research International*, *2015*, 1–10. https://doi.org/10.1155/2015/329481

Kristensen, J. H., Karsdal, M. A., Genovese, F., Johnson, S., Svensson, B., Jacobsen, S., Hägglund, P., & Leeming, D. J. (2014). The Role of Extracellular Matrix Quality in Pulmonary Fibrosis. *Respiration*, *88*(6), 487–499. https://doi.org/10.1159/000368163

Kruger, T. E., Miller, A. H., & Wang, J. (2013). Collagen Scaffolds in Bone Sialoprotein-Mediated Bone Regeneration. *The Scientific World Journal*, *2013*, 1–6. https://doi.org/10.1155/2013/812718

Laporta Hernandez, R., Aguilar Perez, M., Lázaro Carrasco, M., & Ussetti Gil, P. (2018). Lung Transplantation in Idiopathic Pulmonary Fibrosis. *Medical Sciences*, *6*(3), 68. https://doi.org/10.3390/medsci6030068

Lawson, W. E., Cheng, D.-S., Degryse, A. L., Tanjore, H., Polosukhin, V. V., Xu, X. C., Newcomb, D. C., Jones, B. R., Roldan, J., Lane, K. B., Morrisey, E. E., Beers, M. F., Yull, F. E., & Blackwell, T. S. (2011). Endoplasmic reticulum stress enhances fibrotic remodeling in the lungs. *Proceedings of the National Academy of Sciences*, *108*(26), 10562–10567. https://doi.org/10.1073/pnas.1107559108

LeClair, R. J., Durmus, T., Wang, Q., Pyagay, P., Terzic, A., & Lindner, V. (2007). Cthrc1 Is a Novel Inhibitor of Transforming Growth Factor-β Signaling and Neointimal Lesion Formation. *Circulation Research*, *100*(6), 826–833. https://doi.org/10.1161/01.RES.0000260806.99307.72

Leclère, L., Nir, T. S., Bazarsky, M., Braitbard, M., Schneidman-Duhovny, D., & Gat, U. (2020). Dynamic Evolution of the Cthrc1 Genes, a Newly Defined Collagen-Like Family. *Genome Biology and Evolution*, *12*(2), 3957–3970. https://doi.org/10.1093/gbe/evaa020

Lehtonen, S. T., Veijola, A., Karvonen, H., Lappi-Blanco, E., Sormunen, R., Korpela, S., Zagai, U., Sköld, M. C., & Kaarteenaho, R. (2016). Pirfenidone and nintedanib modulate properties of fibroblasts and myofibroblasts in idiopathic pulmonary fibrosis. *Respiratory Research*, *17*(1), 14. https://doi.org/10.1186/s12931-016-0328-5

Lei, G.-S., Kline, H. L., Lee, C.-H., Wilkes, D. S., & Zhang, C. (2016). Regulation of Collagen V Expression and Epithelial-Mesenchymal Transition by miR-185 and miR-186 during Idiopathic Pulmonary Fibrosis. *The American Journal of Pathology*, *186*(9), 2310–2316. https://doi.org/10.1016/j.ajpath.2016.04.015

Ley, B., & Collard, H. (2013). Epidemiology of idiopathic pulmonary fibrosis. *Clinical Epidemiology*, 483. https://doi.org/10.2147/CLEP.S54815

Li, S.-W., Arita, M., Fertala, A., Bao, Y., Kopen, G. C., Långsjö, T. K., Hyttinen, M. M., Helminen, H. J., & Prockop, D. J. (2001). Transgenic mice with inactive alleles for procollagen N-proteinase (ADAMTS-2) develop fragile skin and male sterility. *Biochemical Journal*, *355*(2), 271. https://doi.org/10.1042/0264-6021:3550271

Li, W., Ye, L., Chen, Y., & Chen, P. (2018). P3H4 is correlated with clinicopathological features and prognosis in bladder cancer. *World Journal of Surgical Oncology*, *16*(1), 206. https://doi.org/10.1186/s12957-018-1507-2

Lietman, C. D., Lim, J., Grafe, I., Chen, Y., Ding, H., Bi, X., Ambrose, C. G., Fratzl-Zelman, N., Roschger, P., Klaushofer, K., Wagermaier, W., Schmidt, I., Fratzl, P., Rai, J., Weis, M. A., Eyre, D., Keene, D. R., Krakow, D., & Lee, B. H. (2017). Fkbp10 Deletion in Osteoblasts Leads to Qualitative Defects in Bone. *Journal of Bone and Mineral Research*, *32*(6), 1354–1367. https://doi.org/10.1002/jbmr.3108

Lietman, C. D., Rajagopal, A., Homan, E. P., Munivez, E., Jiang, M.-M., Bertin, T. K., Chen, Y., Hicks, J., Weis, M., Eyre, D., Lee, B., & Krakow, D. (2014). Connective tissue alterations in Fkbp10−/− mice. *Human Molecular Genetics*, *23*(18), 4822–4831. https://doi.org/10.1093/hmg/ddu197

Lindert, U., Weis, M. A., Rai, J., Seeliger, F., Hausser, I., Leeb, T., Eyre, D., Rohrbach, M., & Giunta, C. (2015). Molecular Consequences of the SERPINH1/HSP47 Mutation in the Dachshund Natural Model of Osteogenesis Imperfecta. *Journal of Biological Chemistry*, *290*(29), 17679–17689. https://doi.org/10.1074/jbc.M115.661025

Liu, Gang, Philp, A. M., Corte, T., Travis, M. A., Schilter, H., Hansbro, N. G., Burns, C. J., Eapen, M. S., Sohal, S. S., Burgess, J. K., & Hansbro, P. M. (2021). Therapeutic targets in lung tissue remodelling and fibrosis. *Pharmacology & Therapeutics*, *225*, 107839. https://doi.org/10.1016/j.pharmthera.2021.107839

Liu, Guoxiu, Zhai, H., Zhang, T., Li, S., Li, N., Chen, J., Gu, M., Qin, Z., & Liu, X. (2019). New therapeutic strategies for IPF: Based on the “phagocytosis-secretion-immunization” network regulation mechanism of pulmonary macrophages. *Biomedicine & Pharmacotherapy*, *118*, 109230. https://doi.org/10.1016/j.biopha.2019.109230

Liu, L., Stephens, B., Bergman, M., May, A., & Chiang, T. (2021). Role of Collagen in airway mechanics. *Bioengineering*, *8*(1), 1–13. https://doi.org/10.3390/bioengineering8010013

Liu, X., Rowan, S. C., Liang, J., Yao, C., Huang, G., Deng, N., Xie, T., Wu, D., Wang, Y., Burman, A., Parimon, T., Borok, Z., Chen, P., Parks, W. C., Hogaboam, C. M., Weigt, S. S., Belperio, J., Stripp, B. R., Noble, P. W., & Jiang, D. (2021). Categorization of lung mesenchymal cells in development and fibrosis. *IScience*, *24*(6), 102551. https://doi.org/10.1016/j.isci.2021.102551

Liu, Y., Liu, J., Quimbo, A., Xia, F., Yao, J., Clamme, J.-P., Zabludoff, S., Zhang, J., & Ying, W. (2021). Anti-HSP47 siRNA lipid nanoparticle ND-L02-s0201 reverses interstitial pulmonary fibrosis in preclinical rat models. *ERJ Open Research*, *7*(2), 00733–02020. https://doi.org/10.1183/23120541.00733-2020

López-Ramírez, C., Suarez Valdivia, L., & Rodríguez Portal, J. (2018). Causes of Pulmonary Fibrosis in the Elderly. *Medical Sciences*, *6*(3), 58. https://doi.org/10.3390/medsci6030058

Lucas, T., Waisman, A., Ranjan, R., Roes, J., Krieg, T., Müller, W., Roers, A., & Eming, S. A. (2010). Differential Roles of Macrophages in Diverse Phases of Skin Repair. *The Journal of Immunology*, *184*(7), 3964–3977. https://doi.org/10.4049/jimmunol.0903356

Luo, Y., Xu, W., Chen, H., Warburton, D., Dong, R., Qian, B., Selman, M., Gauldie, J., Kolb, M., & Shi, W. (2015). A novel profibrotic mechanism mediated by TGFβ-stimulated collagen prolyl hydroxylase expression in fibrotic lung mesenchymal cells. *The Journal of Pathology*, *236*(3), 384–394. https://doi.org/10.1002/path.4530

M. Zimmerman, S., Besio, R., E. Heard-Lipsmeyer, M., Dimori, M., Castagnola, P., L. Swain, F., Gaddy, D., B. Diekman, A., & Morello, R. (2018). Expression characterization and functional implication of the collagen-modifying Leprecan proteins in mouse gonadal tissue and mature sperm. *AIMS Genetics*, *5*(1), 24–40. https://doi.org/10.3934/genet.2018.1.24

Ma, H.-Y., N'Diaye, E.-N., Caplazi, P., Huang, Z., Arlantico, A., Jeet, S., Wong, A., Brightbill, H. D., Li, Q., Wong, W. R., Sandoval, W., Tam, L., Newman, R., Roose-Girma, M., & Ding, N. (2022). BMP1 is not required for lung fibrosis in mice. *Scientific Reports*, *12*(1), 5466. https://doi.org/10.1038/s41598-022-09557-3

Maher, T. M., & Strek, M. E. (2019). Antifibrotic therapy for idiopathic pulmonary fibrosis: time to treat. *Respiratory Research*, *20*(1), 205. https://doi.org/10.1186/s12931-019-1161-4

Makley, L. N., & Gestwicki, J. E. (2013). Expanding the Number of 'Druggable' Targets: Non-Enzymes and Protein-Protein Interactions. *Chemical Biology & Drug Design*, *81*(1), 22–32. https://doi.org/10.1111/cbdd.12066

Marini, J. C., Cabral, W. A., & Barnes, A. M. (2010). Null mutations in LEPRE1 and CRTAP cause severe recessive osteogenesis imperfecta. *Cell and Tissue Research*, *339*(1), 59–70. https://doi.org/10.1007/s00441-009-0872-0

Marini, J. C., Cabral, W. A., Barnes, A. M., & Chang, W. (2007). Components of the Collagen Prolyl 3-Hydroxylation Complex are Crucial for Normal Bone Development. *Cell Cycle*, *6*(14), 1675–1681. https://doi.org/10.4161/cc.6.14.4474

Martinez, F. J., Collard, H. R., Pardo, A., Raghu, G., Richeldi, L., Selman, M., Swigris, J. J., Taniguchi, H., & Wells, A. U. (2017). Idiopathic pulmonary fibrosis. *Nature Reviews Disease Primers*, *3*(1), 17074. https://doi.org/10.1038/nrdp.2017.74

Meng, X., Nikolic-Paterson, D. J., & Lan, H. Y. (2016). TGF-β: the master regulator of fibrosis. *Nature Reviews Nephrology*, *12*(6), 325–338. https://doi.org/10.1038/nrneph.2016.48

Merl-Pham, J., Basak, T., Knüppel, L., Ramanujam, D., Athanason, M., Behr, J., Engelhardt, S., Eickelberg, O., Hauck, S. M., Vanacore, R., & Staab-Weijnitz, C. A. (2019). Quantitative proteomic profiling of extracellular matrix and site-specific collagen post-translational modifications in an in vitro model of lung fibrosis. *Matrix Biology Plus*, *1*, 100005. https://doi.org/10.1016/j.mbplus.2019.04.002

Michalski, J. E., & Schwartz, D. A. (2020). Genetic risk factors for idiopathic pulmonary fibrosis: Insights into immunopathogenesis. *Journal of Inflammation Research*, *13*, 1305–1318. https://doi.org/10.2147/JIR.S280958

Michna, A., Schötz, U., Selmansberger, M., Zitzelsberger, H., Lauber, K., Unger, K., & Hess, J. (2016). Transcriptomic analyses of the radiation response in head and neck squamous cell carcinoma subclones with different radiation sensitivity: time-course gene expression profiles and gene association networks. *Radiation Oncology*, *11*(1), 94. https://doi.org/10.1186/s13014-016-0672-0

Millan-Billi, P., Serra, C., Alonso Leon, A., & Castillo, D. (2018). Comorbidities, Complications and Non-Pharmacologic Treatment in Idiopathic Pulmonary Fibrosis. *Medical Sciences*, *6*(3), 59. https://doi.org/10.3390/medsci6030059

Miyamura, T., Sakamoto, N., Kakugawa, T., Taniguchi, H., Akiyama, Y., Okuno, D., Moriyama, S., Hara, A., Kido, T., Ishimoto, H., Yamaguchi, H., Miyazaki, T., Obase, Y., Ishimatsu, Y., Tanaka, Y., & Mukae, H. (2020). Small molecule inhibitor of HSP47 prevents pro-fibrotic

mechanisms of fibroblasts in vitro. *Biochemical and Biophysical Research Communications*, *530*(3), 561–565. https://doi.org/10.1016/j.bbrc.2020.07.085

Morello, R., Bertin, T. K., Chen, Y., Hicks, J., Tonachini, L., Monticone, M., Castagnola, P., Rauch, F., Glorieux, F. H., Vranka, J., Bächinger, H. P., Pace, J. M., Schwarze, U., Byers, P. H., Weis, M., Fernandes, R. J., Eyre, D. R., Yao, Z., Boyce, B. F., & Lee, B. (2006). CRTAP Is Required for Prolyl 3- Hydroxylation and Mutations Cause Recessive Osteogenesis Imperfecta. *Cell*, *127*(2), 291–304. https://doi.org/10.1016/j.cell.2006.08.039

Muiznieks, L. D., & Keeley, F. W. (2013). Molecular assembly and mechanical properties of the extracellular matrix: A fibrous protein perspective. *Biochimica et Biophysica Acta (BBA) - Molecular Basis of Disease*, *1832*(7), 866–875. https://doi.org/10.1016/j.bbadis.2012.11.022

Musiime, M., Chang, J., Hansen, U., Kadler, K. E., Zeltz, C., & Gullberg, D. (2021). Collagen Assembly at the Cell Surface: Dogmas Revisited. *Cells*, *10*(3), 662. https://doi.org/10.3390/cells10030662

Mutsaers, S. E., Marshall, R. P., Goldsack, N. R., Laurent, G. J., & McAnulty, R. J. (1998). Effect of Endothelin Receptor Antagonists (BQ-485, Ro 47-0203) on Collagen Deposition During the Development of Bleomycin-Induced Pulmonary Fibrosis in Rats. *Pulmonary Pharmacology & Therapeutics*, *11*(2–3), 221–225. https://doi.org/10.1006/pupt.1998.0142

Myllärniemi, M., & Kaarteenaho, R. (2015). Pharmacological treatment of idiopathic pulmonary fibrosis – preclinical and clinical studies of pirfenidone, nintedanib, and N-acetylcysteine. *European Clinical Respiratory Journal*, *2*(1), 26385. https://doi.org/10.3402/ecrj.v2.26385

Myllyharju, J. (2003). Prolyl 4-hydroxylases, the key enzymes of collagen biosynthesis. *Matrix Biology*, *22*(1), 15–24. https://doi.org/10.1016/S0945-053X(03)00006-4

Myngbay, A., Manarbek, L., Ludbrook, S., & Kunz, J. (2021). The Role of Collagen Triple Helix Repeat-Containing 1 Protein (CTHRC1) in Rheumatoid Arthritis. *International Journal of Molecular Sciences*, *22*(5), 2426. https://doi.org/10.3390/ijms22052426

Nashchekina, Y., Nikonov, P., Prasolov, N., Sulatsky, M., Chabina, A., & Nashchekin, A. (2022). The Structural Interactions of Molecular and Fibrillar Collagen Type I with Fibronectin and Its Role in the Regulation of Mesenchymal Stem Cell Morphology and Functional Activity. *International Journal of Molecular Sciences*, *23*(20), 12577. https://doi.org/10.3390/ijms232012577

Nemeth, J., Schundner, A., & Frick, M. (2020). Insights Into Development and Progression of Idiopathic Pulmonary Fibrosis From Single Cell RNA Studies. *Frontiers in Medicine*, *7*. https://doi.org/10.3389/fmed.2020.611728

Nizamoglu, M., de Hilster, R. H. J., Zhao, F., Sharma, P. K., Borghuis, T., Harmsen, M. C., & Burgess, J. K. (2022). An in vitro model of fibrosis using crosslinked native extracellular matrix-derived hydrogels to modulate biomechanics without changing composition. *Acta Biomaterialia*, *147*, 50–62. https://doi.org/10.1016/j.actbio.2022.05.031

Noguchi, S., Saito, A., Mikami, Y., Urushiyama, H., Horie, M., Matsuzaki, H., Takeshima, H., Makita, K., Miyashita, N., Mitani, A., Jo, T., Yamauchi, Y., Terasaki, Y., & Nagase, T. (2017). TAZ contributes to pulmonary fibrosis by activating profibrotic functions of lung fibroblasts. *Scientific Reports*, *7*(1), 42595. https://doi.org/10.1038/srep42595

Ochs, R. L., Stein, T. W., Chan, E. K., Ruutu, M., & Tan, E. M. (1996). cDNA cloning and characterization of a novel nucleolar protein. *Molecular Biology of the Cell*, *7*(7), 1015–1024. https://doi.org/10.1091/mbc.7.7.1015

Ogawa, T., Shichino, S., Ueha, S., & Matsushima, K. (2021). Macrophages in lung fibrosis. *International Immunology*, *33*(12), 665–671. https://doi.org/10.1093/intimm/dxab040

Oh, C. K., Ariue, B., Alban, R. F., Shaw, B., & Cho, S. H. (2002). PAI-1 promotes extracellular matrix deposition in the airways of a murine asthma model. *Biochemical and Biophysical Research Communications*, *294*(5), 1155–1160. https://doi.org/10.1016/S0006-291X(02)00577-6

Okano-Kosugi, H., Matsushita, O., Asada, S., Herr, A. B., Kitagawa, K., & Koide, T. (2009).

Development of a high-throughput screening system for the compounds that inhibit collagen–protein interactions. *Analytical Biochemistry*, *394*(1), 125–131. https://doi.org/10.1016/j.ab.2009.07.017

Okuno, D., Sakamoto, N., Tagod, M. S. O., Akiyama, Y., Moriyama, S., Miyamura, T., Hara, A., Kido, T., Ishimoto, H., Ishimatsu, Y., Tanaka, T., Ishihara, J., Takeda, K., Tanaka, Y., & Mukae, H. (2021). Screening of Inhibitors Targeting Heat Shock Protein 47 Involved in the Development of Idiopathic Pulmonary Fibrosis. *ChemMedChem*, *16*(16), 2515–2523. https://doi.org/10.1002/cmdc.202100064

Onursal, C., Dick, E., Angelidis, I., Schiller, H. B., & Staab-Weijnitz, C. A. (2021). Collagen Biosynthesis, Processing, and Maturation in Lung Ageing. *Frontiers in Medicine*, *8*. https://doi.org/10.3389/fmed.2021.593874

Organ, L. A., Duggan, A.-M. R., Oballa, E., Taggart, S. C., Simpson, J. K., Kang'ombe, A. R., Braybrooke, R., Molyneaux, P. L., North, B., Karkera, Y., Leeming, D. J., Karsdal, M. A., Nanthakumar, C. B., Fahy, W. A., Marshall, R. P., Jenkins, R. G., & Maher, T. M. (2019). Biomarkers of collagen synthesis predict progression in the PROFILE idiopathic pulmonary fibrosis cohort. *Respiratory Research*, *20*(1), 148. https://doi.org/10.1186/s12931-019-1118-7

Ortiz-Zapater, E., Signes-Costa, J., Montero, P., & Roger, I. (2022). Lung Fibrosis and Fibrosis in the Lungs: Is It All about Myofibroblasts? *Biomedicines*, *10*(6), 1423. https://doi.org/10.3390/biomedicines10061423

Pardo, A., Cabrera, S., Maldonado, M., & Selman, M. (2016). Role of matrix metalloproteinases in the pathogenesis of idiopathic pulmonary fibrosis. *Respiratory Research*, *17*(1), 23. https://doi.org/10.1186/s12931-016-0343-6

Park, Y., Ahn, C., & Kim, T. H. (2021). Occupational and environmental risk factors of idiopathic pulmonary fibrosis: a systematic review and meta-analyses. *Scientific Reports*, *11*(1), 1–10. https://doi.org/10.1038/s41598-021-81591-z

Parker, M. W., Rossi, D., Peterson, M., Smith, K., Sikström, K., White, E. S., Connett, J. E., Henke, C. A., Larsson, O., & Bitterman, P. B. (2014). Fibrotic extracellular matrix activates a profibrotic positive feedback loop. *Journal of Clinical Investigation*, *124*(4), 1622–1635. https://doi.org/10.1172/JCI71386

Pérez-Mies, B., Caniego-Casas, T., Bardi, T., Carretero-Barrio, I., Benito, A., García-Cosío, M., González-García, I., Pizarro, D., Rosas, M., Cristóbal, E., Ruano, Y., Garrido, M. C., Rigual-Bobillo, J., de Pablo, R., Galán, J. C., Pestaña, D., & Palacios, J. (2022). Progression to lung fibrosis in severe COVID-19 patients: A morphological and transcriptomic study in postmortem samples. *Frontiers in Medicine*, *9*. https://doi.org/10.3389/fmed.2022.976759

Petrides, P. E., & Brenner, D. (2012). From biochemical analysis to targeted therapies. *Fibrogenesis & Tissue Repair*, *5*(S1), S1. https://doi.org/10.1186/1755-1536-5-S1-S1

Philipp, J., Azimzadeh, O., Subramanian, V., Merl-Pham, J., Lowe, D., Hladik, D., Erbeldinger, N., Ktitareva, S., Fournier, C., Atkinson, M. J., Raj, K., & Tapio, S. (2017). Radiation-Induced Endothelial Inflammation Is Transferred via the Secretome to Recipient Cells in a STAT-Mediated Process. *Journal of Proteome Research*, *16*(10), 3903–3916. https://doi.org/10.1021/acs.jproteome.7b00536

Philp, C. J., Siebeke, I., Clements, D., Miller, S., Habgood, A., John, A. E., Navaratnam, V., Hubbard, R. B., Jenkins, G., & Johnson, S. R. (2018). Extracellular Matrix Cross-Linking Enhances Fibroblast Growth and Protects against Matrix Proteolysis in Lung Fibrosis. *American Journal of Respiratory Cell and Molecular Biology*, *58*(5), 594–603. https://doi.org/10.1165/rcmb.2016-0379OC

Piersma, B., & Bank, R. A. (2019). Collagen cross-linking mediated by lysyl hydroxylase 2: an enzymatic battlefield to combat fibrosis. *Essays in Biochemistry*, *63*(3), 377–387. https://doi.org/10.1042/EBC20180051

Pignata, P., Apicella, I., Cicatiello, V., Puglisi, C., Magliacane Trotta, S., Sanges, R., Tarallo, V., & De Falco, S. (2021). Prolyl 3-Hydroxylase 2 Is a Molecular Player of Angiogenesis. *International Journal of Molecular Sciences*, *22*(8), 3896.

https://doi.org/10.3390/ijms22083896

Pleasants, R., & Tighe, R. M. (2019). Management of Idiopathic Pulmonary Fibrosis. *Annals of Pharmacotherapy*, *53*(12), 1238–1248. https://doi.org/10.1177/1060028019862497

Pokidysheva, E., Boudko, S., Vranka, J., Zientek, K., Maddox, K., Moser, M., Fässler, R., Ware, J., & Bächinger, H. P. (2014). Biological role of prolyl 3-hydroxylation in type IV collagen. *Proceedings of the National Academy of Sciences*, *111*(1), 161–166. https://doi.org/10.1073/pnas.1307597111

Pokidysheva, E., Mizuno, K., & Bächinger, H. P. (2013). The Collagen Folding Machinery: Biosynthesis and Post-Translational Modifications of Collagens. *Osteogenesis Imperfecta: A Translational Approach to Brittle Bone Disease*, 57–70. https://doi.org/10.1016/B978-0-12-397165-4.00006-X

Pokidysheva, E., Tufa, S., Bresee, C., Brigande, J. V., & Bächinger, H. P. (2013). Prolyl 3-hydroxylase-1 null mice exhibit hearing impairment and abnormal morphology of the middle ear bone joints. *Matrix Biology*, *32*(1), 39–44. https://doi.org/10.1016/j.matbio.2012.11.006

Pokidysheva, E., Zientek, K. D., Ishikawa, Y., Mizuno, K., Vranka, J. A., Montgomery, N. T., Keene, D. R., Kawaguchi, T., Okuyama, K., & Bächinger, H. P. (2013). Posttranslational Modifications in Type I Collagen from Different Tissues Extracted from Wild Type and Prolyl 3-Hydroxylase 1 Null Mice. *Journal of Biological Chemistry*, *288*(34), 24742–24752. https://doi.org/10.1074/jbc.M113.464156

Prednisone, Azathioprine, and N -Acetylcysteine for Pulmonary Fibrosis. (2012). *New England Journal of Medicine*, *366*(21), 1968–1977. https://doi.org/10.1056/NEJMoa1113354

Puglisi, S., Torrisi, S., Giuliano, R., Vindigni, V., & Vancheri, C. (2016). What We Know About the Pathogenesis of Idiopathic Pulmonary Fibrosis. *Seminars in Respiratory and Critical Care Medicine*, *37*(03), 358–367. https://doi.org/10.1055/s-0036-1580693

Pyott, S. M., Schwarze, U., Christiansen, H. E., Pepin, M. G., Leistritz, D. F., Dineen, R., Harris, C., Burton, B. K., Angle, B., Kim, K., Sussman, M. D., Weis, M., Eyre, D. R., Russell, D. W., McCarthy, K. J., Steiner, R. D., & Byers, P. H. (2011). Mutations in PPIB (cyclophilin B) delay type I procollagen chain association and result in perinatal lethal to moderate osteogenesis imperfecta phenotypes. *Human Molecular Genetics*, *20*(8), 1595–1609. https://doi.org/10.1093/hmg/ddr037

Raghu, G. (2011). Idiopathic pulmonary fibrosis: guidelines for diagnosis and clinical management have advanced from consensus-based in 2000 to evidence-based in 2011. *European Respiratory Journal*, *37*(4), 743–746. https://doi.org/10.1183/09031936.00017711

Raghu, Ganesh, Brown, K. K., Collard, H. R., Cottin, V., Gibson, K. F., Kaner, R. J., Lederer, D. J., Martinez, F. J., Noble, P. W., Song, J. W., Wells, A. U., Whelan, T. P. M., Wuyts, W., Moreau, E., Patterson, S. D., Smith, V., Bayly, S., Chien, J. W., Gong, Q., … O'Riordan, T. G. (2017). Efficacy of simtuzumab versus placebo in patients with idiopathic pulmonary fibrosis: a randomised, double-blind, controlled, phase 2 trial. *The Lancet Respiratory Medicine*, *5*(1), 22–32. https://doi.org/10.1016/S2213-2600(16)30421-0

Rajan, N., Habermehl, J., Coté, M.-F., Doillon, C. J., & Mantovani, D. (2006). Preparation of ready-to-use, storable and reconstituted type I collagen from rat tail tendon for tissue engineering applications. *Nature Protocols*, *1*(6), 2753–2758. https://doi.org/10.1038/nprot.2006.430

Rappu, P., Salo, A. M., Myllyharju, J., & Heino, J. (2019). Role of prolyl hydroxylation in the molecular interactions of collagens. *Essays in Biochemistry*, *63*(3), 325–335. https://doi.org/10.1042/EBC20180053

Reyfman, P. A., Walter, J. M., Joshi, N., Anekalla, K. R., McQuattie-Pimentel, A. C., Chiu, S., Fernandez, R., Akbarpour, M., Chen, C. I., Ren, Z., Verma, R., Abdala-Valencia, H., Nam, K., Chi, M., Han, S. H., Gonzalez-Gonzalez, F. J., Soberanes, S., Watanabe, S., Williams, K. J. N., … Misharin, A. V. (2019). Single-cell transcriptomic analysis of human lung provides insights into the pathobiology of pulmonary fibrosis. *American Journal of Respiratory and Critical Care Medicine*, *199*(12), 1517–1536. https://doi.org/10.1164/rccm.201712-2410OC

Ricard-Blum, S. (2011). The Collagen Family. *Cold Spring Harbor Perspectives in Biology*, *3*(1), a004978–a004978. https://doi.org/10.1101/cshperspect.a004978

Richeldi, L., Cottin, V., Flaherty, K. R., Kolb, M., Inoue, Y., Raghu, G., Taniguchi, H., Hansell, D. M., Nicholson, A. G., Le Maulf, F., Stowasser, S., & Collard, H. R. (2014). Design of the INPULSIS™ trials: Two phase 3 trials of nintedanib in patients with idiopathic pulmonary fibrosis. *Respiratory Medicine*, *108*(7), 1023–1030. https://doi.org/10.1016/j.rmed.2014.04.011

Ritchie, M. E., Phipson, B., Wu, D., Hu, Y., Law, C. W., Shi, W., & Smyth, G. K. (2015). limma powers differential expression analyses for RNA-sequencing and microarray studies. *Nucleic Acids Research*, *43*(7), e47–e47. https://doi.org/10.1093/nar/gkv007

Roach, K. M., Sutcliffe, A., Matthews, L., Elliott, G., Newby, C., Amrani, Y., & Bradding, P. (2018). A model of human lung fibrogenesis for the assessment of anti-fibrotic strategies in idiopathic pulmonary fibrosis. *Scientific Reports*, *8*(1), 342. https://doi.org/10.1038/s41598-017-18555-9

Robert, S., Gicquel, T., Victoni, T., Valença, S., Barreto, E., Bailly-Maître, B., Boichot, E., & Lagente, V. (2016). Involvement of matrix metalloproteinases (MMPs) and inflammasome pathway in molecular mechanisms of fibrosis. *Bioscience Reports*, *36*(4). https://doi.org/10.1042/BSR20160107

Röder, K. (2022). The effects of glycine to alanine mutations on the structure of GPO collagen model peptides. *Physical Chemistry Chemical Physics*, *24*(3), 1610–1619. https://doi.org/10.1039/D1CP04775B

Ruigrok, M. J. R., El Amasi, K. E. M., Leeming, D. J., Sand, J. M. B., Frijlink, H. W., Hinrichs, W. L. J., & Olinga, P. (2021). Silencing Heat Shock Protein 47 (HSP47) in Fibrogenic Precision-Cut Lung Slices: A Surprising Lack of Effects on Fibrogenesis? *Frontiers in Medicine*, *8*. https://doi.org/10.3389/fmed.2021.607962

Sakakibara, S., Inouye, K., Shudo, K., Kishida, Y., Kobayashi, Y., & Prockop, D. J. (1973). Synthesis of (Pro-Hyp-Gly)n of defined molecular weights Evidence for the stabilization of collagen triple helix by hydroxypyroline. *Biochimica et Biophysica Acta (BBA) - Protein Structure*, *303*(1), 198–202. https://doi.org/10.1016/0005-2795(73)90164-5

Salo, A. M., & Myllyharju, J. (2021). Prolyl and lysyl hydroxylases in collagen synthesis. *Experimental Dermatology*, *30*(1), 38–49. https://doi.org/10.1111/exd.14197

Salton, F., Volpe, M., & Confalonieri, M. (2019). Epithelial–Mesenchymal Transition in the Pathogenesis of Idiopathic Pulmonary Fibrosis. *Medicina*, *55*(4), 83. https://doi.org/10.3390/medicina55040083

Sander, H., Wallace, S., Plouse, R., Tiwari, S., & Gomes, A. V. (2019). Ponceau S waste: Ponceau S staining for total protein normalization. *Analytical Biochemistry*, *575*, 44–53. https://doi.org/10.1016/j.ab.2019.03.010

Sato, K., Parag-Sharma, K., Terajima, M., Musicant, A. M., Murphy, R. M., Ramsey, M. R., Hibi, H., Yamauchi, M., & Amelio, A. L. (2021). Lysyl hydroxylase 2-induced collagen cross-link switching promotes metastasis in head and neck squamous cell carcinomas. *Neoplasia*, *23*(6), 594–606. https://doi.org/10.1016/j.neo.2021.05.014

Schäfer, S. C., Funke-Chambour, M., & Berezowska, S. (2020). Idiopathische Lungenfibrose – Epidemiologie, Ursachen und klinischer Verlauf. *Der Pathologe*, *41*(1), 46–51. https://doi.org/10.1007/s00292-019-00747-x

Schiene-Fischer, C. (2015). Multidomain Peptidyl Prolyl cis/trans Isomerases. *Biochimica et Biophysica Acta (BBA) - General Subjects*, *1850*(10), 2005–2016. https://doi.org/10.1016/j.bbagen.2014.11.012

Schiller, H. B., Fernandez, I. E., Burgstaller, G., Schaab, C., Scheltema, R. A., Schwarzmayr, T., Strom, T. M., Eickelberg, O., & Mann, M. (2015). Time- and compartment-resolved proteome profiling of the extracellular niche in lung injury and repair. *Molecular Systems Biology*, *11*(7), 819. https://doi.org/10.15252/msb.20156123

Schiller, H. B., Mayr, C. H., Leuschner, G., Strunz, M., Staab-Weijnitz, C., Preisendörfer, S.,

Eckes, B., Moinzadeh, P., Krieg, T., Schwartz, D. A., Hatz, R. A., Behr, J., Mann, M., & Eickelberg, O. (2017). Deep Proteome Profiling Reveals Common Prevalence of MZB1-Positive Plasma B Cells in Human Lung and Skin Fibrosis. *American Journal of Respiratory and Critical Care Medicine*, *196*(10), 1298–1310. https://doi.org/10.1164/rccm.201611-2263OC

Schwanhäusser, B., Busse, D., Li, N., Dittmar, G., Schuchhardt, J., Wolf, J., Chen, W., & Selbach, M. (2013). Correction: Corrigendum: Global quantification of mammalian gene expression control. *Nature*, *495*(7439), 126–127. https://doi.org/10.1038/nature11848

Schwarze, U., Cundy, T., Pyott, S. M., Christiansen, H. E., Hegde, M. R., Bank, R. A., Pals, G., Ankala, A., Conneely, K., Seaver, L., Yandow, S. M., Raney, E., Babovic-Vuksanovic, D., Stoler, J., Ben-Neriah, Z., Segel, R., Lieberman, S., Siderius, L., Al-Aqeel, A., … Byers, P. H. (2013). Mutations in FKBP10, which result in Bruck syndrome and recessive forms of osteogenesis imperfecta, inhibit the hydroxylation of telopeptide lysines in bone collagen. *Human Molecular Genetics*, *22*(1), 1–17. https://doi.org/10.1093/hmg/dds371

Schwarze, Ulrike, Cundy, T., Pyott, S. M., Christiansen, H. E., Hegde, M. R., Bank, R. A., Pals, G., Ankala, A., Conneely, K., Seaver, L., Yandow, S. M., Raney, E., Babovic-Vuksanovic, D., Stoler, J., Ben-Neriah, Z., Segel, R., Lieberman, S., Siderius, L., Al-Aqeel, A., … Byers, P. H. (2013). Mutations in FKBp10, which result in bruck syndrome and recessive forms of osteogenesis imperfecta, inhibit the hydroxylation of telopeptide lysines in bone collagen. *Human Molecular Genetics*, *22*(1), 1–17. https://doi.org/10.1093/hmg/dds371

Sgalla, G., Kulkarni, T., Antin-Ozerkis, D., Thannickal, V. J., & Richeldi, L. (2019). Update in Pulmonary Fibrosis 2018. *American Journal of Respiratory and Critical Care Medicine*, *200*(3), 292–300. https://doi.org/10.1164/rccm.201903-0542UP

Shao, S., Fang, H., Duan, L., Ye, X., Rao, S., Han, J., Li, Y., Yuan, G., Liu, W., & Zhang, X. (2020). Lysyl hydroxylase 3 increases collagen deposition and promotes pulmonary fibrosis by activating TGFβ1/Smad3 and Wnt/β-catenin pathways. *Archives of Medical Science*, *16*(2), 436–445. https://doi.org/10.5114/aoms.2018.81357

Shao, S., Zhang, X., Duan, L., Fang, H., Rao, S., Liu, W., Guo, B., & Zhang, X. (2018b). Lysyl Hydroxylase Inhibition by Minoxidil Blocks Collagen Deposition and Prevents Pulmonary Fibrosis via TGF-β_1/Smad3 Signaling Pathway. *Medical Science Monitor*, *24*, 8592–8601. https://doi.org/10.12659/MSM.910761

Shin, M., Chan, I. L., Cao, Y., Gruntman, A. M., Lee, J., Sousa, J., Rodríguez, T. C., Echeverria, D., Devi, G., Debacker, A. J., Moazami, M. P., Krishnamurthy, P. M., Rembetsy-Brown, J. M., Kelly, K., Yukselen, O., Donnard, E., Parsons, T. J., Khvorova, A., Sontheimer, E. J., … Watts, J. K. (2022). Intratracheally administered LNA gapmer antisense oligonucleotides induce robust gene silencing in mouse lung fibroblasts. *Nucleic Acids Research*, *50*(15), 8418–8430. https://doi.org/10.1093/nar/gkac630

Shioya, S., Masuda, T., Senoo, T., Horimasu, Y., Miyamoto, S., Nakashima, T., Iwamoto, H., Fujitaka, K., Hamada, H., & Hattori, N. (2018). Plasminogen activator inhibitor-1 serves an important role in radiation-induced pulmonary fibrosis. *Experimental and Therapeutic Medicine*. https://doi.org/10.3892/etm.2018.6550

Silva, J. C., Gorenstein, M. V., Li, G.-Z., Vissers, J. P. C., & Geromanos, S. J. (2006). Absolute Quantification of Proteins by LCMSE. *Molecular & Cellular Proteomics*, *5*(1), 144–156. https://doi.org/10.1074/mcp.M500230-MCP200

Sim, S. L., Kumari, S., Kaur, S., & Khosrotehrani, K. (2022). Macrophages in Skin Wounds: Functions and Therapeutic Potential. *Biomolecules*, *12*(11), 1659. https://doi.org/10.3390/biom12111659

Sime, P. J., Xing, Z., Graham, F. L., Csaky, K. G., & Gauldie, J. (1997). Adenovector-mediated gene transfer of active transforming growth factor-beta1 induces prolonged severe fibrosis in rat lung. *Journal of Clinical Investigation*, *100*(4), 768–776. https://doi.org/10.1172/JCI119590

Singh, P., Carraher, C., & Schwarzbauer, J. E. (2010). Assembly of Fibronectin Extracellular Matrix. *Annual Review of Cell and Developmental Biology*, *26*(1), 397–419.

https://doi.org/10.1146/annurev-cellbio-100109-104020

Sorushanova, A., Delgado, L. M., Wu, Z., Shologu, N., Kshirsagar, A., Raghunath, R., Mullen, A. M., Bayon, Y., Pandit, A., Raghunath, M., & Zeugolis, D. I. (2019b). The Collagen Suprafamily: From Biosynthesis to Advanced Biomaterial Development. *Advanced Materials*, *31*(1), 1801651. https://doi.org/10.1002/adma.201801651

Staab-Weijnitz, C.A., Merl-Pham, J., Basak, T., Knueppel, L., Ramanujam, D., Athanason, M., Behr, J., Engelhardt, S., Eickelberg, O., Hauck, S., & Vanacore, R. (2019). Quantitative Proteomic Profiling of Extracellular Matrix and Collagen Posttranslational Modifications in an In Vitro Model of Lung Fibrosis. *A107. Engineered And Remodelled Matrix Compartments*, A2545–A2545. https://doi.org/10.1164/ajrccm-conference.2019.199.1_MeetingAbstracts.A2545

Staab-Weijnitz, Claudia A. (2022). Fighting the Fiber: Targeting Collagen in Lung Fibrosis. *American Journal of Respiratory Cell and Molecular Biology*, *66*(4), 363–381. https://doi.org/10.1165/rcmb.2021-0342TR

Staab-Weijnitz, Claudia A., Fernandez, I. E., Knüppel, L., Maul, J., Heinzelmann, K., Juan-Guardela, B. M., Hennen, E., Preissler, G., Winter, H., Neurohr, C., Hatz, R., Lindner, M., Behr, J., Kaminski, N., & Eickelberg, O. (2015a). FK506-binding protein 10, a potential novel drug target for idiopathic pulmonary fibrosis. *American Journal of Respiratory and Critical Care Medicine*, *192*(4), 455–467. https://doi.org/10.1164/rccm.201412-2233OC

Steinlein, O. K., Aichinger, E., Trucks, H., & Sander, T. (2011). Mutations in FKBP10 can cause a severe form of isolated Osteogenesis imperfecta. *BMC Medical Genetics*, *12*(1), 152. https://doi.org/10.1186/1471-2350-12-152

Steplewski, A., & Fertala, A. (2012). Inhibition of collagen fibril formation. *Fibrogenesis & Tissue Repair*, *5*(S1), S29. https://doi.org/10.1186/1755-1536-5-S1-S29

Strunz, M., Simon, L. M., Ansari, M., Kathiriya, J. J., Angelidis, I., Mayr, C. H., Tsidiridis, G., Lange, M., Mattner, L. F., Yee, M., Ogar, P., Sengupta, A., Kukhtevich, I., Schneider, R., Zhao, Z., Voss, C., Stoeger, T., Neumann, J. H. L., Hilgendorff, A., … Schiller, H. B. (2020). Alveolar regeneration through a Krt8+ transitional stem cell state that persists in human lung fibrosis. *Nature Communications*, *11*(1), 3559. https://doi.org/10.1038/s41467-020-17358-3

Suki, B., & Bates, J. H. T. (2008). Extracellular matrix mechanics in lung parenchymal diseases. *Respiratory Physiology & Neurobiology*, *163*(1–3), 33–43. https://doi.org/10.1016/j.resp.2008.03.015

Sun, B. (2021). The mechanics of fibrillar collagen extracellular matrix. *Cell Reports Physical Science*, *2*(8), 100515. https://doi.org/10.1016/j.xcrp.2021.100515

Sun, K.-H., Chang, Y., Reed, N. I., & Sheppard, D. (2016). α-Smooth muscle actin is an inconsistent marker of fibroblasts responsible for force-dependent TGFβ activation or collagen production across multiple models of organ fibrosis. *American Journal of Physiology-Lung Cellular and Molecular Physiology*, *310*(9), L824–L836. https://doi.org/10.1152/ajplung.00350.2015

Taguchi, T., & Razzaque, M. S. (2007). The collagen-specific molecular chaperone HSP47: is there a role in fibrosis? *Trends in Molecular Medicine*, *13*(2), 45–53. https://doi.org/10.1016/j.molmed.2006.12.001

Tanabe, N., McDonough, J. E., Vasilescu, D. M., Ikezoe, K., Verleden, S. E., Xu, F., Wuyts, W. A., Vanaudenaerde, B. M., Colby, T. V., & Hogg, J. C. (2020). Pathology of Idiopathic Pulmonary Fibrosis Assessed by a Combination of Microcomputed Tomography, Histology, and Immunohistochemistry. *American Journal of Pathology*, *190*(12), 2427–2435. https://doi.org/10.1016/j.ajpath.2020.09.001

Tanjore, H., Xu, X. C., Polosukhin, V. V., Degryse, A. L., Li, B., Han, W., Sherrill, T. P., Plieth, D., Neilson, E. G., Blackwell, T. S., & Lawson, W. E. (2009). Contribution of Epithelial-derived Fibroblasts to Bleomycin-induced Lung Fibrosis. *American Journal of Respiratory and Critical Care Medicine*, *180*(7), 657–665. https://doi.org/10.1164/rccm.200903-0322OC

Tasab, M., Batten, M. R., & Bulleid, N. J. (2000). Hsp47: a molecular chaperone that interacts

with and stabilizes correctly-folded procollagen. *The EMBO Journal*, *19*(10), 2204–2211. https://doi.org/10.1093/emboj/19.10.2204

Tatro, E. T., Everall, I. P., Kaul, M., & Achim, C. L. (2009). Modulation of glucocorticoid receptor nuclear translocation in neurons by immunophilins FKBP51 and FKBP52: Implications for major depressive disorder. *Brain Research*, *1286*, 1–12. https://doi.org/10.1016/j.brainres.2009.06.036

Tiainen, P., Pasanen, A., Sormunen, R., & Myllyharju, J. (2008). Characterization of Recombinant Human Prolyl 3-Hydroxylase Isoenzyme 2, an Enzyme Modifying the Basement Membrane Collagen IV. *Journal of Biological Chemistry*, *283*(28), 19432–19439. https://doi.org/10.1074/jbc.M802973200

Tjin, G., White, E. S., Faiz, A., Sicard, D., Tschumperlin, D. J., Mahar, A., Kable, E. P. W., & Burgess, J. K. (2017). Lysyl oxidases regulate fibrillar collagen remodelling in idiopathic pulmonary fibrosis. *Disease Models & Mechanisms*, *10*(11), 1301–1312. https://doi.org/10.1242/dmm.030114

Tjin, G., White, E. S., Faiz, A., Sicard, D., Tschumperlin, D. J., Mahar, A., Kable, E. P. W., Burgess, J. K., Tjin, G., White, E. S., Faiz, A., Sicard, D., Tschumperlin, D. J., & Mahar, A. (2017). Correction: Lysyl oxidases regulate fibrillar collagen remodelling in idiopathic pulmonary fibrosis (DMM Disease Models and Mechanisms (2017) 10 (1301-1312) DOI: 10.1242/dmm.030114). *DMM Disease Models and Mechanisms*, *10*(12), 1545. https://doi.org/10.1242/dmm.033191

Todd, N. W., Luzina, I. G., & Atamas, S. P. (2012). Molecular and cellular mechanisms of pulmonary fibrosis. *Fibrogenesis & Tissue Repair*, *5*(1), 11. https://doi.org/10.1186/1755-1536-5-11

Tomasek, J. J., Gabbiani, G., Hinz, B., Chaponnier, C., & Brown, R. A. (2002). Myofibroblasts and mechano-regulation of connective tissue remodelling. *Nature Reviews Molecular Cell Biology*, *3*(5), 349–363. https://doi.org/10.1038/nrm809

Tomasek, J. J., McRae, J., Owens, G. K., & Haaksma, C. J. (2005). Regulation of α-Smooth Muscle Actin Expression in Granulation Tissue Myofibroblasts Is Dependent on the Intronic CArG Element and the Transforming Growth Factor-β1 Control Element. *The American Journal of Pathology*, *166*(5), 1343–1351. https://doi.org/10.1016/S0002-9440(10)62353-X

Tong, M., & Jiang, Y. (2015). FK506-Binding Proteins and Their Diverse Functions. *Current Molecular Pharmacology*, *9*(1), 48–65. https://doi.org/10.2174/1874467208666150519113541

Torrisi, S. E., Kahn, N., Vancheri, C., & Kreuter, M. (2020). Evolution and treatment of idiopathic pulmonary fibrosis. *La Presse Médicale* ,*49*(2),104025. https://doi.org/10.1016/j.lpm.2020.104025

Tsukui, T., Sun, K.-H., Wetter, J. B., Wilson-Kanamori, J. R., Hazelwood, L. A., Henderson, N. C., Adams, T. S., Schupp, J. C., Poli, S. D., Rosas, I. O., Kaminski, N., Matthay, M. A., Wolters, P. J., & Sheppard, D. (2020a). Collagen-producing lung cell atlas identifies multiple subsets with distinct localization and relevance to fibrosis. *Nature Communications*, *11*(1), 1920. https://doi.org/10.1038/s41467-020-15647-5

Tsukui, T., Ueha, S., Shichino, S., Inagaki, Y., & Matsushima, K. (2015). Intratracheal Cell Transfer Demonstrates the Profibrotic Potential of Resident Fibroblasts in Pulmonary Fibrosis. *The American Journal of Pathology*, *185*(11), 2939–2948. https://doi.org/10.1016/j.ajpath.2015.07.022

Turtle, E. D., & Ho, W.-B. (2004). Inhibition of procollagen C-proteinase: fibrosis and beyond. *Expert Opinion on Therapeutic Patents*, *14*(8), 1185–1197. https://doi.org/10.1517/13543776.14.8.1185

Tyanova, S., Temu, T., & Cox, J. (2016). The MaxQuant computational platform for mass spectrometry-based shotgun proteomics. *Nature Protocols*, *11*(12), 2301–2319. https://doi.org/10.1038/nprot.2016.136

Umair, M., Hassan, A., Jan, A., Ahmad, F., Imran, M., Samman, M. I., Basit, S., & Ahmad, W.

(2016). Homozygous sequence variants in the FKBP10 gene underlie osteogenesis imperfecta in consanguineous families. *Journal of Human Genetics*, *61*(3), 207–213. https://doi.org/10.1038/jhg.2015.129

Upagupta, C., Shimbori, C., Alsilmi, R., & Kolb, M. (2018). Matrix abnormalities in pulmonary fibrosis. *European Respiratory Review*, *27*(148), 180033. https://doi.org/10.1183/16000617.0033-2018

Ushakumary, M. G., Riccetti, M., & Perl, A.-K. T. (2021). Resident Interstitial Lung Fibroblasts and their Role in Alveolar Stem Cell Niche Development, Homeostasis, Injury, and Regeneration. *Stem Cells Translational Medicine*, *10*(7), 1021–1032. https://doi.org/10.1002/sctm.20-0526

Valli, M., Barnes, A., Gallanti, A., Cabral, W., Viglio, S., Weis, M., Makareeva, E., Eyre, D., Leikin, S., Antoniazzi, F., Marini, J., & Mottes, M. (2012). Deficiency of CRTAP in non-lethal recessive osteogenesis imperfecta reduces collagen deposition into matrix. *Clinical Genetics*, *82*(5), 453–459. https://doi.org/10.1111/j.1399-0004.2011.01794.x

van der Slot, A. J., Zuurmond, A.-M., Bardoel, A. F. J., Wijmenga, C., Pruijs, H. E. H., Sillence, D. O., Brinckmann, J., Abraham, D. J., Black, C. M., Verzijl, N., DeGroot, J., Hanemaaijer, R., TeKoppele, J. M., Huizinga, T. W. J., & Bank, R. A. (2003). Identification of PLOD2 as Telopeptide Lysyl Hydroxylase, an Important Enzyme in Fibrosis. *Journal of Biological Chemistry*, *278*(42), 40967–40972. https://doi.org/10.1074/jbc.M307380200

van Dijk, F. S., Nesbitt, I. M., Zwikstra, E. H., Nikkels, P. G. J., Piersma, S. R., Fratantoni, S. A., Jimenez, C. R., Huizer, M., Morsman, A. C., Cobben, J. M., van Roij, M. H. H., Elting, M. W., Verbeke, J. I. M. L., Wijnaendts, L. C. D., Shaw, N. J., Högler, W., McKeown, C., Sistermans, E. A., Dalton, A., Pals, G. (2009). PPIB Mutations Cause Severe Osteogenesis Imperfecta. *The American Journal of Human Genetics*, *85*(4), 521–527. https://doi.org/10.1016/j.ajhg.2009.09.001

Vancheri, C., Kreuter, M., Richeldi, L., Ryerson, C. J., Valeyre, D., Grutters, J. C., Wiebe, S., Stansen, W., Quaresma, M., Stowasser, S., & Wuyts, W. A. (2018). Nintedanib with Add-on Pirfenidone in Idiopathic Pulmonary Fibrosis. Results of the INJOURNEY Trial. *American Journal of Respiratory and Critical Care Medicine*, *197*(3), 356–363. https://doi.org/10.1164/rccm.201706-1301OC

Vasta, J. D., & Raines, R. T. (2018). Collagen Prolyl 4-Hydroxylase as a Therapeutic Target. *Journal of Medicinal Chemistry*, *61*(23), 10403–10411. https://doi.org/10.1021/acs.jmedchem.8b00822

Vazquez-Armendariz, A. I., Barroso, M. M., El Agha, E., & Herold, S. (2022). 3D In Vitro Models: Novel Insights into Idiopathic Pulmonary Fibrosis Pathophysiology and Drug Screening. *Cells*, *11*(9), 1526. https://doi.org/10.3390/cells11091526

Vidak, E., Javoršek, U., Vizovišek, M., & Turk, B. (2019). Cysteine Cathepsins and their Extracellular Roles: Shaping the Microenvironment. *Cells*, *8*(3), 264. https://doi.org/10.3390/cells8030264

Vranka, J. A., Pokidysheva, E., Hayashi, L., Zientek, K., Mizuno, K., Ishikawa, Y., Maddox, K., Tufa, S., Keene, D. R., Klein, R., & Bächinger, H. P. (2010). Prolyl 3-Hydroxylase 1 Null Mice Display Abnormalities in Fibrillar Collagen-rich Tissues Such as Tendons, Skin, and Bones. *Journal of Biological Chemistry*, *285*(22), 17253–17262. https://doi.org/10.1074/jbc.M110.102228

Wagenaar-Miller, R. A., Engelholm, L. H., Gavard, J., Yamada, S. S., Gutkind, J. S., Behrendt, N., Bugge, T. H., & Holmbeck, K. (2007). Complementary Roles of Intracellular and Pericellular Collagen Degradation Pathways In Vivo. *Molecular and Cellular Biology*, *27*(18), 6309–6322. https://doi.org/10.1128/MCB.00291-07

Wang, C., Valtavaara, M., & Myllyla, R. (2000). Lack of Collagen Type Specificity for Lysyl Hydroxylase Isoforms. *DNA and Cell Biology*, *19*(2), 71–77. https://doi.org/10.1089/104454900314582

Wang, Q., Wang, Y., Hyde, D. M., Gotwals, P. J., Koteliansky, V. E., Ryan, S. T., & Giri, S. N. (1999). Reduction of bleomycin induced lung fibrosis by transforming growth factor beta

soluble receptor in hamsters. *Thorax*, *54*(9), 805–812. https://doi.org/10.1136/thx.54.9.805

Watson, W. H., Ritzenthaler, J. D., & Roman, J. (2016). Lung extracellular matrix and redox regulation. *Redox Biology*, *8*, 305–315. https://doi.org/10.1016/j.redox.2016.02.005

Wei, P., Xie, Y., Abel, P. W., Huang, Y., Ma, Q., Li, L., Hao, J., Wolff, D. W., Wei, T., & Tu, Y. (2019). Transforming growth factor (TGF)-β1-induced miR-133a inhibits myofibroblast differentiation and pulmonary fibrosis. *Cell Death and Disease*, *10*(9). https://doi.org/10.1038/s41419-019-1873-x

Weill, D., Benden, C., Corris, P. A., Dark, J. H., Davis, R. D., Keshavjee, S., Lederer, D. J., Mulligan, M. J., Patterson, G. A., Singer, L. G., Snell, G. I., Verleden, G. M., Zamora, M. R., & Glanville, A. R. (2015). A consensus document for the selection of lung transplant candidates: 2014—An update from the Pulmonary Transplantation Council of the International Society for Heart and Lung Transplantation. *The Journal of Heart and Lung Transplantation*, *34*(1), 1–15. https://doi.org/10.1016/j.healun.2014.06.014

Weis, M. A., Hudson, D. M., Kim, L., Scott, M., Wu, J.-J., & Eyre, D. R. (2010). Location of 3-Hydroxyproline Residues in Collagen Types I, II, III, and V/XI Implies a Role in Fibril Supramolecular Assembly. *Journal of Biological Chemistry*, *285*(4), 2580–2590. https://doi.org/10.1074/jbc.M109.068726

Wenstrup, R. J., Florer, J. B., Brunskill, E. W., Bell, S. M., Chervoneva, I., & Birk, D. E. (2004). Type V collagen controls the initiation of collagen fibril assembly. *Journal of Biological Chemistry*, *279*(51), 53331–53337. https://doi.org/10.1074/jbc.M409622200

Wierzbicka-Patynowski, I., & Schwarzbauer, J. E. (2003). The ins and outs of fibronectin matrix assembly. *Journal of Cell Science*, *116*(16), 3269–3276. https://doi.org/10.1242/jcs.00670

Wight, T. N., & Potter-Perigo, S. (2011). The extracellular matrix: an active or passive player in fibrosis? *American Journal of Physiology-Gastrointestinal and Liver Physiology*, *301*(6), G950–G955. https://doi.org/10.1152/ajpgi.00132.2011

Willis, B. C. (2006). Epithelial Origin of Myofibroblasts during Fibrosis in the Lung. *Proceedings of the American Thoracic Society*, *3*(4), 377–382. https://doi.org/10.1513/pats.200601-004TK

Willis, Brigham C., Liebler, J. M., Luby-Phelps, K., Nicholson, A. G., Crandall, E. D., du Bois, R. M., & Borok, Z. (2005). Induction of Epithelial-Mesenchymal Transition in Alveolar Epithelial Cells by Transforming Growth Factor-β1. *The American Journal of Pathology*, *166*(5), 1321–1332. https://doi.org/10.1016/S0002-9440(10)62351-6

Winters, N. I., Habermann, A. C., Taylor, C. J., Calvi, C., Blackwell, T. S., Banovich, N., & Kropski, J. (2020). Fibroblast Subtypes Identified by Single Sell RNA Sequencing in Pulmonary Fibrosis. *A95. Novel Insight Into Ipf Pathogenesis*, A2513–A2513. https://doi.org/10.1164/ajrccm-conference.2020.201.1_MeetingAbstracts.A2513

Wollin, S. L., Bonella, F., & Stowasser, S. (2015). Idiopathic pulmonary fibrosis: current treatment options and critical appraisal of nintedanib. *Drug Design, Development and Therapy*, 6407. https://doi.org/10.2147/DDDT.S76648

Yamauchi, M., & Shiiba, M. (n.d.). Lysine Hydroxylation and Cross-linking of Collagen. In *Post-translational Modifi cations of Proteins* (pp. 95–108). Humana Press. https://doi.org/10.1007/978-1-60327-084-7_7

Yamauchi, M., & Sricholpech, M. (2012). Lysine post-translational modifications of collagen. *Essays in Biochemistry*, *52*, 113–133. https://doi.org/10.1042/bse0520113

Yang, M.-Y., Lin, Y.-J., Han, M.-M., Bi, Y.-Y., He, X.-Y., Xing, L., Jeong, J.-H., Zhou, T.-J., & Jiang, H.-L. (2022). Pathological collagen targeting and penetrating liposomes for idiopathic pulmonary fibrosis therapy. *Journal of Controlled Release*, *351*, 623–637. https://doi.org/10.1016/j.jconrel.2022.09.054

Yu, W.-K., Chen, W.-C., Su, V. Y.-F., Shen, H.-C., Wu, H.-H., Chen, H., & Yang, K.-Y. (2022). Nintedanib Inhibits Endothelial Mesenchymal Transition in Bleomycin-Induced Pulmonary Fibrosis via Focal Adhesion Kinase Activity Reduction. *International Journal of Molecular Sciences*, *23*(15), 8193. https://doi.org/10.3390/ijms23158193

Yu, Z., Visse, R., Inouye, M., Nagase, H., & Brodsky, B. (2012). Defining Requirements for Collagenase Cleavage in Collagen Type III Using a Bacterial Collagen System. *Journal of Biological Chemistry*, *287*(27), 22988–22997. https://doi.org/10.1074/jbc.M112.348979

Zanoni, Cortesi, Zamagni, & Tesei. (2019). The Role of Mesenchymal Stem Cells in Radiation-Induced Lung Fibrosis. *International Journal of Molecular Sciences*, *20*(16), 3876. https://doi.org/10.3390/ijms20163876

Zeng, B., Macdonald, J. R., Bann, G. J., Beck, K., Gambee, E. J., Boswell, A. B., & BÄCHINGER, P. H. (1998). Chicken FK506-binding protein, FKBP65, a member of the FKBP family of peptidylprolyl cis–trans isomerases, is only partially inhibited by FK506. *Biochemical Journal*, *330*(1), 109–114. https://doi.org/10.1042/bj3300109

Zepp, J. A., Morley, M. P., Loebel, C., Kremp, M. M., Chaudhry, F. N., Basil, M. C., Leach, J. P., Liberti, D. C., Niethamer, T. K., Ying, Y., Jayachandran, S., Babu, A., Zhou, S., Frank, D. B., Burdick, J. A., & Morrisey, E. E. (2021). Genomic, epigenomic, and biophysical cues controlling the emergence of the lung alveolus. *Science*, *371*(6534). https://doi.org/10.1126/science.abc3172

Zepp, J. A., Zacharias, W. J., Frank, D. B., Cavanaugh, C. A., Zhou, S., Morley, M. P., & Morrisey, E. E. (2017). Distinct Mesenchymal Lineages and Niches Promote Epithelial Self-Renewal and Myofibrogenesis in the Lung. *Cell*, *170*(6), 1134-1148.e10. https://doi.org/10.1016/j.cell.2017.07.034

Zhang, C., Ötjengerdes, R. M., Roewe, J., Mejias, R., & Marschall, A. L. J. (2020). Applying Antibodies Inside Cells: Principles and Recent Advances in Neurobiology, Virology and Oncology. *BioDrugs*, *34*(4), 435–462. https://doi.org/10.1007/s40259-020-00419-w

Zhang, J., Dong, Y., Shi, Z., He, H., Chen, J., Zhang, S., Wu, W., Zhang, Q., Han, C., & Hao, L. (2022). P3H4 and PLOD1 expression associates with poor prognosis in bladder cancer. *Clinical and Translational Oncology*, *24*(8), 1524–1532. https://doi.org/10.1007/s12094-022-02791-1

Zhang, X., Zhang, X., Huang, W., & Ge, X. (2021). The role of heat shock proteins in the regulation of fibrotic diseases. *Biomedicine & Pharmacotherapy*, *135*, 111067. https://doi.org/10.1016/j.biopha.2020.111067

Zhao, M., Chen, S., Qu, X., Abdul-fattah, B., Lai, T., Xie, M., Wu, S., Zhou, Y., & Huang, C. (2018). Increased Cthrc1 Activates Normal Fibroblasts and Suppresses Keloid Fibroblasts by Inhibiting TGF-β/Smad Signal Pathway and Modulating YAP Subcellular Location. *Current Medical Science*, *38*(5), 894–902. https://doi.org/10.1007/s11596-018-1959-1

Zhao, X., Chen, J., Sun, H., Zhang, Y., & Zou, D. (2022). New insights into fibrosis from the ECM degradation perspective: the macrophage-MMP-ECM interaction. *Cell & Bioscience*, *12*(1), 117. https://doi.org/10.1186/s13578-022-00856-w

Zhou, W., Mo, X., Cui, W., Zhang, Z., Li, D., Li, L., Xu, L., Yao, H., & Gao, J. (2016). Nrf2 inhibits epithelial-mesenchymal transition by suppressing snail expression during pulmonary fibrosis. *Scientific Reports*, *6*(1), 38646. https://doi.org/10.1038/srep38646

Zhu, L., Fu, X., Chen, X., Han, X., & Dong, P. (2017). M2 macrophages induce EMT through the TGF-β/Smad2 signaling pathway. *Cell Biology International*, *41*(9), 960–968. https://doi.org/10.1002/cbin.10788

Zimmerman, S. M., Besio, R., Heard-Lipsmeyer, M. E., Dimori, M., Castagnola, P., Swain, F. L., Gaddy, D., Diekman, A. B., & Morello, R. (2018). Expression characterization and functional implication of the collagen-modifying Leprecan proteins in mouse gonadal tissue and mature sperm. *AIMS Genetics*, *05*(01), 024–040. https://doi.org/10.3934/genet.2018.1.24

Zuurmond, A., Vanderslotverhoeven, A., Vandura, E., Degroot, J., & Bank, R. (2005). Minoxidil exerts different inhibitory effects on gene expression of lysyl hydroxylase 1, 2, and 3: Implications for collagen cross-linking and treatment of fibrosis. *Matrix Biology*, *24*(4), 261–270. https://doi.org/10.1016/j.matbio.2005.04.002

List of abbreviation

°C: Degrees Celsius

ANOVA: Analysis of Variance

BLEO: Bleomycin

BSA: Bovine Serum Albumin

CRTAP: Cartilage-associated protein

CTHRC1: Collagen Triple Helix Repeat Containing 1

DAPI: 4',6-diamidino-2-phenylindole

DMEM: Dulbecco's Modified Eagle's Medium

ECM: Extracellular Matrix

ER: Endoplasmic Reticulum

FBS: Fetal Bovine Serum

FFPE: Formalin-Fixed Paraffin-Embedded

FGFR: Fibroblast Growth Factor Receptor

FVC: Forced Vital Capacity

GERD: Gastroesophageal reflux disease

HRP: Horseradish peroxidase

IF: Immunofluorescence

IPF: Idiopathic Pulmonary Fibrosis

LOX: Lysyl Oxidase

mL: Milliliter

MMPs: Matrix metalloproteinases

PAI-1: Plasminogen activator inhibitor-1

PBS. Phosphate buffered saline

PCR: Polymerase Chain Reaction

PDGFR: Platelet-Derived Growth Factor Receptor

PhLF: PhLFs

PPIs: Peptidyl-Prolyl-Isomerases

PTM: Post-Translational Modifications

qRT-PCR: Quantitative Real-Time Reverse-Transcriptase PCR

siRNA: Small interfering RNA

TBS-T: Tris-buffered saline with tween

TGF-β: Transforming Growth Factor beta

TPR: Tetratricopeptide Repeat Receptor

Tris: Tris(hydroxymethyl)aminomethane

VEGFR: Vascular Endothelial Growth Factor Receptor

α-SMA: Alpha Smooth Muscle Actin

List of Symbols

α .....alpha

β .....beta

° .....degree

g .....gram

h .....hour

µ.....micro

min.....minute

O/N.....overnight

%.....percentage

Sec.....seconds

List of figures

List of tables

List of publications

Onursal, C., Dick, E., Angelidis, I., Schiller, H. B.,; Staab-Weijnitz, C. A. (2021). Collagen biosynthesis, processing, and maturation in lung ageing**.** Frontiers in Medicine, 8. https://doi.org/10.3389/fmed.2021.593874

Staab-Weijnitz, C. A., **Onursal C**., Nambiar D., and Vanacore R. "Assessment of collagen in translational models of lung research" in the book titled, “Engineering Translational Models of Lung Homeostasis and Disease.” Book Chapter. Accepted

Acknowledgements

I couldn't have achieved this without the assistance of many people in my life. I'd like to take this opportunity to express my gratitude for their help and support.

First and foremost, I would like to express my heartfelt gratitude to my doctoral supervisor, PD Dr. Claudia Staab-Weijnitz, for her extraordinary guidance and feedback, for providing me with this opportunity to work on this project and gain valuable experience, and for motivating me to grow as a scientist. Your invaluable advice, continuous support, and patience throughout my PhD studies have encouraged me all across my academic research and daily life. I'd also like to thank her for always giving me the chance to present my project at different conferences. I am sure that the experience I have gained over the last three years will be beneficial to me in the near future. Thank you, Claudia, for always being such an amazing mentor and for motivating us in the lab. Thank you so much for everything.

Another special thanks to PD Dr. Claudia Staab-Weijnitz for the activities and training I received from the CPC research school "Lung Biology and Disease" during my PhD studies, as well as to Doreen Franke, Karin Herbert, and the teaching facility for their continuous involvement and support.

I would like to express my deepest appreciation to my thesis advisory committee members Prof. Dr. med. Susanne Mayer and Prof. Dr. Darcy Wagner, for all the fruitful discussions, and for the excellent inputs to this project.

I must also extend my sincere thanks to the CPC bioarchive team for providing valuable human material for this project.

I'm grateful to my former and current Staab-Weijnitz team members, Elisabeth Hennen, Elisabeth Dick, Ashesh Chakraborty, Michal Mastalerz, Marie Zöller, Karolina Pijadina, Natalia Christina Cabeza-Boeddinghaus, Emilia Berthold, and Juliana Giraldo, for their kind support, excellent technical assistance, and also for being such a fantastic team. I'm extremely thankful and feel very lucky to have met such amazing people. Thank you so much for your friendship, your support throughout this process, and everything you do behind the scenes to make our Ph.D. journey easier. I will easily miss all of the enjoyable and memorable times we shared.

Furthermore, I am very thankful for all the support that I received from my collaboration partners from Baylor College of Medicine, Houston, Texas (Dr. Caressa D. Lietman, Dr. Brendan Lee), from CPC/ILBD (Dr. Larissa Knüppel, Dr. Herbert Schiller, PD Dr. med. Anne Hilgendorff, Dr. Janine Schniering), from Klinikum der Ludwig-Maximilians-Universität (Prof. Dr. med. Jürgen Behr, Prof. Rudolf Hatz) and from the Helmholtz Zentrum München (Dr. Juliane Merl-Pham, Dr. Stefanie M. Hauck, Dr.Kristian Unger, Dr.Julia Hess).

I would like to thank to all members of the CPC/LHI and ILBD for their helpful advice and technical assistance.

I furthermore want to also express my thanks to all my colleagues in CPC: Aydan, Ashesh, Vijay, Sara, Pushkar, Mahesh, Shruthi, Vijay, Valeria, Erika, Jeanine, Ayse, Diana, Christoph, Georgia, Marie, Michal, Tankut, Haifeng, Sabine and many more. Thank you all for creating a great work environment, sharing memorable experiences over lunch and coffee breaks ☺, and greatly contributing to making my time at the CPC memorable.

Special thanks to Aydan Sardogan and Ashesh Chakraborty for being such incredible friends and family:), for their constant support during my difficult times and for making the last three years much easier and enjoyable with their motivation, help, and suggestions. I'd also like to thank Dilara Kina for being such an amazing friend and always being a phone call away for discussions about anything I was unsure about.

Last but not least, my heartfelt gratitude goes to my parents (Halit and Asmi), to my brothers and sisters (Alev, Leyla, Dicle, Pinar, Nükeyf, Mert and Resul), as well as Sarya and Ronya, for their unconditional help and emotional support, and for always encouraging and understanding me during difficult times. This work is dedicated to you.